www.rsc.org/greenchem

Plastic bags, sugar cane and advanced vibrational spectroscopy: taking Green Chemistry to the Third World

Martyn Poliakoff of the University of Nottingham, UK, and Isao Noda of the Procter & Gamble Company, USA, discuss the development of an inexpensive plastic made from renewable feedstocks.

DOI:10.1039/b404259j

Part 1 (Martyn Poliakoff)

It is becoming increasingly important for Green Chemists to communicate the message of Green Chemistry to the wider public. The key is to find examples which can catch the audience's imagination. Fortunately, there are many such examples (ibuprofen, *etc.*). However, it is only if you have to lecture in a Third World country that you suddenly realise how heavily these examples rely on the context of a developed country to achieve their effect. This problem was brought forcibly home to me when I was asked to give an impromptu talk on Green Chemistry to a mixed audience of pupils and teachers at Wachamo Comprehensive High School[1] in Hossana, a small isolated town in southern Ethiopia. In essence, how does one convey the spirit of Green Chemistry without resorting to details or to the Twelve Principles[2] and without the help of transparencies or PowerPoint?

My solution was to use a polyethylene bag, bought two days earlier at the town's market, Fig. 1. Such bags are made from oil and are imported as Ethiopia does not have any oil reserves of its own. Once used, the bags are just discarded. I counted 12 discarded bags in just one 100 m stretch of road on my way to the school. By contrast, Ethiopia does produce large quantities of sugar cane, Fig. 1. If the bags could be made from sugar cane, then Ethiopia would not have to import the bags or oil and, more importantly, cows could eat any used bags that were discarded in the street! This point clearly struck home with the audience. "But," I said, "making bags from sugar needs new chemistry and that is Green Chemistry".

It is always hard to judge the impact of a lecture. However, the audience seemed interested and, two weeks later, two sports teachers were overheard discussing bags made from sugar! The unsatisfactory part was that I had no idea of how bags could be made from sugar. However, this problem was resolved, quite by chance, six weeks later. During the lunch break at the International Conference on Advanced Vibrational Spectroscopy in Nottingham, I met Isao Noda, a spectroscopy expert from Procter & Gamble. I told him about my lecture in Ethiopia and explained the chemical problem about making the bags. "Ah" he said "we have solved this problem…"

Fig. 1 Children selling plastic bags and sugar cane in Hossana market.

Part 2 (Isao Noda)

I met Martyn Poliakoff during a spectroscopy conference held in Nottingham in the summer of 2003. Martyn gave a nice talk on spectroscopic monitoring of chemical reactions in supercritical water, and we had a chance to chat about the subject after his talk. That is how I found about his passion for Green Chemistry. Martyn was telling me about his experience in Ethiopia and his surprising interest in making plastic bags from agricultural products, like sugar cane. I knew immediately that we were meant to meet on that day, because this has been my major area of research for some time.

For the last 15 years or so, the Procter & Gamble Company in Cincinnati, Ohio, USA, has been quietly working on the development of a totally new plastic material which can be produced from renewable feedstocks, like sugars and fats.[3] This bio-based plastic, now known under the registered trademark of *Nodax*™, is made by bacterial fermentation of common agricultural products. Bacteria produce these materials as an energy storage mechanism, very much the way higher organisms accumulate fats in their body, by metabolizing vegetable oil or sugar.

Nodax™ belongs to a class of aliphatic polyesters, known as poly(hydroxyalkanoate)s or PHAs. It has the general structure given below consisting of random repeat units of (*R*)-3-hydroxybutyrate (3HB) and additional medium chain length (*R*)-3-hydroxyalkanoates (*mcl*-3HA) (Fig. 2).

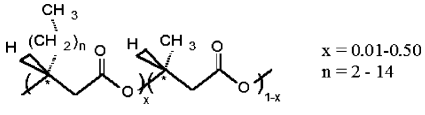

Fig. 2 *Nodax*™ poly(hydroxyalkanoate) copolymers

Bacterially produced poly[(*R*)-3-hydroxybutyrate] homopolymer consisting exclusively of 3HB units was actually known for many years.[4] Unfortunately, it has very high crystallinity and melting point, so that the material becomes too brittle and difficult to process for most standard applications. Copolymerization with other small monomer units, like 3-

Fig. 3 Injection moulded utensils, coated paper cup, and plastic bag all made of bio-based biodegradable *Nodax*™ PHA copolymers.

hydroxyvalerate, was tried with relatively little success in improving the desired properties.[5] Thus, although wonderfully romantic in concept, PHA plastics made by bacteria did not find much use in practice.

In the late 1980s, we had the idea of incorporating a small amount of *mcl*-3HA to make this type of polymer much less crystalline. The idea of using short branches to control plastics properties was well known among polymer chemists to produce soft and ductile linear low density polyethylene. We thought we could make the analogous linear low density polyesters with improved properties.

By carefully examining the known metabolic pathways used for biosynthesis of PHAs in bacteria, we concluded that there should be some wild microorganisms somewhere out there, which could produce PHAs with specific *Nodax*™-type structure. The problem was we had not found such bugs yet at that time, so we had to do the job of making polymers by ourselves. A series of *Nodax*™ copolymers were synthesized by chiral ring-opening copolymerization of substituted β-propiolactones. The properties of the resulting materials were unexpectedly good. They all showed surprisingly ductile and tough characteristics reminiscent of conventional polyolefins like polypropylene and polyethylene.[6] We knew then that we were on to something very exciting: the possibility of deriving truly useful plastics from bio-based feedstocks.

Today, as a result of collaboration with universities, research institutes and other companies active in the field such as the Kaneka Corporation of Japan, we now have multiple strains of bacteria which can efficiently produce *Nodax*™ PHA copolymers. Some were found wild in nature, and others were developed by modern genetic engineering. The biotechnology itself has advanced so much in the last decade or so that fermentation has become a viable industrial means to produce relatively inexpensive plastic. With continued collaboration with Kaneka, we are in the process of completing the R&D to fully commercialize *Nodax*™ polymers.

By using conventional processing equipment for plastics, *Nodax*™ can be converted to various basic forms, like films, sheets, fibres, moulded articles, foams, and coatings. The stiffness range of *Nodax*™ is readily controlled by the amount of *mcl*-3HA from very soft and flexible to hard and tough at will. Some examples are shown in Fig. 3, including the plastic bag made from a renewable source, just as Martyn wanted.

For further information contact Martyn Poliakoff, email: martyn.poliakoff@nottingham.ac.uk, Fax: +44 115 9513058 or Isao Noda, email: noda.i@pg.com, Fax: +1-513-634-9342.

References

1 http://www.ethiopia.org.uk.
2 P. T. Anastas and J. Warner, *Green Chemistry Theory and Practice*, Oxford University Press, Oxford, 1998.
3 http://www.nodax.com.
4 M. Limoigne, *C. R. Seances Soc. Biol. Ses Fil.*, 1926, **94**, 1291.
5 P. P. King, *J. Chem. Technol. Biotechnol.*, 1982, **32**, 2.
6 M. M. Satkowski, D. H. Melik, J.-P. Autran, P. R. Green, I. Noda and L. A. Schechtman, in *Biopolymers*, eds. Y. Doi and A. Steinbüchel, Wiley, Weinheim 2001, **vol. 3b**, p. 231.

Highlights

Markus Hölscher reviews some of the recent literature in green chemistry

DOI:10.1039/b404774p

In situ spectroscopy of heterogeneous catalysts in supercritical solvents

The combination of asymmetric heterogeneous catalysis and supercritical solvents is an especially elegant and green method for the production of enantiopure chemical compounds. It is not surprising that Cinchona alkaloid-modified heterogeneous catalysts, which constitute the most promising catalyst class of this kind, are used in combination with supercritical solvents, thus enabling all the advantages of these unique reaction, extraction and transport media to be applied to asymmetric catalysis. However, rational catalyst design needs definite information about the active species. Baiker and coworkers from ETH Zürich developed an ***in situ*** spectroscopic method for use in supercritical solvents (*Chem. Commun.*, 2004, 744–745). They showed that by *in situ* FTIR investigation of the supercritical fluid phase and the catalytically active solid surface (ATR measurements) it is possible to obtain precise information about the stereochemistry and the coordination of the substrate to the solid. They studied the hydrogenation of ethyl pyruvate, which in solution predominantly occurs in the *trans* form. Upon adsorption on Pt/Al_2O_3 modified with cinchonidine using supercritical ethane as the solvent this equilibrium is shifted to the *cis* form. Insights like this are of great importance for the correct interpretation of experimental data and thus show the relevance of the *in situ* monitoring of heterogeneous catalysts.

Vapor phase epoxidation of propene over mesoporous titanosilicate with gold nanoparticles

A direct gas-phase epoxidation of propene would be a tremendously important and highly advantageous green alternative to the current chlorohydrin and hydroperoxide processes. Among the many attempts to develop a suitable catalyst, Haruta and coworkers from the Research Institute for Green Technology, Tsukuba, succeeded in depositing gold nanoparticles in a three dimensional mesoporous titanosilicate, which in its silylated form serves as an efficient catalyst for the epoxidation of propene with oxygen (*Angew. Chem.*, 2004, **116**, 1572–1574).

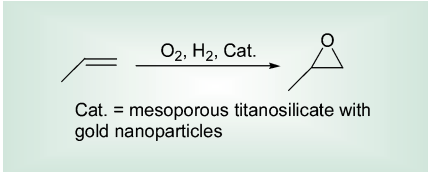

In a systematic study they showed that treatment of these catalysts with $Ba(NO_3)_2$ improves the catalyst performance further. The best catalyst yielded a selectivity for propylene oxide of 92.3% with a propene conversion of 6.3% and a H_2 conversion of 16.7% (time on stream: 4 h; H_2 efficiency was 34.6%).

Solvent-resistant nanofiltration for the recycling of the Co-Jacobsen catalyst

Nanofiltration as a means for recycling of homogeneous transition metal catalysts is one of the promising alternatives to solve the inherent problem of homogeneous catalysis: the efficient separation of products and catalysts under mild and feasible conditions. Jacobs and coworkers from the university of Leuven contributed a novel approach for the separation of the Co-Jacobsen catalyst, which is used for the hydrolytic kinetic resolution of epoxides (*Chem. Commun.*, 2004, 710–711). The authors developed a novel membrane named COK M2, which is a silicon based material with an inorganic filler. The reaction of (±)-1,2-epoxyethane with H_2O in diethyl ether in the presence of (*S*,*S*)-Co(III)-Jacobsen catalyst yielding (*R*)-1,2-hexanediol and (*S*)-1,2-epoxyethane was accomplished successfully four times yielding conversions of *ca.* 80% with *ee*'s higher than 95% for the diol.

The reaction mixture was allowed to react for 30 h, then pressurized with N_2 until half of the reaction volume had permeated and subsequently recharged with fresh reactant solution. A slight decrease of conversion was attributed to an incomplete catalyst retention by the membrane and partial catalyst deactivation.

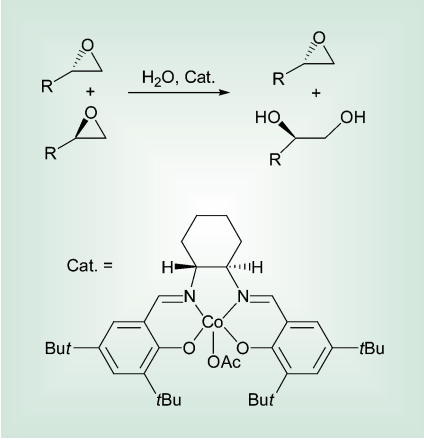

Green hydration of nitriles in water

The development of an efficient and intrinsically non-waste-producing catalytic hydration for the synthesis of amides from nitriles would be of great importance, since common methods for the hydration of nitriles generate large amounts of salts and also undesired by-products such as carboxylic acids. Mizuno and coworkers approached this problem by developing a $Ru(OH)_x/Al_2O_3$ catalyst that can be used in water as the solvent (*Angew. Chem.*, 2004, **126**, 1602–1605).

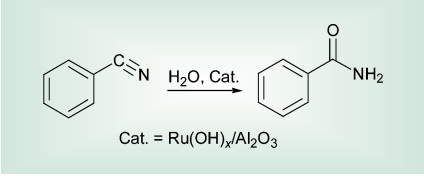

The hydration of benzonitrile was employed as test reaction. The $Ru(OH)_x/Al_2O_3$ catalyst yields benzamide at 413 K with more than 99% conversion and selectivity. The catalyst can be reused at least three times and the scope of nitriles usable turned out to be large (conversions and selectivities were in the 99% region for many nitriles). Workup is simply accomplished by filtration, and the filtrate, from which the products can be crystallized in analytically pure form by

cooling the mixture to 273 K, contains no ruthenium compounds (ICP-AES; detection limit 7 ppb) and is catalytically inactive.

Theoretical insights in reactions related to processes with potential for environmentally benign developments

Many natural or synthetic catalyzed reactions suffer from incomplete understanding of the reaction mechanism, which has important implications related to the academic and industrial evaluation of the practical and economical usefulness and environmental sustainability of these transformations. Computationally based investigations of the corresponding reaction mechanisms are nowadays a well established tool to help understand the underlying single microscopic steps of such chemical reactions and ultimately show clear trends for future developments. In this context a number of theoretical studies have recently contributed significantly to the mechanisms of some important reactions:

• Modeling of the **active site of acetyl-coenzyme A synthase** by Hall and coworkers from Texas A&M University.
• Understanding the role of ligands and substrates in **ruthenium metathesis** catalysts contributed by Chen and Adlhart from ETH Zürich.
• Investigation of the reasons for ***cis*-diole formation *versus* C–C bond cleavage in the presence of OsO_4 and RuO_4** catalysts by Frenking and coworkers from the University of Marburg.

Acetyl-coenzyme A synthase/carbon monoxide dehydrogenase is found in certain anaerobic chemoautotrophic bacteria, in which it synthesizes acetyl CoA from CO and CH_3^+. The active site was identified as a dinuclear metal complex with one nickel centre coordinated by two carboxyamido N and two cysteinyl S atoms and another metal atom (Ni, Cu or Zn) also coordinated by the same S atoms and the sulfur centre of an additional cysteinyl moiety.

Controversies have emerged about the nature of the second metal centre, the

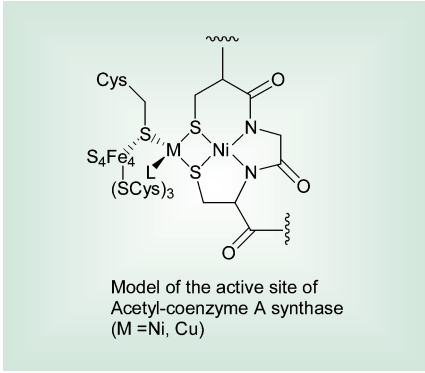

Model of the active site of Acetyl-coenzyme A synthase (M =Ni, Cu)

details of the reductive activation of the active site and other issues of the reaction. Hall and coworkers undertook density functional studies to elucidate these subjects (*J. Am. Chem. Soc.*, 2004, **126**, 3410–3411). According to their work the second metal centre could be identified as nickel (Zn could be excluded due to its acknowledged inactivity and Cu is energetically less favorable compared to Ni). Furthermore a bimetallic CO-insertion/CH_3-migration mechanism could be excluded and the authors favor a mechanism in which methylation occurs first and is followed by CO coordination. The CO-insertion/CH_3-migration then occurs on one metal centre and finally the addition of thiolate yields the thioester.

Olefin metathesis is a powerful method for the formation of carbon–carbon double bonds, which developed into a broadly applicable reaction with a scope ranging from bulk chemistry to the synthesis of natural products. Despite its versatility and usefulness, certain details of the reaction mechanism are still under investigation. One particular concern is the lack of understanding of the reactivity differences between the first and second generation catalysts.

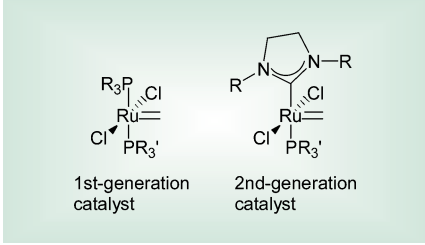

1st-generation catalyst 2nd-generation catalyst

Chen and Adlhart set out to clarify this and other open questions (*J. Am. Chem. Soc.*, 2004, **126**, 3496–3510): is the metallacyclobutane an intermediate or a transition state? Is the configuration of the halides *cis* or *trans* in the metallacyclobutane? Is the rate-limiting step the phosphane dissociation, the metallacyclobutane formation or the cycloreversion? One of the interesting answers they found is that in first generation ruthenium metathesis catalysts the rate-limiting step is metallacyclobutane formation, whereas with second generation catalysts it is the dissociation of one phosphane ligand.

Despite the elegant formation of *cis*-diols by OsO_4, which was established mainly by Sharpless *et al.*, RuO_4, which is neither explosive nor poisonous, cleaves

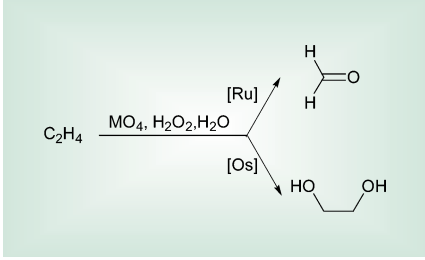

C–C double bonds in the presence of oxidants yielding carbonyl compounds.

This method of cleaving C–C bonds is advantageous over ozonolysis and chromium oxide cleavage. Frenking and coworkers undertook a detailed density functional study of the reaction between MO_4 (M = Os, Ru), ethylene and H_2O_2 to clarify this reactivity difference (*J. Am. Chem. Soc.*, 2004, **126**, 3642–3652). Among other differences between the two metal oxides they found that prior to C–C bond cleavage a second ethylene molecule reacts with relevant complexes, which after oxidation show significantly different activation energies for C–C bond cleavage: the corresponding Ru compound has a very low activation barrier of only 2.5 kcal mol^{-1}, whereas for the Os compound the activation barrier amounts to 18.9 kcal mol^{-1}, thus rendering this option unfeasible for the Os complex.

Sustainable Chemistry in Dessau – a workshop report

Klaus Günter Steinhäuser, Steffi Richter and Jutta Penning
Federal Environmental Agency Berlin

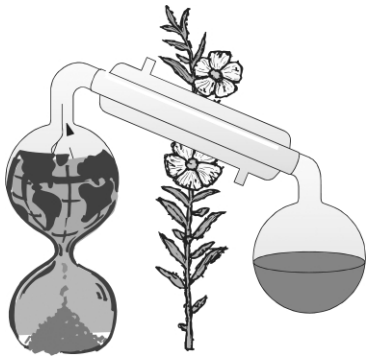

How can 150 experts from 14 countries be tempted into the small town of Dessau? The Federal Environmental Agency (UBA), in cooperation with the OECD, the Federal Institute for Occupational Health and Safety (BAuA) and the German Federal Ministry of Environment, Nature Conservation and Nuclear Safety (BMU), invited delegates to Saxony-Anhalt to discuss an unwieldy but nevertheless widely discussed issue – *Sustainable Chemistry.* Under the title "Sustainable Chemistry – Integrated Management of Chemicals, Products and Processes", a workshop was held from 27–29th January 2004, which provided scientists and experts from university, industry, environmental NGOs and authorities with a forum to discuss and reflect steps to put sustainable chemistry in more concrete terms. As part of the global programme of the OECD on sustainable chemistry, this workshop should focus on specific elements of sustainable chemistry, criteria and indicators, methods for evaluation and instruments for implementation. The workshop was not held in Dessau by accident. *Andreas Troge*, President of the UBA, said "The workshop will make a contribution to an economy that is competitive, dynamic, and based on knowledge. It is important to sustain the efficiency of chemical production as well as to safeguard the natural means of livelihood for future generations. Dessau is not only the future location of the UBA, it is also situated near a region which is a symbol for the transformation from a dirty to a resource-saving chemical production". *Ulrich Schlottmann* from the hosting Ministry (BMU) brought the title of the workshop into an international context. He recalled the World Summit for Sustainable Development in Johannesburg in 2002, aimed at minimization of significant negative impacts of chemicals on human health and environment by 2020. *Laurence Musset* from the OECD Environment Directorate stated, "Sustainable chemistry will raise the overall level of environmental protection and job and consumer safety" and highlighted the role of OECD as an engine for international chemical safety.

Introduction

At the beginning of the conference overarching views on the issue were presented. As the most prominent guest *Paul Anastas*, Science Advisor in the US Whitehouse and often called the "Father of Green Chemistry", fascinated participants with his vision of a change of chemistry from a "mature science" to one which faces new challenges questioning the "irrevocable" rules for chemical synthesis, such as the use of solvents which must later be evaporated or synthetic processes incorporating several steps that use protecting groups which must be removed at a later stage. Atom economy and consideration of structure–activity relationships may be key instruments in research and development. His 12 principles are widely approved as the basis for future "Green Chemistry" (P. T. Anastas and J. C. Warner, *Green Chemistry: Theory and Practice*, Oxford University Press, Oxford, 1998). He pleaded for voluntary and informatory measures including acceptance and application of the green chemistry principles rather than for legal requirements when making progress towards sustainability.

Jan van der Kolk from the Dutch Ministry of Environment agreed that progress can not be achieved by legislation alone. A sustainable chemistry needs cooperation with industry, which should take its responsibilities beyond legal requirements. In contrast, *Michael Warhurst* from WWF (UK) pointed out that a demanding legal framework is essential to induce industry to accept its responsibilities. *Klaus Steinhäuser* from UBA expressed his view that, in spite of the progress made during the last decades, sustainable chemistry is far from being already achieved. Further efforts are needed. It will be necessary to create win–win situations connecting economic and ecologic benefits and enhancing the competitiveness of the chemical industry.

As a common understanding it was emphasized that "Sustainable Chemistry" has to be implemented on a global scale and "dirty" productions cannot be exported to developing countries.

Chemicals in the environment and at workplaces

Today, discussing sustainable chemistry is not possible without mentioning REACH, the new chemicals policy of the European Community. *Reinhard Schulte-Braucks* from the EC-Commission, GD Enterprise, presented the contents of the current draft of the regulation. *Utz Tillmann* from the European Association of Chemical Industry (CEFIC) expressed his view that REACH is not balanced between economic, ecologic and social demands. He predicted that many chemicals will vanish from the market, resulting in a decrease of innovations for greater sustainability. *Patricia Cameron* from BUND, a German environmental NGO,

DOI:10.1039/b404170b

contradicted this view and asked for a necessary change to a policy of consequent substitution of hazardous chemicals. An interesting contribution came from *Joel Tickner* from the University of Massachusetts Lowell (USA), who explained the great interest in the USA in the European efforts to make progress in the safety of chemicals through REACH and – based upon American experience – argued for simple and practicable tools to set priorities and choose sustainable alternatives.

However, will REACH guarantee that only sustainable chemicals are produced and used? Experts for occupational safety said 'no' to this question and pointed out that small and medium enterprises do not have the capability to cope with all the requirements for safe handling of dangerous substances. *Norbert Kluger* from the German Bau-Berufsgenossenschaft presented the information system GISBAU giving downstream users data for safe handling, on substitute products and procedures beyond safety data sheets whereas *Herbert Bender* from BASF highlighted the efforts of big chemical manufacturers to inform their customers comprehensively. A tiered approach was presented by *Rolf Packroff* from the BAuA derived from classification and labeling and aiming at a hierarchy of management options. This model defines categories of chemicals, named as "inherently safe", "safe-to-apply" or "use-supported" chemicals. Some examples from representatives of industry underlined the usefulness of such an approach: *Philippe Class* (Thermal Ceramics, F – biosoluble mineral fibres), *Friedrich Sosna* (Degussa, D – polymeric disinfectants), *Bernd Burchardt* (SIKA, CH – adhesives) and *Gerald Altnau* (Invista, D – dibasic esters as solvents). Sosna and Burchardt emphasized that extensive legal requirements may prevent development and marketing of innovative products.

For environmental protection purposes it may also be possible to derive criteria for the inherent safety of chemicals, delegates concluded, but it cannot be based on classification and labeling. *Leena Ylä-Mononen* from the EC-Commission, GD Environment, presented characteristics which sustainable chemicals should not exhibit: **P**ersistence, **B**ioaccumulation potential and **T**oxicity (PBT). *Martin Scheringer* from the ETH Zürich explained his approach of short-range chemicals which do not remain in the environment for longer periods and are not distributed over long ranges, thus protecting future generations from unknown risks.

The debate on the topic whether legal requirements are necessary to substitute hazardous chemicals was controversial. *Alf Lundgren* from the Swedish National Chemicals Inspectorate (KEMI) stated that Sweden intends to do more than REACH requires. Others in the auditorium stated that substitution should only be a matter of self-responsibility of producers and industrial downstream users governed by market forces. *Andreas Ahrens* from the Institute of Political Ecology (Ökopol) pointed out that this approach will work only if professional and private users are informed about the risks of chemicals and their alternatives to enable them to choose less dangerous alternatives. An efficient flow of information will be a crucial point for functioning of the new European chemicals policy.

Summarizing this session it was concluded that a clear and demanding legal framework should be assisted by voluntary initiatives, programmes for funding and information measures.

Production and processing

Experts agreed that sustainable processes are signified by:

- reduced resource demand,
- reduced energy consumption,
- minimization of waste and releases to water and air,
- reduced amounts of chemicals and elimination of auxiliaries, in particular hazardous ones,
- increase of selectivity, atom economy,
- elimination/minimization of unintended by-products,
- inherent safety of processes regarding accidents.

Jürgen Metzger from the University of Oldenburg discussed the shift of feedstocks used in chemical production towards renewables as an element of sustainable chemistry. Currently only 8% of chemical production is based on renewables; in the USA a share of 25% shall be achieved by 2030.

Peter Eder from the EU Joint Research Centre in Sevilla presented a study on new innovative processes for chemicals production and processing highlighting that new synthetic pathways using heterogeneous catalysis or biotechnology are of great potential. *Chris Adams* from the Institute of Applied Catalysis (UK), *Matthias Beller* from the University of Rostock and *Georg Markowz* from Degussa presented catalysis, alternative solvents (*e.g.* ionic liquids) and microprocessing as key technologies for achieving progress.

However, why are these new sustainable technologies not introduced much faster, especially since they are economically feasible in most cases? Not having a comprehensive answer, experts felt that high starting investments tend to be avoided whereas time-to-market aspects are most decisive for implementing innovative chemical production processes. A "quick and dirty" approach in order to meet the need for short times to market may conflict with a sound, but time consuming integrated approach. Further obstacles are a lack of knowledge on new techniques and often low readiness for cooperation of most chemists working in classical chemical synthesis. What is needed are guidelines considering sustainability aspects to speed up implementation, a sphere of activity for consultants. *Malcolm Wilkinson* (Crystal Faraday Partnership, UK) underscored this by presenting his "Sustainable Manufacturing Protocol". There is a need for a sound strategy to get to know these new approaches and to overcome the cultural impediments of classical chemistry.

Products

An Integrated Product Policy (IPP) is needed as a frame for sustainable products, experts reiterated in this session. *Natalie Eckelt* from German BUND explained that IPP makes efforts to enhance the market share of sustainable products and called for minimum standards for sustainable products. For this reason, the entire life cycle of the products needs to be reflected from the 'cradle to the grave'. *Rainer Griesshammer* from Eco Institute and *Walter Klöpffer* from LCA Consult & Review confirmed this through their presentations on Substance Flow Management and Lifecycle Assessment (LCA). In the process of evaluation, economic, ecologic and social aspects have to be taken into consideration. All participants of the value chain should be involved, as is realized in Denmark through the so-called 'product panels' described by *Preben Kristensen* from the Danish Toxicology Centre. An impressive and successful example of a dialogue-oriented approach was demonstrated by *Hans-Jürgen Klüppel* (Henkel) who explained a project in the detergent industry for sustainable washing, also involving private consumer organizations. Last, but not least, an important part of IPP is management-oriented service concepts, such as "Chemical leasing", presented by *Barbara Perthen-Palmisano* from the Austrian Environment Ministry and *Thomas May* from DuPont who stated that these approaches may reduce costs and use of chemicals.

Implementation

Finally the discussion was focused upon how sustainable chemistry can be put in concrete terms and implemented. *Dirk*

Bunke from Eco-Institute and *Arseen Seys* from EuroChlor presented indicators for sustainable chemistry which are developed to measure progress towards sustainability and to set targets to be applied by authorities and enterprises. Regarding several aspects the chlorine industry can demonstrate significant progress.

Which are the main obstacles that prevent innovation and substitution? Which means are appropriate to foster sustainable chemistry? *Armin von Gleich* from the University of Bremen asked these questions and stated that the inertia of the system, the complexity and non-predictability of the results of severe changes are the most important impediments. He pleaded for smooth changes and mentioned market forces, a critical public, an effective information network throughout the supply chain and liability requirements as the main drivers in a demand driven economy. In every case it is necessary to deal with uncertainty in such a manner that gaps in knowledge should not prevent risk management. *Martin Führ* from the University of Darmstadt discussed the role of the regulatory and institutional framework, which may be an obstacle or a target-setter, and reminded that the behavioural habits and perceptions of all people involved should be considered when deciding on measures.

Bernd Jastorff from the University of Bremen convinced the participants that fundamental changes in the education of chemists and neighbouring scientists are necessary if aiming at the implementation of thinking and acting in sustainability terms. This includes *e.g.* reflection of the relationship between structure and activity, planning of synthetic pathways by avoidance of unnecessary steps, avoidance of hazardous components and by-products, atom economy. By this, he closed the loop

to the beginning lecture given by Paul Anastas.

Finally, *Hans Jochen Luhmann* from the Wuppertal Institute reflected upon why men often close their eyes, perceiving scientific findings on risks only with great delay after they have been published.

Final impression

Many participants left their impression that the three days of intensive discussion and dialogue should be the starting point for the development of a network and asked the organizers to continue work on this issue. The social events, with visits in the Hugo Junckers museum and the 'Bauhaus', helped people to perceive themselves as a community thinking in the same direction. The report of the workshop will be published at http://www.sustainable-chemistry.com.

TUTORIAL REVIEW

www.rsc.org/greenchem

"Green" amino acid-based surfactants

Ma Carmen Morán,[a] Aurora Pinazo,[a] Lourdes Pérez,[a] Pere Clapés,[a] Marta Angelet,[a] Ma Teresa García,[a] Ma Pilar Vinardell[b] and Ma Rosa Infante*[a]

[a] *Instituto de Investigaciones Químicas y Ambientales de Barcelona-C.S.I.C., Jordi Girona 18-26, 08034 Barcelona, Spain. E-mail: rimste@cid.csic.es; Fax: +34 932045904; Tel: +34 934006 100*

[b] *Facultad de Farmacia, Universidad de Barcelona, Unidad Asociada de Investigacion del CSIC, Avd. Juan XXIII s/n. Edificio B 3ª planta, 08028 Barcelona, Spain; Fax: +34 934035901; Tel: +34 934024505*

Received 9th January 2004, Accepted 8th March 2004
First published as an Advance Article on the web 26th March 2004

The value of amino acids and vegetable oil derivatives as raw materials for the preparation of surfactants was recognized as soon as they were discovered early in the last century. Amino acid-based surfactants, which have an amino acid residue as a hydrophilic moiety, are reviewed with respect to their synthesis, properties and some applications. The review covers three main categories of amino acid-based surfactants: N^{α}-acyl, *N*-alkyl amide and *O*-alkyl ester derivatives among the linear or single chain amino acid-based surfactants; N^{α}, N^{ω}-bis(N^{α}-acylarginine)α,ω-alkylendiamides, which are *gemini* amino acid-based surfactants; and 1-monoacyl-*rac*-glycero-3-*O*-(N^{α}-acetyl-L-amino acid) and 1,2-diacyl-*rac*-glycero-3-*O*-(N^{α}-acetyl-L-amino acid), both amino acid-based surfactants with glycerolipid-like structures.

1 Introduction

Surfactants are one of the most representative chemical products, which are consumed in large quantities every day on a worldwide scale. Since it is known that surface-active compounds can adversely affect the aquatic environment, the biodegradability and biocompatibility of surfactants have become almost as important as their functional performance to the consumer. Because of this, there is a pressing need for development of efficient novel surfactants that are biodegradable and biocompatible.[1]

Surfactants of this kind can be obtained by designing molecules that mimic natural amphiphilic structures, *e.g.* phospholipids,[2] N^{α}-acyl amino acids[3] and alkyl-glucosides.[4] Surfactant molecules from renewable raw materials that mimic natural lipoamino acids are one of the preferred choices for food, pharmaceutical and cosmetic applications. Given their natural and simple structure they show low toxicity and quick biodegradation.[5] They can be produced by biotechnological and chemical methods using renewable raw materials such as amino acids and vegetable oils.[6–12] The value of amino acids as raw materials for the preparation of surfactants was recognized as soon as they were discovered early in the last century.[13] Initially they were used as preservatives for medical and cosmetic applications. Moreover, they were found to be active against various disease-causing bacteria, tumors, and viruses.[14–16] The combination of polar amino acids/peptides (hydrophilic moiety) and non-polar long chain compounds (hydrophobic moiety) for building up the amphiphilic structure has produced molecules with high surface activity. There is a large variety of amino acid/peptide structures. Moreover, the fatty acid chains can vary in their structure, length and number. These facts explain their wide structural diversity and different physicochemical and biological properties.[5,10,17,18]

The amino acid or peptide moiety determines the main differences of adsorption, aggregation and biological activity between the amino acid/peptide-based surfactants. Hence, cationic, anionic, non-ionic and amphoteric surfactants can be obtained depending on the free functional groups. Further modification of these groups allows a fine-tuning of their properties to meet almost every particular application.

The amino acids and long aliphatic chains can be combined with each other to generate three main structures (Scheme 1) of amino acid-based surfactants namely linear or single chain **1**, dimeric or *gemini* **2** and glycerolipid-like structures **3**. Linear structures **1**

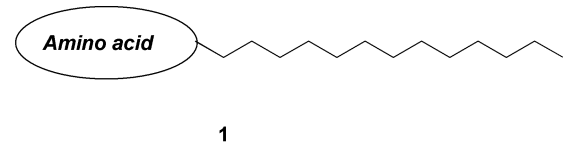

1

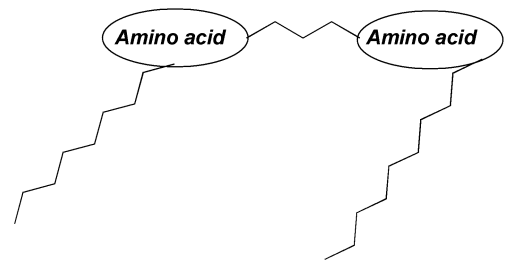

2

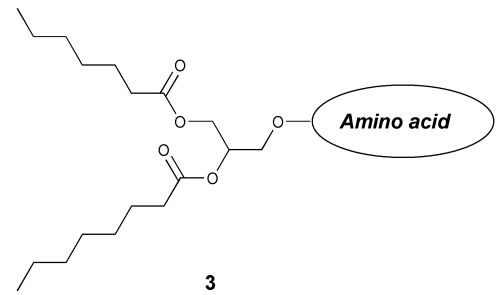

3

Scheme 1 Structures of amino acid-based surfactants: (**1**) Linear or single chain, (**2**) Dimeric or *Gemini* and (3) Glycerolipid-like structures. The amino acid constitutes the polar head of the surfactant. The hydrocarbon alkyl chain constitutes the hydrophobic moiety.

DOI: 10.1039/b400293h

consist of an amino acid bearing at least one hydrophobic tail. *Gemini* or dimeric are amphipathic structures **2** with two polar heads (*i.e.* two amino acids) and two hydrophobic tails per molecule separated by a covalently bonded spacer. Glycerolipid-like structures **3** can be considered analogues of mono-, diglycerides and phospholipids, and consist of one polar head and one or two hydrophobic moieties linked together through a glycerol skeleton.

This review is concerned with the preparation and the structure–activity relationship studies of amino acid-based surfactants of single chain, double chain *gemini* and glycerolipid-like structures for adsorption, self-assembling, and biological properties.

2 Single chain amino acid/peptide surfactants

2.1 Synthesis

Acidic, basic, or neutral amino acids such as aspartic acid, glutamic acid, arginina, alanine, glycine, leucine, proline, serine, and protein hydrolysates have been used as starting materials to synthesize single chain amino acid surfactants commercially and experimentally.[10]

Amino acids are linked to long aliphatic chains through the α-amino, α-COOH or side chain groups (Scheme 2).

Thus, fatty acids or alkyl halides can react with amino groups yielding the corresponding *N*-acyl and *N*-alkyl derivatives (Scheme 2, compounds **1** and **2**), respectively. Alternatively, the carboxyl group of the amino acid can be condensed with alkyl amines or aliphatic alcohols to give *N*-alkyl amides and esters (Scheme 2, compounds **3** and **4**, respectively).

Among the different types of linkages between the long aliphatic chain and the amino acid, the *N*-acyl (Scheme 3, series 1), *N*-alkyl amides (Scheme 3, series 2) and *O*- alkyl esters (Scheme 3, series 3) of arginine have attracted much interest in our group due to their low toxicity and high biodegradability in combination with their antimicrobial activity.[19–25]

The *N*-acylation of the amino terminal arginine (series 1) was prepared by condensation of fatty acids to arginine methyl ester hydrochloride using classical chemical methods.[5] The application of biotechnological procedures was not efficient for these compounds.[25] Series 2 was at first prepared by chemical procedures,[23] however papain from *Carica papaya* latex was found to be a suitable catalyst for the formation of amide (series 2) and ester bonds (series 3) between Cbz–Arg–OMe and various long chain alkyl amines and fatty alcohols.[24] In all cases, papain deposited onto polyamide was found to be the best biocatalyst configuration. The preparation of arginine alkyl esters was carried out in solvent free systems using the same alcohol reagent. Both series were enzymatically synthesized at multigram scale with a purity higher than 99%.

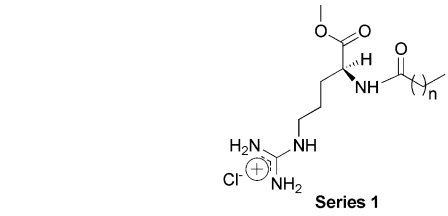

N^{α}-acyl-Arginine-methyl ester hydrochloride

CAM: n= 8
LAM: n= 10
MAM: n= 12
PAM: n= 14

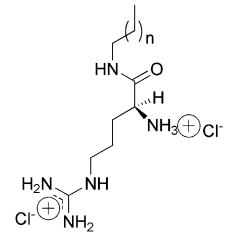

Arginine-N-alkyl amide dihydrochloride

ACA: n= 8
ALA: n= 10
AMA: n= 12

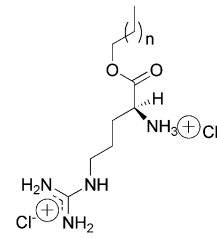

Arginine-O-alkyl ester dihydrochloride

AOE: n= 6
ACE: n= 8
ALE: n= 10

Scheme 3 Chemical structure of single chain arginine-based cationic surfactants.

N-Alkyl amide and ester derivatives of N^{α}-protected amino acids have also been prepared by lipases. In a study carried out with *Candida antarctica* and *Rhizomucor miehei* lipases, it was found that these enzymes could readily catalyse the condensation of a number of N^{α}-Cbz-amino acids with α,ω-alkyldiamines or fatty alcohols.[26]

N-Alkyl amide and side chain-substituted lipoamino acids have also been prepared by proteases and lipases. It was found that these enzymes could readily catalyse the condensation of a number of amino acids with fatty acids and triglycerides.[27]

2.2 Properties

Our group has reported that long chain N^{α}-acyl arginine methyl ester compounds (series 1 Scheme 3) are cationic surfactants with a satisfactory toxicity profile, high biodegradability and a surface activity comparable to that of conventional long chain quaternary ammonium salts. We have demonstrated that the morphology of

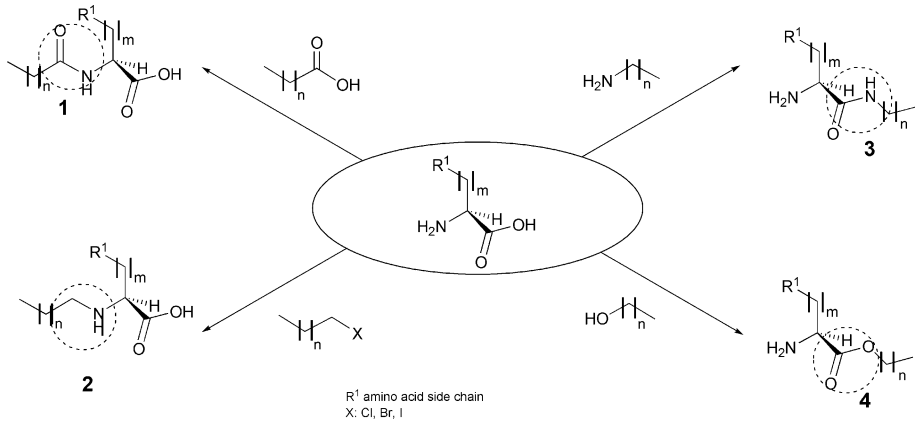

Scheme 2 Different types of linkages between an amino acid and a hydrophobic alkyl chain: acyl bond derivatives (**1**), alkyl bond derivatives (**2**), amide bond derivatives (**3**) and ester bond derivatives (**4**).

their micelle aggregates and lyotropic phases depends on the hydrophobic moiety, temperature, composition and electrolyte content in the system. As a result, we have found that compounds of series 1 show a rich and unusual phase behavior.[28–30] For instance, reversed vesicles (dispersion of lamellar liquid crystals in non-polar media) with biocompatible properties occurred in the lecithin-LAM–squalane system.[31] The PAM homologue was the only compound that showed lamellar lyotropic liquid crystals in the binary water–surfactant system.[30] These properties make them good alternatives for a wide range of industrial applications in the personal care, pharmaceutical and food sectors as well as in the design and synthesis of biomaterials. Furthermore, the arginine residue gives antimicrobial activity to the amphipathic molecule, a valuable property for a biocompatible surfactant.[32]

Compared to series 1, the series 2 and 3 compounds (Scheme 3) have two positive charged groups in the hydrophilic moiety, one in the primary amine and a second in the guanidine function. From the surface tension/concentration curves at 25 °C the critical micelle concentration (CMC) which is associated with the hydrophobicity of the molecule, the maximum surface excess concentration at the air–aqueous solution interface (Γ_m) and the area per molecule whose value indicates the minimum area per surfactant molecule at the air–aqueous solution interface (A_{min}) were calculated. Table 1

Table 1 Surface active properties of single chain surfactants from arginine at 25 °C[27–29,39]

Compound	γ_{cmc}[a]/ 10^{-3} N m^{-1}	CMC[b]/ 10^{-3} mol dm^{-3}	Γ_m[c]/ 10^{14} mol m^{-2}	A_{min}[d]/ 10^2 nm^2
CAM[e]	40	16		
LAM[e]	32	5.8		67
MAM[e]	32	2		62
ACA[f]	35	26	1.79	62
ALA[f]	37	1.8	1.24	90
AMA[f]	33	0.7	0.97	114
AOE[g]	35	38	1.15	96
ACE[g]	34	13	1.54	72
ALE[g]	30	5	0.91	122

[a] Surface tension at the critical micelle concentration. [b] Critical micelle concentration. [c] Maximum surface excess concentration at the air–aqueous solution interface. [d] Minimum area per surfactant molecule at the air–aqueous solution interface. [e] Compounds of series 1 (Scheme 3). [f] Compounds of series 2 (Scheme 3). [g] Compounds of series 3 (Scheme 3).

summarizes the surface parameters of the three series of compounds using the Gibbs adsorption equation.[33] In all cases they have the ability to decrease the surface tension of water until a constant value is reached, γ_{CMC}, and show a clear CMC in the surface tension–log C curves in the millimolar range. This indicates that they can be classified as surfactants with a surface activity similar to that of conventional cationic ones. Table 1 shows that the CMC depends on the straight alkyl chain and the nature of the hydrophilic moiety. For the three series of surfactants, the larger the number of methylene groups in the alkyl chain the lower the CMC, as would be expected from the increase in the hydrophobic character of the molecule. The smaller the A_{min}, the more effective its adsorption at the interfaces. We found that the A_{min} values for series 2 and 3 (62–114 $\times$ 10^{-2} nm^2 and 96–122 $\times$ 10^{-2} nm^2, respectively) were higher than that for series 1 with the same alkyl chain length (67 and 62 $\times$ 10 nm^2). This result indicates that the new molecules are less packed at the interface than those of series 1. The two charged groups in series 2 and 3 tend to spread themselves out on the interface due to an increase in the inter–intramolecular electrostatic repulsion forces.

One important milestone in our research is the design and development of new amino acid-based surfactants with antimicrobial properties, which mimic natural amphiphilic cationic peptides.[21,34] To this end, Lys and Arg derivatives of long chain N^{α}-acyl, COO-ester and *N*-alkyl amide have been prepared. In particular, the N^{α}-acyl arginine methyl ester derivatives series 1 (Scheme 3) have turned out to be an important class of cationic surface active compounds with a wide bactericidal activity, high biodegradability and low toxicity profile. The antimicrobial activities were determined *in vitro* on the basis of the minimum inhibitory concentration (MIC) values, defined as the lowest concentration of antimicrobial agent which inhibits the development of visible growth after 24 h of incubation at 37 °C. We have shown that essential structural factors for their antimicrobial activity include both the length of the fatty residue (akin with their solubility and surface activity) and the presence of the protonated guanidine function.[34,35] Amphoteric lipopeptide surfactants with antimicrobial activity comparable to those of LAM were found when neutral Gly or Phe amino acids were condensed to the N^{α}-lauroyl arginine.[10] More interestingly, condensation of a N^{α}-acyl-arginine residue to an acid-hydrolyzed collagen gave rise to a family of amphoteric protein-based surfactants with antimicrobial activity, the homologue of C_{14} carbon atoms being the most active.[10] The activity of all these amphoteric N^{α}-acyl arginine surfactants could be due to the presence of the long chain N^{α}-acyl-arginine residue and to the absence of intramolecular ionic interactions in the molecule. The free guanidine group together with the surface activity of these compounds could interact with the polyanionic components of the cell surface triggering the biocide mechanisms of these surfactants. In accordance with Ferguson's principle,[36] the antimicrobial activity might be related to the combination of several physicochemical properties such as surface activity, adsorption and solubility.

The ultimate biodegradability[37] measurements for the three series of arginine-based cationic surfactants showed that all homologues (except AMA) can be considered biodegradable.[38] Interestingly, using ester type bonds (series 3, Scheme 3) to link the hydrophobic and hydrophilic moieties accelerates their biodegradation considerably. This fact has also been described for sugar-based surfactants.[39]

The haemolytic activity, HC_{50}, which is the concentration of surfactant that causes 50% of haemolysis of red blood cells from healthy human donors[40] and the HC_{50}/D ratio, where D is the haemoglobin denaturising index, are the parameters commonly measured for evaluating the potential toxicity of the surfactants. The HC_{50}/D or L/D is used for predicting the potential ocular irritation relative to sodium dodecyl sulfate (SDS) (L/D_{SDS}: 0.44; irritant). The values of HC_{50} for series 1, 2 and 3 (Scheme 3) demonstrated that these compounds can be considered non-haemolysing agents (HC_{50} < 1000 μg mL^{-1}). For comparison's sake, commercial cationic surfactants have HC_{50} ranging from 4 to 15 μg mL^{-1}. Furthermore, according to the results of the L/D ratio first and by the *in vivo* eye irritation Draize test later, these linear arginine-based surfactants have no irritant effect on the eyes (non eye-irritants, L/D > 100).[40]

2.3 Applications

The application of synthetic acyl amino acid/peptide vesicles as drug carriers as well as for the preparation of functional liposomes with lipopeptide ligands have been examined by several authors in recent years.[41,42] Vesicles of long aliphatic chain N^{α} acyl amino acids showed encapsulation efficiencies for solutes comparable to that of conventional liposomes of lecithin. Recently, a new technology has emerged for the transfer of foreign DNA into cells forming non-toxic hydrophobic ion-paired complexes between long chain arginine alkyl esters (Scheme 3 series 3) with DNA.[43]

Lipoamino acids are also particularly attractive as antiviral agents. Certain acyl amino acid derivatives have been found to produce inhibition on influenza neuraminidase.[44] A number of N^{α}-palmitoylated amino acids/peptides have been incorporated into model membranes affecting the transition temperature between the

bilayer to hexagonal aggregation, a property associated with antiviral activity against the Cantell strain of the Sendai virus (parainfluenza type 1).[45]

Polymeric amino acid-based surfactants for enantiomeric separations using capillary electrokinetic chromatography (EKC) has been reported in the bibliography.[46–48] The effect of the position and number of chiral centers, amino acid order and steric effects have been evaluated.[48]

3 Amino acid-based *gemini* surfactants

Gemini surfactants are a novel class of amphipathic compounds consisting of two hydrophilic and two hydrophobic groups per molecule linked through a spacer chain. These molecules can be considered dimers of the single chain conventional surfactants of one hydrophilic and one hydrophobic group. Their interest lies in the number of unexpected surface activity properties, which make them superior to the conventional surfactants. These molecules show extremely low CMC (CMC, a fundamental parameter of surfactants close related to their hydrophobicity), solubilizing, wetting, foaming, antimicrobial and lime soap dispersion properties.[49–56]

3.1 Synthesis

In the past 15 years, many different types of *gemini* surfactants have been synthesized.[57] Reviews concerning the synthesis and structures of *gemini* surfactants have been published.[58–61]

A number of surfactant structures with a variety of hydrophilic head groups and hydrophobic tails of different chain lengths have been reported in an effort to increase their surface-active properties.[62–66] Several papers have been published addressing the synthesis and properties of a new type of bifunctional amphiphilic cationic compounds with an effective surfactant and antimicrobial behaviour of the *gemini* type called bis quaternary ammonium halide surfactants, or bis(Quats).[67] These are double-headed surfactants in which two alkyldimethyl quaternary ammonium groups per molecule are linked by a hydrocarbon spacer chain. Owing to their extraordinary activity, they are regarded as an outstanding new generation of cationic surfactants with excellent performance with regard to solubilization, soil cleaning, and oil recovery. However, they are very stable molecules with a questionable chemical and biological degradability.[68]

A strategy to reduce the environmental impact and potential toxicity is to build up *gemini* structures from environmentally friendly single chain arginine-based surfactants. To this end, our group has chemically synthesized and studied a new class of *gemini* cationic surfactants derived from the arginine: the N^{α},N^{ω}-bis(N^{α}-acylarginine)α,ω-alkylendiamides or bis(Args).[25,69–73] These compounds consist of two symmetrical long chain N^{α}-acyl-L-arginine residues of twelve N^{α},N^{ω}-bis(N$^{\alpha}$-lauroylarginine)α,ω-alkylendiamides [$C_n(LA)_2$ series], and ten carbons atoms, N^{α},N^{ω}-bis(N$^{\alpha}$-caproylarginine)α,ω-alkylendiamides [$C_n(CA)_2$ series], linked by amide bonds to an α,ω-alkylenediamine spacer chain of varying length (n = 2–10) (Scheme 4). This particular alkylenediamine spacer chain was chosen to control the distance between the charged sites of the molecule which modify the inter- and intra-hydrophilic–hydrophobic interactions. The bis(Args) were investigated in an attempt to develop a new class of environmentally friendly amino acid-based surfactants with surface activity exceeding that of CAM and LAM, and with at least the same antimicrobial, toxicity and biodegradability properties.

Recently a series of bis(Args) have been prepared at multigram scale by a chemoenzymatic approach using papain deposited onto Celite for the best results[70,74] (Scheme 4 right).

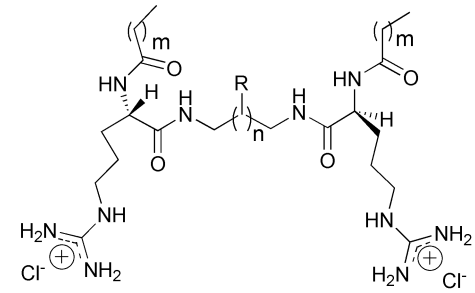

$C_3(OA)_2$: m=6; n=1; R= H
$C_2(CA)_2$: m=8; n=0; R=H
$C_3(CA)_2$: m=8; n=1; R=H
$C_4(CA)_2$: m=8; n=2; R=H
$C_6(CA)_2$: m=8; n=4; R=H
$C_9(CA)_2$: m=8; n=7; R=H
$C_{10}(CA)_2$: m=8; n=8; R=H
$C_2LA)_2$: m=10; n=0; R=H
$C_3(LA)_2$: m=10; n=1; R=H
$C_4(LA)_2$: m=10; n=2; R=H
$C_6(LA)_2$: m=10; n=4; R=H
$C_9(LA)_2$: m=10; n=7; R=H
$C_{10}(LA)_2$: m=10; n=8; R=H

$C_3(OA)_2$: m=6, n=1, R: H
$C_3(CA)_2$: m=8, n=1, R: H
$C_3(LA)_2$: m=10, n=1, R: H
$C_3OH(LA)_2$: m=10, n=1, R: OH
$C_6(CA)_2$: m=8, n=4, R: H
$C_9(CA)_2$: m=8, n=7, R: H

Scheme 4 Structures of bis(Args) *gemini* cationic surfactants prepared by chemical procedures (left) and chemo-enzymatic procedures (right).

3.2 Properties

In the light of our studies, most *gemini* surfactant properties are superior to the corresponding conventional monomeric surfactants. They were found to be more efficient surface active molecules than the single chain structures: Their CMC are at least one order of magnitude lower than that of the corresponding monomeric surfactants[71] and they are 10–100 times more efficient at reducing the surface tension of water and in foam stability.[75]

To establish the effect of the dimerization on the antimicrobial activity as well as the influence of the alkyl and the spacer chain length of bis(Args), the evaluation of *in vivo* membrane-disrupting properties was made using cell bacteria as biological membranes. The dilution antimicrobial susceptibility test was carried out and the minimum inhibitory concentration (MIC) values were determined. Bis(Args) exhibited a broad spectrum of preservation capacity at MIC values in the range from 4 to 125 μg mL^{-1}.[69] The dimerization enhanced the antimicrobial activity for the *gemini* $C_n(CA)_2$ compared with CAM. Given the peculiar structure of bis(Args), the compounds of the $C_n(CA)_2$ series have a hydrophobicity which is more than twice the hydrophobicity of CAM. However, the presence of two ionic arginine groups in one molecule of $C_n(CA)_2$ can make a positive contribution to the degree of the hydration of this series, showing a water-solubility similar to that of CAM. These two characteristics in the molecule can result in a more effective adsorption and diffusion of $C_n(CA)_2$ on the cell interface, resulting in an antimicrobial action at lower concentrations.

Bearing in mind that biological membranes are essentially nonpolar interfaces, evidence exists that the toxicity of surfactants against the aquatic species tested is caused by the ability of the monomers to disrupt the integral membrane by a hydrophobic/ionic adsorption phenomenon at the cell membrane–water interface in a similar way to that of the antimicrobial mode action. Acute toxicity tests on freshwater crustacea (*Daphnia magna*), a very sensitive invertebrate,[76] as well as on saltwater bacteria (*Photobacterium phosphoreum*)[77] were carried out to assess the aquatic toxicity. These standard tests represent two of the trophic levels which can be exposed to the cationic surfactants. Concentration values that cause inmobilization in 50% of the Daphnia after 24 hours exposure (IC_{50}) and 50% reduction in the light emitted by the bacteria after 30 minutes exposure (EC_{50}) were determined. Values of IC_{50} and EC_{50} for the bis(Args) together with those of LAM and CAM are summarised in Table 2.[78] Values reported for two series of

Table 2 Aquatic toxicity values of $C_n(LA)_2$, $C_n(CA)_2$ series and CAM, LAM, DTAB and HTAB.[77]

	Daphnia magna IC_{50}[a]/mg L^{-1}		*Photobacterium phosphoreum* EC_{50}[b]/mg L^{-1}	
Compounds	mean	95% confidence range	mean	95% confidence range
$C_2(LA)_2$	4.4	(3.5–5.3)	28	(18–43)
$C_3(LA)_2$	2.1	(1.8–2.4)	2.4	(2.2–2.7)
$C_4(LA)_2$	4.6	(3.9–5.2)	5.8	(4.3–8.0)
$C_6(LA)_2$	2.4	(1.9–2.5)	3.0	(2.0–4.5)
$C_9(LA)_2$	2.2	(1.9–2.5)	13	(10–17)
$C_{10}(LA)_2$	16	(11–20)	20	(15–28)
LAM	15	(12–18)	12	(10–14)
DTAB	0.38	(0.36–0.40)	0.24	(0.20–0.30)
HTAB	0.13	(0.11–0.15)	0.63	(0.40–0.98)
$C_2(CA)_2$	16	(11–20)	1.5	(1.2–1.9)
$C_3(CA)_2$	16	(11–20)	1.1	(0.5–2.1)
$C_4(CA)_2$	12	(7–17)	0.9	(0.4–2.2)
$C_6(CA)_2$	15	(11–19)	1.3	(0.3–5.6)
$C_9(CA)_2$	5.5	(2.7–8.2)	1.1	(0.7–1.7)
$C_{10}(CA)_2$	7.5	(5.0–10)	2.7	(1.2–5.8)
CAM	77	(56–98)	4.0	(3.1–5.3)

[a] Concentration values that cause 50% inhibition in the crustacean mobility after 24 h of exposure. [b] Concentration values that cause 50% reduction in the light emitted by the bacteria after 30 min of exposure.

conventional mono(Quats) dodecyltriammonium bromide (DTAB) and hexadecyltriammonium bromide (HTAB) are also indicated. When increasing the hydrophobicity of the molecule, the acute toxicity raised for each series of surfactants is in agreement with their CMC values, Table 3. Thus, $C_n(CA)_2$ were less toxic than the

Table 3 CMC values (g L^{-1}) and HC_{50} (mg L^{-1}) of CAM, LAM and bis(Args) homologues on human red blood cells.[77]

Compound	CMC[a]/g L^{-1}	HC_{50}[b]/mg L^{-1}
CAM	6.05	38.5
$C_3(CA)_2$	1.53	110.5
$C_6(CA)_2$	1.29	9.0
$C_9(CA)_2$	9.35	8.7
LAM	2.44	20.8
$C_3(LA)_2$	4.60	80.7
$C_3(OH)(LA)_2$	5.89	> 200
$C_3(OA)_2$	49.77	> 200

[a] Critical micelle concentration. [b] Hemolysis value.

$C_n(LA)_2$ compounds due to their lower hydrophobic character. Interestingly, IC_{50} values for $C_n(CA)_2$ compounds were similar to that of LAM. Furthermore, all of them were one order of magnitude less toxic than the conventional mono(Quats).

Due to the complexity and hydrophobicity of the *gemini* compared with the single chain structures, the biodegradation rate of single chain structures such as LAM (90% in 14 days), was higher than that of the bis(Args) (50–90% in 14 days). The biodegradation rate of bis(Args) decreased when both the spacer chain and the alkyl chain length increased. Hence, the higher the hydrophobicity of the surfactants the lower their biodegradation rate[78].

The haemolysis test showed again that the highest HC_{50} values were obtained for the compounds with the highest hydrophobic character, namely, those with the longest alkyl and spacer chain lengths. There is considerable difference between the HC_{50} of these new *gemini* surfactants and those bearing a quaternary ammonium group at the polar head. MonoQuats have HC_{50} values between 0.05 and 0.1 μg m^{-1}. The introduction of a hydroxyl function to the spacer chain make the compound more hydrophilic, in consequence the CMC increases and the HC_{50} increases.

Dimerization of LAM and CAM yields environmentally friendly antimicrobial *gemini* surfactants with lower hemolytic activity, aquatic toxicity and efficient surface activity than other cationic surfactants, (*i.e.* monoQuats). The increase of hydrophobicity of these molecules is a negative structural parameter for their environmental behaviour.

3.3 Applications

Gene therapy is an important topic in life science. It depends on effective techniques for safe introduction of the selected gene into living cells. Recently, *Gemini* surfactants have been found to be particularly promising as potential vehicles for the transport of bioactive molecules. Lysine and 2,4-diaminobutyric acid form polycationic *gemini* surfactants, by relatively simple synthesis using standard peptide chemistry.[79,80] These polycationic *gemini* surfactants and spermine-based *gemini* surfactants are attracting much attention as efficient agents in gene delivery.[81–86]

4 Amino acid glyceride conjugates

4.1 Synthesis

Amino acid glyceride conjugates (*i.e.* glycero amino acids) constitute a novel class of lipoamino acids, which can be considered analogues of mono and diacylglycerides and phospholipids (1 and 2 Scheme 5). They consist of one or two aliphatic chains and one amino acid, as the polar head, linked together through ester bonds in the glycerol backbone.

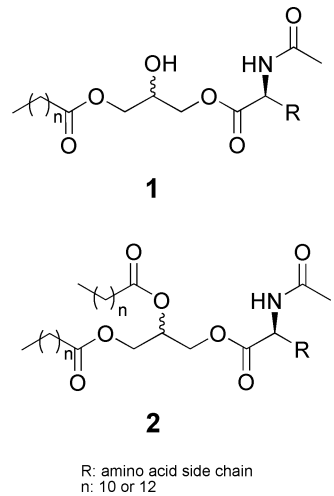

Scheme 5 Structures of amino acid glyceride conjugates: mono acyl derivatives (**1**) and diacyl derivatives (**2**).

Our group has synthesized these products using chemical and enzymatic methodologies.[25,87–89] The first enzymochemical synthetic strategy of amino acid glyceride conjugates was described by Valivety *et al.*[90] The synthesis started with the preparation of amino acid glyceryl esters namely 1-*O*-(N^{α}-protected-aminoacyl)glycerols. The preparation of these compounds was performed using an acid catalyst such as BF_3 at elevated temperatures in glycerol, which served as solvent and reactant. Alternatively, they can be obtained by enzymatic methodology using hydrolases (Scheme 6). Proteases and lipases were found to be a versatile catalyst for this reaction.[91–92] A variety of protected amino acid glyceryl ester derivatives were obtained in 46–98% yield under mild and selective conditions.

In a second step, the free hydroxyl groups of the glyceryl moiety were acylated with fatty acid using lipases as catalyst. According to Valivety *et al.*,[60,90] both Novozyme and Lipozyme can be successfully used as biocatalysts showing a high regioselectivity towards the primary hydroxyl group of the amino acid glyceryl ester derivative. Hence, by this methodology only the 1(3)-aminoacyl monoglycerides are likely to be prepared.

We have developed a novel methodology to obtain both 1-monoacyl- and 1,2-diacyl-3-aminoacyl glycerol[88] (see Scheme 5,

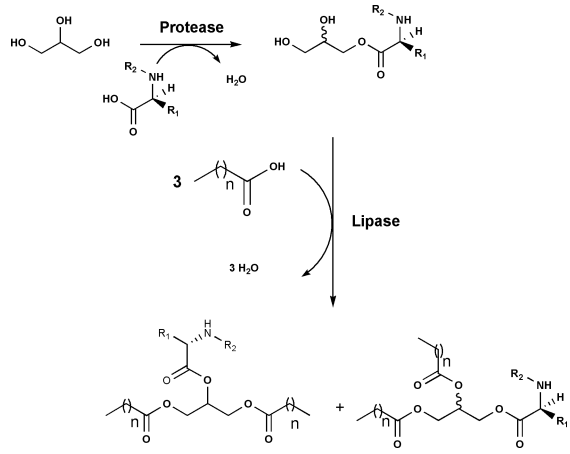

Scheme 6 Reaction pathway for the synthesis of mono and diacylglycerol amino acid conjugates.

1 and 2, respectively). Mono and diacylation of amino acid glyceryl ester may be carried out using selective lipases by taking advantage of the spontaneous intramolecular acyl-migration reaction that occurs in partial glycerides.[93–95] Thus, the 1(3)-acylated product may undergo intramolecular 1(3)→2 acyl migration and the resulting 1,2(2,3)-isomer subsequently be acylated at the free primary hydroxyl group by the lipase. Accordingly, the yield of diacylated product will depend on both the rate of intramolecular acyl-migration and the enzymatic esterification of the newly free primary hydroxyl of the monoacylated derivative. Both processes are influenced by the reaction conditions, such as solvent, support for enzyme immobilization, buffer salts and by the amino acid glyceryl ester derivative. All the enzymatic acylations were carried out in solvent free media, at a temperature around the melting point of the corresponding fatty acid.

We have found that the 1,2-diacyl-3-aminoacyl glycerol derivatives were in fact a mixture of two regioisomers: 1,2-diacyl-*rac*-glycero-3-(amino acid) derivative as the major one, and 1,3-dilauroyl-glycero-2-(amino acid) derivative. With this methodology a series of mono and dilauroylated glycerol derivatives of arginine, aspartic acid, glutamic acid, asparagine, glutamine and tyrosine were prepared.[88] All of them were mixtures of diastereoisomers and regioisomers except the dilauroylated derivative of glutamine. Here, both 1,3-dilauroyl-glycero-2-*O*-(N^{α}-acetyl-L-glutamine) and 1,2-dilauroyl-*rac*-glycero-3-*O*-(N^{α}-acetyl-L-glutamine) were separarated by flash chromatography on silica.

Chemically, two biocompatible cationic surfactants from the amino acid argininine were prepared (Scheme 5, **2**, *n*: 10, 12).[96] The first compound is 1,2-dilauroyl-*rac*-glycero-3-*O*-(N^{α}-acetyl-L-arginine), with 12 carbon atoms in the alkyl chains (Scheme 5, **2**, *n*: 10) . The second one is the 1,2-dimiristoyl-*rac*-glycero-3-*O*-(N^{α}-acetyl-L-arginine), with 14 carbon atoms in the alkyl chains (Scheme 5, **2**, **n**: 12). Henceforth, we shall refer to these compounds as 1212RAc and 1414RAc, respectively.

The synthesis of 1212RAc and 1414RAc compounds was achieved following a two step procedure. The first step involves the enzymatic preparation of the arginine glyceryl ester derivative as described in Morán *et al.*[92] This reaction consisted of the selective protease-catalysed esterification of one of the primary hydroxyl groups of the glycerol with the carboxylate group of the N^{α}-protected amino acid. The reaction yield was 80%. The second step consists of the preparation of 1,2-diacyl-*rac*-glycero-3-*O*-(N^{α}-acetyl-L-arginine) by acylation of the two remaining free hydroxyls groups of the arginine glyceryl ester derivative with the corresponding long chain acid chloride.[96] The progress control of the reaction showed that the arginine glyceryl ester derivative was first esterified with 1 mol of acyl chloride to give the corresponding monoacyl derivatives. With a molar ratio acid chloride : arginine glyceryl ester derivative (1 : 3), the main reaction products were 1212RAc and 1414RAc with conversions higher than 98%. The overall yield of these reactions after purification was in the range of about 85–70%.

New surfactants that are analogues of lecithin have been synthesized[97–101] The structure of these non-ionic amphiphilic compounds is based on natural dibasic (lysine) or diacidic (glutamic or aspartic acids) amino acids. As with the lecithins, these amino acid-based compounds have two hydrophobic tails and one hydrophilic head. However, in the latter compounds the polar head is of the non-ionic type (one or two chains of monomethyletherpolyoxyethylene glycol) whereas in the lecithins it is of the zwitterionic type. The central pivot in the structure of lecithins, *i.e.* the glycerol, is imitated by the natural trifunctional amino acids lysine,[91–101] aspartic acid[99,101] and glutamic acid.[99,101] The hydrophobic (fatty acids or fatty amines) and hydrophilic (monomethyletherpolyoxyethylene amine or monomethyletherpolyethylene carboxylic acid) moieties were introduced into their amino or carboxylic functions through amine bonds, in place of the ester bonds in lecithins. The latest variation on this theme contains two different hydrophobes; thus creating an asymmetric structure that displays lower water solubility and higher surface activity as well as a slightly increased toxicity.

4.2 Properties

The physicochemical and biological properties of amino acid glyceride conjugates have not been extensively explored yet. From preliminary observations carried out in our lab, these novel compounds combine the advantages of both partial glycerides and lipoamino acids.

The influence of the temperature as a function of time on the stability properties was studied in order to ascertain whether chemical degradation of 1212RAc and 1414RAc compounds occurred.[102] As expected, the hydrolysis rate was higher when the temperature increases, reaching 10% in the case of the 1414RAc and 8.9% in the case of the 1212RAc at 40 °C after 144 hours. The hydrolysis of 1212RAc and 1414RAc compounds is related to their structure in which three ester bonds are present. The ester bonds hydrolyzed under acid pH conditions. Owing to the presence of a weak acid group, the guanidine group, aqueous solutions of these surfactants have a slightly acid pH (pH = 4). Slow hydrolysis of the ester bonds was promoted at this pH.

The aqueous aggregation behavior, studied by conductivity, showed a linear increase with concentration up to a break point of 0.12 mM for 1212RAc and 0.09 mM for 14141RAc. Results for similar nonacetylated compounds suggest that the break points from conductivity for this new family of compounds do not correspond to a true CMC (monomer to micelle) but some other transition (*i.e.* vesicle to ribbon).[102]

Qualitative phase behavior studies applying the flooding method revealed the formation of anisotropic phases in all the binary surfactant systems studied. The compound 1212RAc forms lamellar liquid crystals at room temperature (25 °C) and this structure is stable and remains stable until high temperatures are reached. The 1414RAc also forms anisotropic phases that developed in lamellar liquid crystals at 45 °C. Dispersions of 1212RAc and 1414RAc 0.1% in water at 35 °C revealed that their lamellar structures (Fig. 1) spontaneously form stable multilamellar vesicles (Fig. 2) spontaneously and easily, of diverse size and number of bilayers.

The 1212RAc and 1414RAc surfactants can simultaneously stabilize water-in-oil (W/O) droplets and oil-in-water droplets (O/W), forming multiple emulsions. On account of this behavior, these surfactants constitute an interesting alternative to the diglycerides and lecithins in formulations that need antimicrobial properties.

The phase behaviour in the dry state of pure and regioisomeric mixtures has been studied by differential scanning calorimetry and small-angle X-ray diffraction complemented by polarized light microscopy.[103] The study showed the influence of the bilayer packing as a function of the temperature.

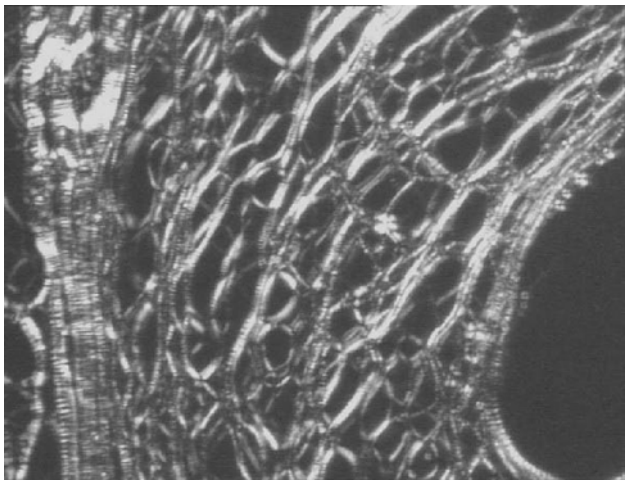

Fig. 1 Polarized microscopy of lamellar liquid crystals for the 1414RAc/H_2O system (**1**).

Fig. 2 Polarized microscopy of vesicles for the 1212RAc/H_2O system (**2**).

We have shown that a novel family of 1,2-diacylglycerol amino acid-based surfactants exhibits a monolayer behaviour similar to that found in natural phospholipids, suggesting that they may be viable substitutes for these compounds in industrial applications, which need multifunctional compounds.[104] Use of Brewster Angle Microscopy (BAM) image analysis of the inner textures has revealed that condensed phases of the diacyl glycerol compounds with 14 carbon atoms in the hydrocarbon chain exhibit hexatic order. Variations in the chain length introduce similar changes to those commonly found in lipid monolayers. Generally, compounds with a 1,2-substitution pattern in the glycerol backbone exhibit a tendency to form continuous monolayers (expanded phases) at significantly lower molecular densities than their natural phospholipid counterparts.

Our investigations with a compound bearing a 1,3-substitution pattern [1,3-dilauroyl-glycero-2-(N^{α}-acetyl-L-glutamine)] show that it forms rough and compact LC domains, very different from those observed in phospholipid monolayers.[104]

In summary, amino acid-based surfactants constitute a class of bio-based surfactants with excellent surface properties, wide biological activity, low potential toxicity and low environmental impact. Moreover, they can be prepared efficiently by chemical and enzymatic catalysis. All these features make them an outstanding clean and safe alternative to conventional specialty surfactants. Hence, this new generation of surfactants will contribute to meet the increasing demand for environmentally friendly surfactants for pharmaceutical and food industries.

Acknowledgement

This work was supported by the MEC, Projects QUI97-0570 and PPQ2000-1687-CO2-01 and UA-CSIC *Interaccion de Tensioactivos con membranas.*

References

1 K. Holmberg, Novel Surfactants. Preparation, Applications and Biodegradability, Second Edition, Revised and Expanded, *Surfactant Science Series*, ed. K. Holberg, Marcel Dekker, New York, 2004.
2 Y. Okahata, S. Tammamachi, M. Magai, T. Kunitake and J. Colloid, *Interface Sci.*, 1981, **82**, 401.
3 Ma R. Infante, J. Molinero, P. Erra, R. Juliá, J. J. García Domínguez and M. Robert, *Fette Seifen Anstrichm.*, 1986, **88**, 108.
4 T. Kida, N. Morishima, A. Masuyama and Y. Nakatsuji, *J. Am. Oil Chem. Soc.*, 1994, **71**, 705.
5 Ma R. Infante, A. Pinazo and J. Seguer, *Colloids Surf., A*, 1997, **123–124**, 49.
6 T. Furutani, H. Ooshima and J. Kato, *Enzyme Microb. Technol.*, 1997, **20**, 214.
7 B. Gallot and H. H. Hassan, *Mol. Cryst. Liq. Cryst.*, 1989, **170**, 195.
8 S. E. Godtfredsen and F. Bjoerkling, World Patent No. 90/14429, 1990.
9 A. Nagao and M. Kito, *J. Am. Oil Chem. Soc.*, 1989, **66**, 710.
10 I. A. Nnanna and J. Xia. Protein Based Surfactants: Synthesis, *Physicochemical Properties and Applications*, Marcel Dekker, New York, 2001.
11 A. Vonderhagen, H.-C. Raths and E. Eilers, Ger. Offen. DE *19749555 A1 12 May* Henkel K.-G.a.A., Germany, 1999, 4.
12 R. Valivety, P. Jauregui and E. N. Vulfson, *J. Am. Oil Chem. Soc.*, 1997, **74**, 879.
13 W. Heutrich, H. Keppler and K. Hintzmann, Ger Patent 635522, 1936.
14 H. Yokota, K. Sagawa, Ch. Eguchi and M. Takehara, *J. Am. Oil Chem. Soc.*, 1985, **62**, 1716.
15 G. Baschang, A. Hartmann and O. Wacker, US patent 4666886 A, 1987.
16 D. B. Braun, *Cosmet. Toiletries*, 1989, **104**, 92.
17 P. Presenz, *Pharmazie*, 1996, **51**, 755.
18 M. Takehara, *Colloids Surf.*, 1989, **38**, 149.
19 Ma R. Infante, J. J. García Domínguez, P. Erra, Ma R. Juliá and M. Prats, *Int. J. Cosmet. Sci.*, 1984, **6**, 27.
20 Ma R. Infante, J. Molinero, P. Bosch, Ma R. Juliá and P. Erra, *J. Am. Oil Chem. Soc.*, 1992, **69**, 647.
21 Ma R. Infante and V. Moses, *Int. J. Pept. Protein Res.*, 1994, **43**, 173.
22 J. Seguer, J. Molinero, A. Manresa, J. Caelles and Ma R. Infante, *J. Soc. Cosmet. Chem.*, 1994, **45**, 53.
23 E. Piera, F. Comelles, P. Erra and Ma R. Infante, *J. Chem. Soc., Perkin Trans. 2*, 1998, 335.
24 P. Clapés, C. Morán and Ma R. Infante, *Biotechnol. Bioeng.*, 1999, **63**, 333.
25 P. Clapés and Ma R. Infante, *Biocatal. Biotransform.*, 2002, **20**, 215.
26 R. Valivety, I. S. Gill and E. N. Vulfson, *J. Surf. Deterg.*, 1998, **1**, 177.
27 E. L. Soo, A. B. Salleh, M. Basri, R. N. Z. R. A. Rahman and K. Kamaruddin, *J. Biosci. Bioeng.*, 2003, **95**(4), 361.
28 C. Solans, N. Azemar, Ma R. Infante and T. Warnheim, *Prog. Colloid Polym. Sci.*, 1989, **79**, 70.
29 H. Fördedal, J. Sjöblom and Ma R. Infante, *Colloids Surf., A*, 1993, **79**, 81.
30 M. A. Pés. Doctoral Thesis, University of Barcelona, 1992.
31 H. Kunieda, K. Nakamura, Ma R. Infante and C. Solans, *Adv. Mater.*, 1992, **4**, 291.
32 T. J. Franklin and G. A. Snow, *Biochemistry of Antimicrobial Action*, 3rd edn., Chapman & Hall, New York, 1981.
33 M. J. Rosen, *Surfactants and Interfacial Phenomena*, Wiley & Sons, New York, 1987.
34 M. R. Infante, J. Molinero, P. Erra, M. R. Juliá and J. J. García Dominguez, *Fett. Wiss. Technol.*, 1998, **87**, 309.
35 H. Gibson and J. T. Holah, in *Preservation of Surfactant Formulations*, ed. F. F. Morpeth, Blackie Academic and Professional, Glasgow, 1995, p. 30.
36 J. Ferguson, *Proc. R. Soc. London, Ser. B.*, 1939, **127**, 387.
37 Organisation for Economic Cooperation and Development (OECD) Chemicals Group, Revised Guidelines for tests for Ready Biodegradability, 301E. Paris, 1993 and OECD guidelines for testing of Chemicals. Vol. 1, section 2.

38 C. Morán, P. Clapés, F. Comelles, M. T. García, L. Pérez, Ma Vinardell, M. Mitjans and Ma R. Infante, *Langmuir*, 2001, **17**, 5071.
39 O. Kirk, F. D. Pedersen and C. C. Fuglsang, *J. Surfactants Deterg.*, 1998, **1**, 37.
40 W. J. W. Pape and U. Hopper, *Drug Res.*, 1990, **4**, 498.
41 C. Boeckler, B. Frisch and F. Schuber, *Bioorg. Med. Chem. Lett.*, 1998, **8**, 2055.
42 N. Yagi, Y. Ogawa, M. Kodaka, T. Okada, T. Tomohiro, T. Konakahara and H. Okuno, *Lipids*, 2000, **35**, 673.
43 D. J. Claffey, J. D. Meyer, R. Beauvais, T. Brandt, E. Shefter, D. J. Kroll, J. A. Ruth and M. C. Manning, *Biochem. Cell Biol.*, 2000, **78**, 59.
44 M. Kondoh, T. Furutani, M. Azuma, H. Oshima and J. Kato, *Biosci., Biotechnol., Biochem.*, 1997, **61**, 870.
45 R. F. Epand, Ma R. Infante, T. D. Flanagan and R. M. Epand, *BBA-Biomembranes*, 1998, **1373**, 67.
46 J. Wang and I. M. Warner, *Anal. Chem.*, 1994, **66**, 3773.
47 S. Hara and A. Dobashi, Jpn. Pat. 04 149 205 1993.
48 E. Billiot and I. Warner, *Anal. Chem.*, 2000, **72**, 1740.
49 M. J. Rosen, *CHEMTECH*, 1993, 30.
50 R. Zana, in *Specialist Surfactants*, ed. D. Robb, Blackie, London, 1997, p. 81.
51 F. M. Menger and C. A. Littau, *J. Am. Chem. Soc.*, 1993, **115**, 10083.
52 F. Devinsky, I. Lacko, F. Bittererova and D. Mlynarcik, *Chem. Pap.*, 1987, **41**, 803.
53 M. El Achouri, Ma R. Infante, F. Izquierdo, F. Kertit, H. M. Gouttaya and B. Nciri, *Corros. Sci.*, 2001, **43**, 19.
54 F. M. Menger and J. S. Keiper, *Angew. Chem., Int. Ed.*, 2000, **39**, 1906.
55 A. Pinazo, M. Diz, A. Pés, P. Erra and M. R. Infante, *J. Am. Oil Chem. Soc.*, 1993, **70**, 37.
56 M. Diz, A. Manresa, A. Pinazo, P. Erra and M. R. Infante, *J. Chem. Soc., Perkin. Trans. 2*, 1994, 1871.
57 I. Ikeda, in Novel Surfactants. Synthesis of Gemini (Dimeric) and Related Surfactants, *Surfactant Science Series*, ed. K. Holberg, Marcel Dekker, New York, 2004, pp. 9–35.
58 M. J. Rosen, *CHEMTECH*, 1993, **23**, 30; Y. Nakatsuji and I. Ikeda, *Chim. Oggi.*, 1997, 40.
59 R. Zana, in Novel Surfactants. Preparation, Applications and Biodegradability, *Surfactant Science Series*, ed. K. Holberg, Marcel Dekker, New York, 1998, pp. 241–277.
60 E. Vulfson, in Novel Surfactants. Enzymatic Synthesis of Surfactants, *Surfactant Science Series*, K. Holberg, Marcel Dekker, New York, 2004, pp. 279–300 (and references therein).
61 T. W. Davey, in Gemini Surfactants. Special Gemini Surfactants: Nonionic, Zwitterionic, Fluorinated, and Amino Acid Based, *Surfactant Science Series*, K. Holberg, Marcel Dekker, New York, 2004, pp. 253–280 (and references therein).
62 M. Brock, *Tenside Surfactants Deterg.*, 1993, **30**, 394.
63 R. Puchta, P. Krigs and F. Schambil, Comite Español De La Detergencia Tensioactivos Y Afines (C.E.D.), Barcelona, 1993.
64 Kationische Zuckertenside, *Seifen Oele Fette Waschse*, 1994, **120**, 423.
65 R. Pi Subirana, N. Bonastre, E. Prat Queralt and J. Bigorra Lloses, Ger. Patent 195 39 876 to Henkel K._G.a.A. 1996.
66 R. Valivety, I. S. Gill and E. N. Vulfson, *J. Surfactants Deterg.*, 1998, **1**(2), 177.
67 M. Biermann, F. Lange, R. Piorr, U. Ploog, H. Rutzen, J. Schindler and R. Schmidt, in *Surfactants in Consumer Products*, ed. J. Falbe, Springer-Verlag, Heidelberg, 1987, pp. 110–114.
68 L. Edebo, M. Lindstedt, S. Allenmark and R. A. Thompson, *Antimicrob. Agents Chemother.*, 1990, **34**, 1949.
69 L. Pérez, J. L. Torres, A. Manresa, C. Solans and Ma R. Infante, *Langmuir*, 1996, **12**, 5296.
70 E. Piera, Ma R. Infante and P. Clapés, *Biotechnol. Bioeng.*, 2000, **70**, 323.
71 L. Pérez, A. Pinazo, M. J. Rosen and M. R. Infante, *Langmuir*, 1998, **14**, 2307.
72 A. Pinazo, X. Wen, L. Pérez, M. R. Infante and E. I. Franses, *Langmuir*, 1999, **15**, 3134.
73 L. Pérez, Doctoral Thesis, University of Barcelona, 1997.
74 E. Piera, Doctoral Thesis, University of Barcelona, 2000.
75 A. Pinazo, L. Pérez, M. R. Infante and E. I. Franses, *Colloids Surf., A*, 2001, **189**, 225.
76 OECD guidelines for testing of Chemicals. Vol. 1, section 2: *Effects on Biotic system*, 202, Paris, France, 1993.
77 J. M. Ribó and K. L. M. Kaiser, *Toxic. Assess.*, 1987, **2**, 305.
78 L. Perez, T. García;, I. Ribosa, P. Vinardell, A. Manresa and Ma R. Infante, *Environ. Toxicol. Chem.*, 2002, **21**, 1279.
79 C. McGregor, C. Perrin, M. Monck, P. Camilleri and A. Kirby, *J. Am. Chem. Soc.*, 2001, **123**, 6215.
80 P. Camilleri, A. Kremer, A. J. Edwards, K. H. Jennings, O. Jenkins and I. Marshall, *Chem. Commun.*, 2000, 1253.
81 C. McGregor, C. Perrin, M. Monck, P. Camilleri and A. Kirby, *J. Am. Chem. Soc.*, 2001, **123**, 6215.
82 G. Ronsin, C. Perrin, P. Guedat, A. Kremer, P. Camilleri and A. Kirby, *Chem. Commun.*, 2001, 2234.
83 G. Ronsin, A. J. Kirby, S. Rittenhouse, G. Woodnutt and P. Camilleri, *J. Chem. Soc., Perkin. Trans. 2*, 2002, 1302.
84 P. Camilleri, A. Kremer, A. J. Edwards, K. H. Jennings, O. Jenkins and I. Marshall, *Chem. Commun.*, 2000, 1253.
85 P. Camilleri, C. McGregor, A. J. Kirby and C. Perrin, WO 0230957, September 2002.
86 K. H. Jennings, I. C. B. Marshall, M. Wilkinson, A. Kremer, A. J. Kirby and P. Camilleri, *Langmuir*, 2002, **18**, 2426.
87 S. Pegiadou, L. Pérez and Ma R. Infante, *J. Surfactants Deterg.*, 2000, **3**, 517.
88 C. Morán, Ma R. Infante and P. Clapés, *J. Chem. Soc., Perkin. Trans. 2*, 2001, 2063.
89 M. C. Morán, Doctoral Thesis, University of Barcelona, 2002.
90 R. Valivety, P. Jauregui and E. N. Vulfson, *J. Am. Oil Chem. Soc.*, 1997, **74**, 879.
91 Y. V. Mitin, K. Braun and P. Kuhl, *Biotechnol. Bioeng.*, 1997, **54**, 287.
92 C. Morán, M. R. Infante and P. Clapés, *J. Chem. Soc., Perkin Trans. 1*, 2001, 2063.
93 M. Berger, K. Laumen and M. P. Schneider, *J. Am. Oil Chem. Soc.*, 1992, **69**, 955.
94 A. Millqvist-Fureby, C. Virto, P. Adlercreutz and B. Mattiason, *Biocatal. Biotransform.*, 1996, **14**, 89.
95 C. Virto, I. Svensson and P. Adlercreutz, *Enzyme Microb. Technol.*, 1999, **24**, 651.
96 L. Pérez, M. R. Infante, R. Pons, C. Moran, P. Vinardell, M. Mitjans and A. Pinazo, *Colloids Surf., B*, 2003, in press.
97 M. R. Infante, J. Seguer, A. Pinazo and M. P. Vinardell, *J. Dispersion Sci. Technol.*, 1999, **20**, 621.
98 J. Seguer, C. Selve, M. Allouch and M. R. Infante, *J. Am. Oil Chem. Soc.*, 1996, **73**(1), 79.
99 J. Seguer, M. R. Infante, M. Allouch, L. Mansuy, C. Selve and P. Vinardell, *New J. Chem.*, 1994, **18**, 765.
100 M. Macian, J. Seguer, Ma R. Infante, C. Selve and Ma P. Vinardell, *Toxicology*, 1996, **106**, 1.
101 J. Seguer, Doctoral Thesis, UB, 1993.
102 A. Pinazo, L. Perez, M. R. Infante and R. Pons, *Phys. Chem. Chem. Phys.*, 2004, **6**, in press10.1039/b313313n.
103 M. C. Morán, A. Pinazo, P. Clapés, L. Pérez, M. R. Infante and R. Pons, *J. Phys. Chem. B*, 2004, (submitted).
104 R. Albalat, J. Claret, J. Ignés-Mullol, F. Sagués, C. Morán, L. Pérez, P. Clapés and A. Pinazo, *Langmuir*, 2003, **19**, 10878.

PAPER

www.rsc.org/greenchem

Organometallic reactions in ionic liquids. Alkylation of aldehydes with diethylzinc

Man Chun Law,[ab] Kwok-Yin Wong[b] and Tak Hang Chan*[ab]

[a] *Department of Chemistry, McGill University, Montreal, Quebec, Canada H3A 2K6*

[b] *Department of Applied Biology and Chemical Technology, The Hong Kong Polytechnic University, Hung Hom, Hong Kong SAR, China. E-mail: bcchanth@polyu.edu.hk; Fax: +852-2364-9932; Tel: +852-2766-5605*

Received 2nd February 2004, Accepted 9th March 2004
First published as an Advance Article on the web 25th March 2004

The ionic liquids, [bmim][Br] (**2a**), [bmim][BF_4] (**2b**), [bmim][PF_6] (**2c**), [bdmim][BF_4] (**8**) and [bpy][BF_4] (**9**), were examined as the solvent media for dialkylzinc addition to aldehydes giving the corresponding alcohols. The ionic liquid [bpy][BF_4] was found to be the solvent of choice, giving the best yields, easily recovered and reused.

Because of the concern for the environment, there has been considerable recent research into replacing the use of volatile organic solvents with clean solvents[1] as reaction media for chemical synthesis.[2] Water,[3] supercritical carbon dioxide[4] and ionic liquids[5] are currently the clean solvents being investigated most extensively. A common problem that is faced by these solvents is their reactivity towards reactive organometallic reagents such as the Grignard or the organolithium reagents. These organometallic reagents are very useful in organic synthesis for the formation of carbon–carbon bonds. They are well known to react with water or carbon dioxide. It is also likely that Grignard or organolithium reagents will react with quaternary salts, structures which are common for ionic liquids.[6] Alternative organometallic reactions must be sought for these solvents to replace the role of Grignard or organolithium reactions. Recently, we and others have investigated the Barbier–Grignard type reactions in aqueous media using In,[7] Zn[8] and Sn[9] and other metals as alternatives to the classical magnesium based Grignard reaction.[10] While these aqueous organometallic reactions have been found to be useful in organic synthesis, they also have limitations. Firstly, the types of reactions have been largely limited to allylation and its variations.[11] Efforts to extend them to alkylation reactions have only limited success.[12] Secondly, water sensitive substrates such as hydrolytically reactive imines cannot be used.[13] Finally, highly hydrophobic compounds insoluble in water tend to present difficulties in these reactions. We are therefore interested in examining organometallic reactions in ionic liquids and comparing their chemistry with those in aqueous media and in conventional organic solvents. The hope is that a broader range of organometallic reactions can be carried out in ionic liquids than in aqueous media. Thus far, few stoichiometric organometallic reactions in ionic liquids have been examined.[14,15] Recently we and others have found that zinc was quite effective in mediating the coupling of allyl bromide with carbonyl compounds in the ionic liquid 3-butyl-1-methylimidazolium tetrafluoroborate, [bmim][BF_4], to give the product homoallylic alcohols in good yields.[16,17] The results suggested that the presumed allylzinc intermediate, if formed under those conditions, may not have reacted with the ionic liquid solvent. This observation prompted us to examine the possibility of conducting alkylation reactions with the more reactive diethylzinc in ionic liquids.

Initially, we examined the reaction of neat diethylzinc (**1**) with [bmim][Br] (**2a**) at room temperature. Gas bubbles evolved quickly and the ionic liquid turned from pale yellow to white with increased viscosity. Based on ^{1}H and ^{13}C NMR together with mass spectral studies and in analogy with the known *bis*(imidazolylidene)palladium and nickel dibromide complexes,[18] the products of the reaction were assigned to have the [$ZnBr_2$(bmiy)$_2$] (**3**) and [Zn(μ-Br)(Br)(bmiy)$_2$]$_2$ (**4**) (bmiy = 3-butyl-1-methyl-2-imidazolylidene) structures (Scheme 1). Previously, imidazol-2-ylidene zinc adducts have been prepared by a different route.[19] However, when the reaction of diethylzinc with [bmim][BF_4] (**2b**) was examined, the reaction was found to be slow and the conversion to the carbene zinc complexes was incomplete. The reaction could be accelerated by the addition of NaBr. We suspected therefore that the carbene formation in [bmim][BF_4] may actually be due to the contamination of the precursor – [bmim][Br]. Indeed, when [bmim][BF_4] had been meticulously purified using the chromatography method to be free of bromide ion,[20] its reaction with diethylzinc was now sufficiently slow that it could be used as solvent for the alkylation reactions. The results are summarized in Table 1. Using [bmim][BF_4] as solvent, various aldehydes **5** were alkylated by diethylzinc to the alkylated product alcohols **6** together with the reduced alcohols **7** as the minor product (Scheme 2). In many cases where a small amount (0.05 mL) of the ionic liquid was used, a 0.5 mole ratio of Et_2Zn was able to give good yield of the adduct **6**, suggesting that both ethyl groups can be transferred to the carbonyl compound. This is distinctly different from organozinc reactions in organic solvents which have been generally described as sluggish: diorganozincs usually add to aldehydes in synthetically useful yields only in the presence of catalysts such as Lewis acids and Lewis bases.[21] For example, the reaction of diethylzinc and 4-chlorobenzaldehyde in organic solvent without catalyst gave a mixture of the adduct alcohol **6** in 38% yield together with 45% of the reduction product **7**.[21c] Aliphatic aldehydes (entry 20) were alkylated similarly in IL. For conjugated aldehydes such as *trans*-cinnamaldehyde (entry 21), alkylation occurred in a 1,2-fashion. 4-Hydroxybenzaldehyde (entry 19) was alkylated without the need to protect the hydroxyl group. However, excess diethylzinc was required to give a good yield. When [bmim][PF_6] (**2c**) was used as the ionic liquid in place of [bmim][BF_4] (**2b**), the yield of the adduct **6** was much reduced (entry 7). The major product was found to be the reduction of the aldehyde to the corresponding alcohol **7** due to hydride transfer from diethylzinc. It should be pointed out that under the solvent-free conditions,[22] reaction of aldehyde with diethylzinc did not give a satisfactory result as the reaction mixture solidified readily and gave incomplete reaction (entry 8). This is typical of the reactions of solid substrates in solvent-free conditions.

In spite of these results, the use of [bmim][BF_4] as solvent was considered unsatisfactory due to the difficulty of its purification. Chromatographic purification of [bmim][BF_4] according to literature procedures[20] was tedious and the recovery was low. The alternative method of using $AgBF_4$ to remove bromide ion was expensive[20] and the trace of silver ion remaining was found to catalyze the decomposition of diethylzinc. In addition, the reaction

DOI: 10.1039/b401520g

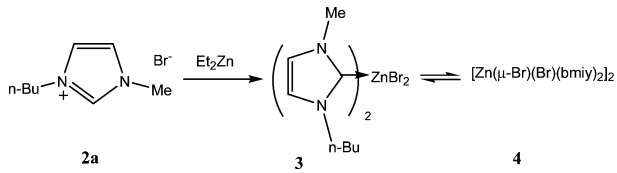

Scheme 1

Table 1 Yields of alkylation reactions of various carbonyl compounds with diethylzinc in ionic liquid **2b**[a]

Entry	Carbonyl compound	Mole ratio Et_2Zn : C=O	Vol. of IL/mL	Yield **6** (%)[b]
1	PhCHO	0.5 : 1	0.05	71
2	2-FC_6H_4CHO	0.5 : 1	0.05	93
3	4-FC_6H_4CHO	0.5 : 1	0.05	68
4	2-ClC_6H_4CHO	0.5 : 1	0.05	61
5	3-ClC_6H_4CHO	0.5 : 1	0.05	99
6	2,6-$Cl_2C_6H_3CHO$	2 : 1	2.00	68
7[c]	2,6-$Cl_2C_6H_3CHO$	1 : 1	1.00	39
8[d]	2,6-$Cl_2C_6H_3CHO$	1 : 1	neat	29
9	4-EtC_6H_4CHO	0.5 : 1	0.05	40
10	2-$MeOC_6H_4CHO$	2 : 1	2.00	69
11	3-$MeOC_6H_4CHO$	0.5 : 1	0.05	38
12	4-$MeOC_6H_4CHO$	2 : 1	2.00	75
13	2-MeC_6H_4CHO	0.5 : 1	0.05	70
14	3-MeC_6H_4CHO	0.5 : 1	0.05	(59)
15	3-MeC_6H_4CHO	1 : 1	0.05	84
16	4-MeC_6H_4CHO	0.5 : 1	0.05	(30)
17	4-MeC_6H_4CHO	1 : 1	0.05	91
18	1-naphthaldehyde	0.5 : 1	0.05	50
19	4-HOC_6H_4CHO	2 : 1	1.00	78[e]
20	2-methylvaleraldehyde	0.5 : 1	0.05	94
21	*trans*-cinnamaldehyde	0.5 : 1	0.05	67
22	4-CNC_6H_4CHO	2 : 1	0.50	86

[a] Addition of diethylzinc to carbonyl compounds was carried out at 1 mmol scale of the carbonyl compound at 0° → room temperature in ionic liquid (**2b**) overnight. [b] Isolated yields (NMR yield in parenthesis). [c] [bmim][PF_6] (**2c**) was used as the ionic liquid. [d] Reaction was carried out neat without IL. The reaction stopped in 5 minutes and could not be stirred further. [e] 4-Hydroxybenzaldehyde was first dissolved in ionic liquid before addition to diethylzinc.

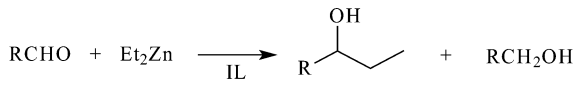

Scheme 2

often had to be carried out at 0 °C to reduce the reaction of bmim with diethylzinc. We therefore examined two other ionic liquids, 3-butyl-1,2-dimethylimidazolium tetrafluoro-borate [bdmim][BF_4] (**8**) and N-butylpyridinium tetrafluoroborate [bpy][BF_4] (**9**), for the alkylation reactions. These two solvents do not react with diethylzinc to give the carbene complexes since they do not have the relatively acidic hydrogen at the C2 position of the imidazole ring. There was no need for extensive purification to remove bromide ion from these two ionic liquids. The reactions of diethylzinc with aldehydes are summarized in Tables 2 and 3. Using 2,6-dichlorobenzaldehyde as the common substrate, 1 mL of the ionic liquid as solvent and reaction with one mole of diethylzinc at room temperature for two hours as the standard conditions, [bpy][BF_4] was the best solvent in giving essentially quantitative yield of **6**, with little of the reduction product **7** (Table 3, entry 1). Though inferior to [bpy][BF_4], [bbdmim][BF_4] appeared to be superior to [bmim][PF_6] and [bmim][BF_4] (Table 2, entry 1).

We have also studied the diethylzinc alkylation of a number of other aldehydes in these two solvents. In all cases, excellent isolated yields of the adducts could be obtained using [bpy][BF_4] as the solvent. The yields in [bdmim][BF_4], though generally inferior,

Table 2 Yields of alkylation reactions of various carbonyl compounds with diethylzinc in IL **8**[a]

Entry	Substrate (**5**)	Mole ratio **5** : **1**	Time	Yield (%)[b] **6**	**7**
1	2,6-$Cl_2C_6H_5CHO$	1 : 1	2 h	73	6
2	PhCHO[c]	1 : 0.7	2 h	80	17
3	PhCHO[c]	1 : 1	2 h	85	6
4	PhCHO	1 : 1	2 h	88	8
5	4-CNC_6H_4CHO	1 : 1	6 h	(48)	19
6	2,3-$Cl_2C_6H_5CHO$	1 : 1	5 h	(70)	0
7	4-HOC_6H_4CHO	1 : 2	10 min[d]	33	2
8	4-$CH_3COC_6H_4CHO$	1 : 1	5 min	(86)	0
9	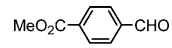	1 : 1	5 min	(63)	0
10		1 : 1	3 h	(58)	—
11	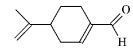	1 : 2	12 h	(81)	4
12	PhCH=CHCHO	1 : 1	12 h	(97)	—
13	Hexanal	1 : 1	3 h	(61)	—

[a] Addition of diethylzinc to carbonyl compound was carried out at a 1 mmol scale of carbonyl compound at room temperature in ionic liquid **8** (1 mL unless noted otherwise) with vigorous stirring of the reaction mixture. [b] Measured by ^1H NMR (isolated yields in parentheses). [c] 0.1 mL of IL **8** was used. [d] The reaction mixture could not be further stirred and the reaction was stopped.

Table 3 Yields of alkylation reactions of various carbonyl compounds with diethylzinc in IL **9**[a]

Entry	Substrate (**5**)	Mole ratio **5** : **1**	Time	Yield (%)[b] **6**	**7**
1	2,6-$Cl_2C_6H_5CHO$	1 : 1	2 h	(90)	0
2	PhCHO	1 : 0.7	2 h	(87)	8
3	4-CNC_6H_4CHO	1 : 1	6 h	(89)	8
4	2,3-$Cl_2C_6H_5CHO$	1 : 1	5 h	(88)	5
5	4-HOC_6H_4CHO	1 : 1	6 h	34	3
6	4-HOC_6H_4CHO	1 : 2	6 h	72	4
7	4-HOC_6H_4CHO	1 : 3	6 h	(76)	6
8	4-$CH_3COC_6H_4CHO$	1 : 1	5 min	(86)	0
9	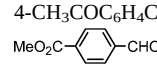	1 : 1	5 min	(90)	0
10		1 : 1	3 h	(82)	12
11	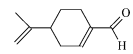	1 : 2	12 h	(96)	0
12	PhCH=CHCHO	1 : 1	12 h	(92)	0
13	Hexanal	1 : 1	3 h	(75)	—

[a] Addition of diethylzinc to carbonyl compound was carried out at a 1 mmol scale of carbonyl compound at room temperature in ionic liquid **9** (1 mL) with vigorous stirring of the reaction mixture. [b] Measured by ^1H NMR (isolated yields in parentheses).

were still adequate. It is interesting to note that the ethylation reaction was chemoselective. Aryl ketone and ester functions (entries 8 and 9 in Tables 2 and 3) were not alkylated under these conditions. Aliphatic aldehydes were alkylated readily to give adducts in satisfactory yields (entries 10 and 13). Ethylation of conjugated aldehydes occurred in a 1,2-fashion (entry 12). In many cases, the side reaction, due to hydride transfer, leading to the reduced alcohols **7** appeared to have been suppressed when [bpy][BF_4] was used as the solvent.

One problem anticipated in the use of ionic liquids as solvents for organometallic reactions is the issue of recycling of the ionic liquids. In the present reaction, the inorganic zinc salt [presumably $Zn(OH)_2$] after aqueous work-up would remain in the recovered ionic liquid and may interfere with subsequent alkylation reactions. Indeed, when [bpy][BF_4] was recovered, dried vigorously under vacuum at 100 °C and reused as solvent for the ethylation of benzaldehyde, the yield of the product alcohol **6** was reduced to

Table 4 Recycling of $[bpy][BF_4]$[a]

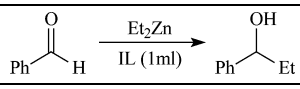

	Yield[b]			
IL/No. of cycle	1	2	3	4
Drying alone	68	50		
CH_2Cl_2 treatment	92	89	88	85
Oxalic acid treatment	93	86		

[a] Addition of diethylzinc to carbonyl compound was carried out at a 1 mmol scale of each reagent at room temperature in ionic liquid **9** (1 mL) with vigorous stirring. [b] Isolated yield.

68% (Table 4). The yield was further reduced to 50% on the next cycle. We found, however, if the inorganic zinc salt was removed from the recovered $[bpy][BF_4]$ by addition of a small amount of methylene chloride, the ionic liquid can be reused readily to give the alkylation product with qualitatively the same rates and similar yields for several cycles (Table 4). Alternately, the reaction mixture could be quenched with oxalic acid instead of water, and the resultant zinc oxalate removed from the recovered ionic liquid by the addition of a small amount of acetone. The $[bpy][BF_4]$ thus recovered could also be reused for the reaction to give the ethylated product in similar yields. There was little loss of the ionic liquid in the recycling process since the extract in each work-up was free of ionic liquid according to its NMR.

In conclusion, we have found that alkylation of aldehydes with diethylzinc can be conducted in ionic liquids. Using N-butylpyridinium tetrafluoroborate as the solvent, the reaction proceeded cleanly with high yield. This is in contrast to the reaction in aqueous media where diethylzinc is hydrolyzed readily, or in conventional volatile organic solvents where the addition of diethylzinc to aldehyde is generally sluggish and gives a low yield.[21] Finally, it was recently reported that $[bmim][F{\cdot}H_2O]$ was identified as a decomposition product during purification of $[bmim][PF_6]$.[23] Since HF is considered toxic, it has been cautioned that ionic liquids are not always green.[23] Even though at this time, we do not have evidence to suggest that either $[bdmim][BF_4]$, or $[bpy][BF_4]$ decompose to give HF containing products, caution must be exercised as with any ionic liquids with no supporting toxicological data.

Experimental

Neat diethylzinc was purchased from Aldrich and was used without further purification. All manipulations were carried out using Schlenk techniques under inert nitrogen atmosphere. The liquid diethylzinc was kept under nitrogen and transferred with a syringe into the reaction mixture. Nitrogen gas must flow into the container by piercing through the septum fitted on top with a needle during withdrawal of diethylzinc. Excess diethylzinc was quenched with acetone. Diethylzinc should be handled with care and not be exposed to aqueous media as this will lead to a fire hazard.[24]

Preparation of ionic liquids

Ionic liquids $[bmim][PF_6]$, $[bmim][BF_4]$, $[bdmim][BF_4]$ and $[bpy][BF_4]$ were prepared by metathesis with sodium tetrafluoroborate from its bromide precursors which were in turn prepared from the microwave-assisted method.[25] The ionic liquids were vacuum-dried overnight at 70 °C (0.1 mmHg) and stored under argon.

General procedure for alkylation with diethylzinc in ionic liquid

A 30 mL three-necked round-bottomed flask was charged with the ionic liquid (0.1 to 1 mL, as specified in Tables 1 and 2). Diethylzinc (0.5 to 3 mmol) was added dropwise *via* syringe to the ionic liquid at room temperature under nitrogen. The aldehyde (1 mmol) was then added dropwise under nitrogen flow throughout the addition process and the reaction mixture was stirred vigorously at room temperature for the specified time. The resulting mixture was quenched with a few drops of water followed by extraction with Et_2O (2×5 mL).† After removal of the ether solvent *in vacuo*, the residue was purified by flash chromatography (10 : 1 hexane : EtOAc as eluent) on silica gel to yield the pure adduct alcohol **6**. Specific conditions and yields of the alkylation of aldehydes are given in Tables 1, 2 and 3.

Recycling and reuse of ionic liquids

After the reaction was completed and work-up carried out as described above, the ionic liquid could be reused after drying at 100 °C (0.1 mmHg) without further treatment. However this would result in the accumulation of inorganic zinc salt residues and reduce the yield of subsequent reactions. Method A: the zinc residue was removed by dissolution of the ionic liquid (1 mL) in methylene chloride (4 mL) and the solid precipitate of $Zn(OH)_2$ was filtered. The ionic liquid was recovered on removal of methylene chloride and dried by further heating overnight at 70 °C (0.1 mmHg). The experimental procedure for alkylation with diethylzinc in recycled ionic liquid was the same as described above. Method B: after complete reaction, 1 equiv. of oxalic acid dissolved in acetone (1 mL) was added to quench the reaction and stirred for 1 hour. More acetone (3 mL) was added to the mixture and the solid precipitate of ZnC_2O_4 was filtered. The filtrate was subjected to rotary evaporation to remove the acetone, followed by extraction with diethyl ether. The ionic liquid, recovered on removal of the diethyl ether, was dried by further heating at 70 °C (0.1 mmHg). The experimental procedure for alkylation with diethylzinc in the recycled ionic liquid was the same as described above except the reaction mixture was heated at 40 °C after stirring overnight for a few hours.

3-Butyl-1-methylimidazolylidene zinc complexes

A three-necked 50 ml round bottom flask was charged with 1-methyl-3-butyl-1-methylimlidazolium bromide (0.5 g, 2.28 mmol) followed by dropwise addition of diethylzinc (0.11 mL, 1.14 mmol). The flask was capped with a septum, and the rate of gas evolution was monitored by a cranial tube connected to an oil-filled bubbler. After completion of the reaction as indicated by the cessation of gas evolution in 5 mins, the mixture was examined by NMR. The product was found to be a mixture of **3** and **4** in a ratio of about 1 : 4.

$[ZnBr_2(bmiy)_2]$ (3)

^1H NMR (CD_3CN): 7.46 (s, 2H), 7.43 (s, 2H,), 4.16 (t, 4H), 3.77 (s, 6H), 1.70 (m, 4H), 1.30 (m, 4H), 0.89 (t, 6H). ^{13}C NMR (CD_3CN): 173.9, 124.0, 122.3, 50.3, 37.7, 33.7, 20.0, 13.6.

$[Zn(\mu\text{-}Br)(Br)(bmiy)_2]_2$ (4)

^1H NMR (CD_3CN): 7.34 (s, 2H), 7.31 (s, 2H), 4.37 (t, 4H), 3.96 (s, 6H), 1.77 (m, 4H), 1.35 (m, 4H), 0.94 (t, 6H); ^{13}C NMR (CD_3CN): 173.6, 123.4, 121.7, 50.1, 37.7, 34.0, 19.9, 13.7.

MS (FAB): *m*/*z* 139 (100); 203 (18), cluster; 281 (2.7), cluster; 419 (1.6), cluster; 289 (2.1), 303 (4.3), 317 (9.0), 331 (11.4), 345 (8.5), 359 (4.3) and 373 (1.4) clusters; 413 (0.8), 427 (1.0), 441 (1.7), 455 (3.2), 469 (4.1), 483 (2.8), 497 (1.3) and 511 (0.4) clusters; 760 (0.4), 774 (0.9), 788 (1.5), 802 (2.2), 816 (2.6), 830 (2.5), 844 (1.7), 858 (0.8), 872 (0.3) and 886 (0.1) clusters.

† It is assumed generally that, if necessary, extraction of organic substrates from ionic liquids can be carried out with supercritical carbon dioxide in place of non-polar organic solvents. See ref. 26.

Acknowledgements

We thank NSERC and HKRGC for financial support of this research.

References

1 *Clean Solvents: Alternative Media for Chemical Reactions and Processing*, ed. M. Abraham and L. Moens, ACS Symp. Ser. No. 819, American Chemical Society, Washington, DC, 2001.
2 P. T. Anastas and J. C. Warner, *Green Chemistry: Theory and Practice*, Oxford Science Publications, Oxford, 1998.
3 C. J. Li and T. H. Chan, *Organic Reactions in Aqueous Media*, John Wiley & Sons, New York, 1997.
4 *Chemical Synthesis Using Supercritical Fluids*, ed. P. Jessop and W. Leitner, Wiley-VCH, Weinheim, 1999.
5 J. D. Holbrey and K. R. Seddon, *J. Chem. Soc., Dalton Trans.*, 1999, 2701; J. S. Wilkes, *Green Chem.*, 2002, **4**, 73.
6 For recent examples of reactions of ionic liquids with reactive organometallic reagents, see D. S. McGuinness, W. Mueller, P. Wasserscheid, K. J. Cavell, B. W. Skelton, A. H. White and U. Englert, *Organometallics*, 2002, **21**, 175.
7 C. J. Li and T. H. Chan, *Tetrahedron Lett.*, 1991, **32**, 7017; T. H. Chan and Y. Yang, *J. Am. Chem. Soc.*, 1999, **121**, 3228.
8 C. Petrier and J. L. Luche, *J. Org. Chem.*, 1983, **50**, 910.
9 T. H. Chan, Y. Yang and C. J. Li, *J. Org. Chem.*, 1999, **64**, 4452.
10 T. H. Chan, C. J. Li, M. C. Lee and Z. Y. Wei, *Can. J. Chem.*, 1994, **72**, 1181.
11 C. J. Li and T. H. Chan, *Tetrahedron*, 1999, **55**, 11149.
12 C. C. K. Keh, C. Wei and C. J. Li, *J. Am. Chem. Soc.*, 2003, **125**, 4062.
13 T. Vilaivan, C. Winotapan, T. Shinada and Y. Ohfune, *Tetrahedron Lett.*, 2001, **42**, 9073.
14 T. Kitazume and K. Kasai, *Green Chem.*, 2001, **3**, 30.
15 C. M. Gordon and A. Mccluskey, *Chem. Commun.*, 1999, 1431.
16 M. C. Law, K. Y. Wong and T. H. Chan, *Green Chem.*, 2002, **4**, 161.
17 C. M. Gordon and C. Ritchie, *Green Chem.*, 2002, **4**, 124.
18 (*a*) C. J. Mathews, P. J. Smith, T. Welton, A. J. P. White and D. J. Williams, *Organometallics*, 2001, **20**, 3848; (*b*) L. Xu, W. Chen and J. Xiao, *Organometallics*, 2000, **19**, 1123.
19 A. J. Arduengo III, H. V. Rasika Dias, F. Davidson and R. L. Harlow, *J. Organomet. Chem.*, 1993, **462**, 13.
20 S. Park and R. J. Kazlauskas, *J. Org. Chem.*, 2001, **66**, 8395.
21 (*a*) P. Knochel and R. D. Singer, *Chem. Rev.*, 1993, **93**, 2117; (*b*) K. Soai and S. Niwa, *Chem. Rev.*, 1992, **92**, 833; (*c*) B. Marx, *C. R. Hebd. Seances Acad. Sci., Ser. C*, 1968, **266**, 1646.
22 K. Tanaka and T. Toda, *Chem. Rev.*, 2000, **100**, 1025.
23 R. P. Swatloski, J. D. Holbrey and R. D. Rogers, *Green Chem.*, 2003, **5**, 361.
24 For the preparation and safe handling of dialkylzinc, see; *Synthetic Methods of Organometallic and Inorganic Chemistry*, ed. W. A. Herrmann, vol. 5, Thieme, Stuttgart, 1999.
25 M. C. Law, K. Y. Wong and T. H. Chan, *Green Chem.*, 2002, **4**, 328.
26 L. A. Blanchard, D. Hancu, E. J. Beckman and J. F. Brennecke, *Nature*, 1999, **399**, 28.

PAPER

www.rsc.org/greenchem

Triflic acid-promoted transacylation and deacylation reactions in ionic liquid solvents

Viorel D. Sarca† and Kenneth K. Laali*
Department of Chemistry, Kent State University, Kent, OH 44242, USA.
E-mail: klaali@kent.edu; Fax: 011-330-6722988

Received 7th January 2004, Accepted 17th March 2004
First published as an Advance Article on the web 31st March 2004

A convenient process for transacylation by sterically crowded aromatic ketones (namely acetylmesitylene **1**, acetyldurene **2**, acetylprehnitene **3**, acetylpentamethylbenzene **4** and diacetyldurene **5**) to activated aromatic compounds such as anisole has been developed using triflic acid (TfOH) as catalyst and employing various room temperature imidazolium ionic liquids as "eco-friendly" solvents under relatively mild conditions (at 70 °C). The yields have been optimized based on the arene to TfOH molar ratios and the reaction temperature. Deacetylation to transacylation product ratios depend on the reaction conditions and increase on raising temperature. In the absence of an activated arene receptor, hindered ketones are efficiently deacetylated by TfOH in the ionic liquid solvents. The simple process employed avoids the use of large excess of $AlCl_3$ or TFA, and chlorinated or nitrated solvents which were previously utilized to effect this transformation.

Introduction

Acid-catalyzed transfer of an acyl group from an aromatic ketone to an activated aromatic substrate is known as transacylation reaction (Fig. 1). It constitutes the reverse of the Friedel–Crafts acylation

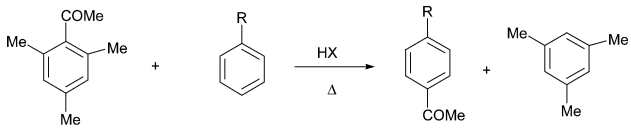

Fig. 1

process. The reaction is facilitated in the presence of *ortho* alkyl substituents which force the –COMe group out of coplanarity with the ring and weaken the Ar–COMe bond (Fig. 1).

Transacylation of acetophenones was previously observed in $AlCl_3$–HCl in 1,2-dichloroethane, $CHCl_3$, or $MeNO_2$ solvents accompanied by side reactions.[1] The significance of the *ortho* steric effect was shown in an early kinetic study[2] in 89.8% H_2SO_4, which also indicated that the presence of a second acetyl group in the *para* position (as in diacetyldurene) has a significant rate retardation effect because it destabilizes the benzenium ion of *ipso* protonation (Fig. 2).

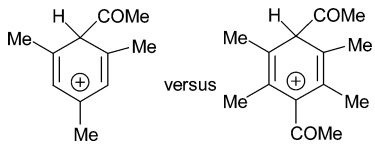

Fig. 2

Observation of slow "acetyl exchange" between acetylmesitylene and ^{14}C-labelled acetyl chloride and between acetyl[3,5-$^2H_2$]mesitylene and ^{14}C-labelled acetyl chloride in $AlCl_3$–$MeNO_2$ led Gore *et al.*[3] to postulate a synchronous reaction involving the *ipso* σ-complex of acetylation rather than *via* a stepwise acylation–deacylation or deacylation–reacylation (Fig. 3).

† Visiting scientist from Baldwin Wallace College, Berea, OH 44017, USA.

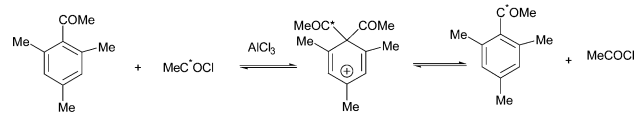

Fig. 3

Roberts and associates[4] employed a large excess of $AlCl_3 \cdot H_2O$ at 100 °C to effect transacylation and reported on the importance of catalyst concentration and temperature on the yields. To explain the formation of both transacylation product and diarylethenes under their reaction conditions, Roberts *et al.*[4] proposed a Lewis acid-catalyzed condensation reaction involving the $AlCl_3$-coordinated carboxonium ion derived from acetylmesitylene.

A detailed mechanistic study of transacylation by acetylpentamethylbenzene (AcPMB) was reported by Keumi and associates[5] in boiling TFA (100 fold excess) by means of product analysis, kinetics, and deuterium labelling. The combined data suggested a two-step deacylation–reacylation process (see Fig. 4) involving

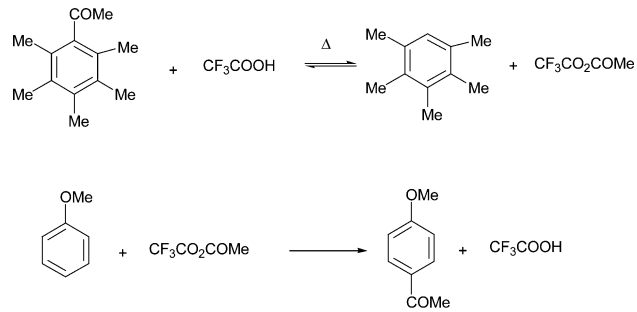

Fig. 4

initial ring protonation at the C-3/C-5 (*meta*) followed by proton shift to produce the benzenium ion of *ipso* attack which undergoes deacylation to give PMB and acetic trifluoroacetic mixed anhydride which then rapidly acylates the arene.

In a model stable ion study, Keumi *et al.*[5] showed that whereas PMB is CO-protonated in FSO_3H–SO_2ClF to form a carboxonium ion, a C,O-diprotonated carboxonium-benzenium dication is formed in FSO_3H–SbF_5/SO_2ClF, which on raising the temperature gives the pentamethylbenzenium ion and acetyl cation.

Olah and coworkers[6] found that various sterically crowded aromatic ketones can be deacetylated over Nafion-H perfluorinated resin sulfonic acid in refluxing toluene as solvent. Under these conditions little or no transacylation products were formed even

DOI: 10.1039/b400113c

with anisole. It was proposed that under solid superacid catalysis, the acylium ion formed *via* deacetylation of the *ipso* protonated benzenium ion forms ketene which is then polymerized (Fig. 5).

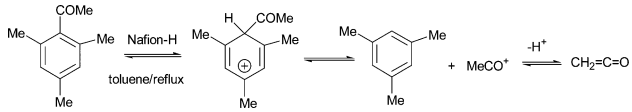

Fig. 5

Application of room temperature ionic liquids (RTILs), especially the imidazolium-based ILs, as "designer solvents", for organic synthesis is a subject of ongoing intense research effort in an emerging agenda for "green chemistry", and the rapidly growing literature include an ever-increasing number of organic and organometallic transformations.[7–13]

Friedel–Crafts acylation of representative aromatics has been reported in [emim]-$AlCl_3$ and in [bmim][BF_4]/$Cu(OTf)_2$.[14,15] Interestingly, the classical Friedel–Crafts acetylation mechanism is not altered in ionic liquid solvents.[16] However, no examples of transacylation of aromatics in ionic liquid solvents have been reported.

In relation to our continuing interest in electrophilic/carbocationic reactions and onium ion chemistry in ionic liquids and our previous studies of aromatic nitration,[17] electrophilic fluorination of arenes with NF reagents,[18] and fluorodediazoniation[19] in ILs, we report here on transacetylation and deacetylation of hindered acetophenones in several imidazolium ILs in the presence of TfOH. In favorable cases, quantitative conversions are achieved under mild conditions with little or no side reactions. The simple one-pot process employed avoids the use of a large excess of $AlCl_3$, TFA, high temperatures, as well as chlorinated or nitrated solvents which were previously utilized to bring about this transformation.

Results and discussion

Sterically crowded acetophenones acetylmesitylene **1**, acetyldurene **2**, acetylprehnitene **3**, acetylpentamethylbenzene **4** and diacetyldurene **5** (Fig. 6) were examined as substrates for transacylation to activated aromatics (typically anisole and toluene).

Ethylmethylimidazolium (EMIM) and butylmethylimidazolium (BMIM) salts with OTf, PF_6 and BF_4 counter ions (Fig. 7) were employed for this study. The data are summarized in Table 1.

Addition of solid acetyldurene **2** to [EMIM][BF_4] in a Schlenk tube gave a suspension which slowly dissolved upon sonication at rt. Addition of anisole (8 equivalents) followed by TfOH (8 equivalents) under nitrogen with cooling produced a viscous red solution which upon gentle heating (4 h at 70 °C) gave acetylanisole and durene nearly quantitatively (GC and GC-MS) (run 1, Table 1).

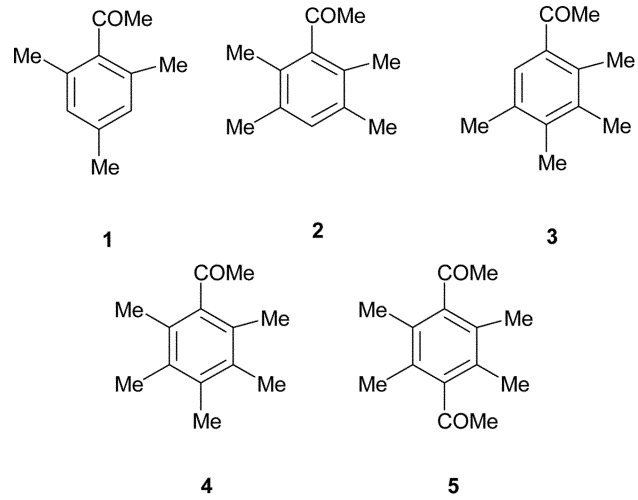

Fig. 6

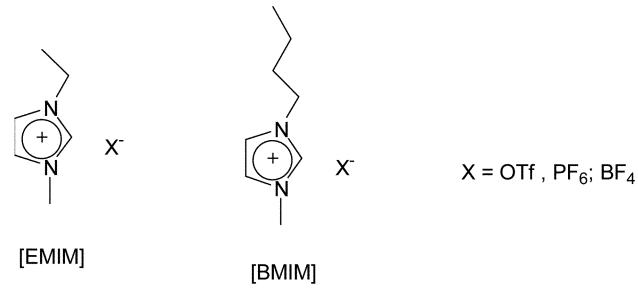

Fig. 7

Under similar conditions, **2** underwent transacylation to anisole in about 90% yield in [BMIM][PF_6] (run 2, Table 1). Acetylmesitylene **1** reacted in [EMIM][OTf] and in [BMIM][PF_6] ionic liquids to produce (after 5 h at 70 °C) acetylanisole and mesitylene quantitatively (runs 3–4, Table 1). Transacylation by **1** in [BMIM][OTf] to the less reactive nucleophile, toluene, employing 4 fold excess of TfOH proceeded less efficiently (run 5, Table 1). In this case, the yield of transacylation product (*p*-methylacetophenone) was substantially lower than the deacylation product (mesitylene). The outcome is similar to the findings of Keumi *et al.* in refluxing TFA solvent,[5] and reflects a two-step process in which the 2nd step (acylation of toluene with the *in situ* produced acetic trifluoromethanesulfonic mixed anhydride AcOTf) is less efficient than deacylation *via* the *ipso* σ-complex. Formation of AcOTf *via* Ac_2O–TfOH mixtures and its protonation and heterolytic cleavage to $MeCO^+$ have previously been reported in the literature.[20]

Table 1 Transacylation to arenes by sterically crowded acetophenones promoted by TfOH in imidazolium ILs at 70 °C

						Composition of rxn mixture (%)		
Run #	ArCOMe	ArH	ArCOMe : ArH : TfOH (molar ratio)	IL	Rxn time/h	Unreacted ArCOMe	New ArCOMe[a]	Arene formed
1	**2**	Anisole	1 : 8 : 8	[EMIM][BF_4]	4	0	98	100
2	**2**	Anisole	1 : 8 : 8	[BMIM][PF_6]	4	9	> 100	91
3	**1**	Anisole	1 : 8 : 8	[EMIM][OTf]	5	0	> 100	100
4	**1**	Anisole	1 : 8 : 8	[BMIM][PF_6]	5	0	> 100	100
5	**1**	Toluene	1 : 8 : 4	[BMIM][OTf]	5	15	15	85
6	**2**	Anisole	1 : 4 : 0	[EMIM][OTf]	24	8	98	91
7	**3**	Anisole	1 : 4 : 0	[EMIM][OTf]	24	0	> 100	100
8	**5**	Anisole	1 : 4 : 5	[EMIM][OTf]	48	49	46	40
9	**5**	Anisole	1 : 4 : 5	[EMIM][BF_4]	48	49	48	45
10	**3**	Toluene	1 : 4 : 4	[EMIM][OTf]	8	11	12	88
11	**1**	Toluene	1 : 8 : 4	[BMIM][OTf]	24	2	20	98
12	**5**	Anisole	1 : 4 : 16	[BMIM][OTf]	24	7	81	92
13	**5**	Anisole	1 : 4 : 6	[BMIM][OTf]	5	53	46	46

[a] For entries marked with > 100%, the calculated conversions for the new ketones were between 101–108%. This possibly stems from incomplete deprotonation/Et_2O extraction in earlier runs (see discussion).

Unlike previous studies in $AlCl_3$–HCl[4] or TFA[5] where the products are isolated following neutralization of a large quantity of acid so as to deprotonate and release the new ketones into the organic phase, isolation of the products in the IL version is accomplished by several extractions with diethyl ether and without aqueous work-up, which also allows the cycle to be repeated without addition of fresh TfOH (see later discussion). The combined ether extracts are neutralized as a precaution for GC and GC-MS analysis. NMR analysis of the IL phase following Et_2O extraction showed that apart from the IL, traces of the reaction mixture remained in the IL phase (estimated between 5–7% by NMR). Therefore, deprotonation of $ArCOH^+Me$ product and any remaining unreacted starting ketone with excess Et_2O must occur efficiently, but incompletely [for a relative comparison: pK_a for Et_2OH^+ = −3.6;[21a] H_o (TfOH) ~ −14;[21b] H_o for *p*-MeC_6H_4COMe in FSO_3H ~ −12[21c] and pK_{HB} for *p*-MeC_6H_4COMe = −5.7[21c]], and this is believed to be the origin of "higher than quantitative" conversions calculated for the new ketones in several entries in Table 1 based on GC and after response factor correction. Similar results were obtained in [BMIM][PF_6].

By addition of acetyldurene and anisole (1 : 4 ratio) to the used [EMIM][OTf] without further addition of fresh TfOH (run 6, Table 1) it was possible to repeat the process. A further reaction cycle was effected after removal of the organic phase from run 6 by reacting acetylprehnitene with anisole, (run 7, Table 1), in both cases with little or no reduction in the conversions.

In line with the early kinetic study,[2] reaction of diacetyldurene with anisole in [EMIM][OTf] or in [EMIM][BF_4] ILs with TfOH (4 equivalents) proceeded less efficiently to give acetylanisole and durene (double deacetylation; with only traces of acetyldurene being detected) in 40–50% yields (runs 8–9, Table 1). The outcome of the reaction of acetylprehnitene with toluene (run 10, Table 1) was similar to that of acetylmesitylene with toluene (run 5), resulting in higher yields of deacetylation product relative to transacylation product.

Comparison between runs 5 and 11 (acetylmesitylene with toluene and TfOH in [BMIM][OTf]) shows that increased conversions can be achieved at longer reaction times. Comparing the outcomes of experiments 12 and 13 in conjunction with runs 8 and 9 for the reaction of diacetyldurene with anisole demonstrates that the amount of TfOH employed and the reaction time are both important in the reaction, with the TfOH : arene ratio being a more dominant factor in increasing conversion.

The transacylation to deacylation product ratios changed significantly in favor of deacylation upon increasing the reaction temperature from 70 to 100 °C, even in the presence of anisole. The results are summarized in Table 2. Thus acetylpentamethylbenzene **4** and diacetyldurene **5** were efficiently deacetylated with TfOH (4 equivalents) in the IL solvents [BMIM][PF_6], [BMIM][OTf] or [EMIM][OTf] after 10 h, with no acetylanisole being detected (runs 1–3). Employing acetophenones **1**, **3**, and **5**, in reaction with toluene, *p*-diethylbenzene or anisole, but with shorter reaction times (5 h) (runs 4–6; Table 2), resulted in deacetylation in lower yields (50–55%).

In experiments 7–8, diacetydurene is readily deacetylated, and the conversion is noticeably higher with 8 fold excess of TfOH as compared to 4 fold excess. This double deacetylation process, which is most likely stepwise, occurs efficiently in the imidazolium IL solvents despite destabilization of the first benzenium ion intermediate (see Fig. 2). In runs 9–12, deacetylations were effected in the absence of the aromatic substrates by simply heating acetophenones **3** and **5** in [EMIM][OTf] or [BMIM][OTf] in the presence of TfOH. The yields, once again, point to the significance of the acetophenone : TfOH molar ratios, with near quantitative conversions being obtained by employing 8 equivalents of TfOH.

Absence of transacylation product on increasing temperature is likely due to the decomposition of the mixed anhydride AcOTf formed *in situ via* the deacylation step (as in the proposed Scheme for TFA; Fig. 4). *In situ* deacetylation of the transacylation product (*e.g.* 4-methoxyacetophenone, 4-methylacetophenone) is unlikely as Roberts *et al.* found no reaction with these substrates at 100 °C in $AlCl_3 \cdot H_2O$.[4]

In conclusion, the present study demonstrates that transacylation and deacylation of hindered acetophenones can be conveniently accomplished in imidazolium ILs as solvent with TfOH as promoter under relatively mild conditions. Chemoselectivity (transacylation *versus* deacylation) depends on the reaction temperature. By tweaking the reaction conditions (arene to TfOH ratio, the choice of arene receptor, and reaction time), high conversions could be reached. Examples have been provided where the reaction cycle could be repeated in the used ionic liquid without addition of fresh TfOH. The present method appears superior to previous methods utilizing excess TFA or $AlCl_3$–H_2O at high temperatures or $AlCl_3$ in chlorinated or nitrated solvents.

Experimental

General

All glassware were oven-dried at 120 °C and flushed with nitrogen immediately prior to use.

Transfer of reagents was performed under a blanket of dry nitrogen. Reactions were performed in small Schlenk tubes under nitrogen. Imidazolium ionic liquids employed were purchased from Aldrich, Merck, or were available from previous studies[17–19] in our laboratory (they were used without any pre-treatment). Hindered acetophenones were synthesized and purified according to previously published procedures.[22]

The aromatic substrates and other chemicals were highest purity commercial samples which were used as received. Et_2O was dried

Table 2 Deacylation of sterically crowded acetophenones promoted by TfOH in imidazolium ILs at 100 °C

						Composition of rxn mixture (%)		
Run #	ArCOMe	ArH	ArCOMe : ArH : TfOH (molar ratio)	IL	Rxn time/h	Unreacted ArCOMe	New ArCOMe	Arene formed
1	**4**	Anisole	1 : 4 : 4	[BMIM][PF_6]	10	8	0	92
2	**5**	Anisole	1 : 4 : 4	[EMIM][OTf]	10	16	0	84
3	**5**	Anisole	1 : 4 : 4	[BMIM][OTf]	10	15	0	85
4	**1**	Toluene	1 : 8 : 4	[BMIM][OTf]	5	47	0	52
5	**3**	*p*-Et_2Ph	1 : 8 :4	[EMIM][OTf]	5	44	0	55
6	**5**	Anisole	1 : 8 : 4	[BMIM][OTf]	5	46	0	53
7	**5**	EtPh	1 : 4 : 4	[EMIM][OTf]	8	38	0	62
8	**5**	p-Et_2Ph	1 : 4 : 8	[BMIM][OTf]	8	14	0	87
9	**3**	none	1 : 0 : 4	[EMIM][OTf]	5	47	0	52
10	**5**	none	1 : 0 : 4	[EMIM][OTf]	5	57	0	42
11	**5**	none	1 : 0 : 8	[BMIM][OTf]	4	2	0	98
12	**5**	none	1 : 0 : 8	[EMIM][OTf]	5	0	0	100

over sodium. TfOH (Aldrich) was distilled under nitrogen and stored in a Nalgene bottle in the freezer.

The reaction mixtures were analyzed by capillary GC and an ion-trap GC-MS with MS/MS capability. Product identification was accomplished either by co-injection with authentic samples and/or by GC-MS. The reported conversions are based on GC after response factor correction. The GC response factors were corrected by analysis of various authentic mixtures of hindered ketones, the aromatic products and the acetyl transfer products (for example, acetylmesitylene, mesitylene and acetylanisole). As was found previously,[5] only the *para* isomer is formed in transacylation reaction. Regioselectivity was verified in the present study by GC-MS using authentic 2-methoxyacetophenone and 2-methylacetophenone.

Typical procedure. The [EMIM][OTf] (1.15 g, 4.43 mmol) was charged into a Schlenk tube and acetylmesitylene **1** (0.162 g, 1 mmol) was added to the IL under nitrogen. The closed Schlenk tube was placed in an ultrasonic bath at rt for 10 minutes to increase solubility. After addition of anisole (0.865 g, 8 mmol) and magnetic stirring at rt for 10 min, the Schlenk tube was cooled to 0 °C and TfOH (0.6 mL, 8 mmol) was added under a nitrogen atmosphere. The Schlenk tube was re-sealed and placed in a thermostatic bath at 70 °C under magnetic stirring, whereupon the medium turned red. The work-up procedure involved addition of dry Et_2O (4 mL × 5) and neutralization of the combined ether extracts (as a precaution for subsequent GC and GC-MS analysis) by washing with water (4 mL × 2), with 5% $NaHCO_3$ solution (4 mL × 2), and water (3 mL × 2) respectively, followed by separation of the organic phase, drying ($MgSO_4$) and simple filtration. The procedure was similar when using other ILs. Addition of TfOH to [BMIM][PF_6], [EMIM][BF_4] or [BMIM][BF_4] results in competing counter-ion exchange, but as was shown previously for aromatic nitration,[17] this process did not cause noticeable changes in conversions under a comparable set of conditions. The procedure for deacetylation reactions was similar except for the reaction temperature (100 °C) and that in some runs no aromatic compound was used.

Recovery/regeneration of IL. This was accomplished by heating the used imidazolium ILs under high vacuum at 100 °C to remove the aromatic compounds and any remaining TfOH or other acidic impurities.

Acknowledgement

V. D. S. thanks Dr. M. Gangoda for assistance with GC and GC-MS, postgraduate student M. Khairuddean for assistance with NMR, and is grateful for the opportunity to conduct this research as a visiting scientist in Laali laboratory at Kent State.

References

1 A. D. Andreou, R. V. Bulbulian and P. H. Gore, *J. Chem. Res.(S)*, 1980, 225.
2 P. H. Gore and B. S. Moonga, *J. Chem. Res. (S)*, 1989, 292.
3 A. D. Andreou, R. V. Bulbulian, P. H. Gore, D. F. C. Morris and E. L. Short, *J. Chem. Soc., Perkin Trans. 2*, 1981, 830.
4 A. M. El-Khawaga, R. M. Roberts and K. M. Sweeney, *J. Org. Chem.*, 1985, **50**, 2055.
5 T. Keumi, T. Morita, T. Shimada, N. Teshima, H. Kitajima and G. K. S. Prakash, *J. Chem. Soc., Perkin Trans. 2*, 1986, 847.
6 G. A. Olah, K Laali and A. K. Malhotra, *J. Org. Chem.*, 1983, **48**, 3360.
7 H. Zhao and S. V. Malhotra, *Aldrichimica Acta*, 2002, **35**, 75.
8 H. Olivier-Bourbigou and L. Magna, *J. Mol. Catal., A: Chem.*, 2002, **182–183**, 419.
9 T. Welton, *Chem. Rev.*, 1999, **99**, 2071.
10 J. Dupont, R. F. de Souza and P. A. Z. Suarez, *Chem. Rev.*, 2002, **102**, 3667.
11 P. Wasserscheid and W. Keim, *Angew. Chem., Int. Ed.*, 2000, **39**, 3772.
12 *Ionic Liquids in Synthesis*, ed. P. Wasserscheid and T. Welton, Wiley-VCH, Weinheim, 2003.
13 *Ionic Liquids, Industrial Applications to Green Chemistry*, ed. R. D. Rogers and K. R. Seddon, ACS Symp. Ser. 818, American Chemical Society, Washington, DC, 2002.
14 C. J. Adams, M. J. Earl, G. Glyn and K. R. Seddon, *Chem. Commun.*, 1998, 2097.
15 J. Ross and J. Xiao, *Green Chem.*, 2002, **4**, 129.
16 S. Csihony, H. Mehdi and I. T. Horvath, *Green Chem.*, 2001, **3**, 307.
17 K. K. Laali and V. J. Gettwert, *J. Org. Chem.*, 2001, **66**, 35.
18 K. K. Laali and G. L. Borodkin, *J. Chem. Soc., Perkin Trans. 2*, 2002, 953.
19 K. K. Laali and V. J. Gettwert, *J. Fluorine Chem*, 2001, **107**, 31.
20 (*a*) A. Germain and A. Commeyras, *J. Chem. Soc., Chem. Commun.*, 1972, 1345; (*b*) A. Germain, A. Commeyras and A. Casadevall, *Bull. Chem. Soc. Fr.*, 1973, **7–8**, 2527.
21 (*a*) S. Ege, *Organic Chemistry, Structure and Reactivity*, 5th edn., Houghton-Mifflin, Boston, 2004; (*b*) D. A. Klumpp and S. Lau, *J. Org. Chem.*, 1999, **64**, 7309; (*c*) V. Gold, K. Laali, K. P. Morris and L. Zdunek, *J. Chem. Soc., Chem. Commun.*, 1981, 769.
22 A. D. Andreou, R. V. Bulbulian and P. H. Gore, *Tetrahedron*, 1980, **36**, 2101.

PAPER

Synthesis of metallophthalocyanine end-capped polymers and their catalytic activity for the copolymerization of CO_2 and propylene oxide

Y. Z. Meng,*[ab] W. Wan,[a] M. Xiao[a] and Allan S. Hay*[c]

[a] *Institute of Energy & Environmental Materials, School of Physics & Engineering, Sun Yat-Sen University, Guangzhou 510275, P. R. China. E-mail: stdpmeng@zsu.edu.cn; Fax: +8620-85232337*

[b] *Guangzhou Institute of Chemistry, Chinese Academy of Sciences, P.O. Box 1122, Guangzhou 510650, P. R. China*

[c] *Department of Chemistry, McGill University, 801 Sherbrooke St. West, Montreal, Quebec H3A 2K6, Canada. E-mail: allan.hay@mcgill.ca*

Received 14th January 2004, Accepted 12th March 2004
First published as an Advance Article on the web 31st March 2004

A series of metallophthalocyanine end-capped poly(arylene ether sulfone)s containing zinc were synthesized from reduced phenolphthalein by an improved method. The molecular structure of zinc metallophthalocyanine-containing polymer was confirmed by Fourier-transform spectroscopy, wide-angle X-ray diffraction technique, UV-visible spectra, and ^{1}H-NMR spectra. The zinc metallophthalocyanine-containing polymer was found to be soluble in some solvents, and the colored polymer showed maximum visible absorption at 665 nm. Copolymerization between carbon dioxide and propylene oxide (PO) was performed using the zinc metallophthalocyanine end-capped poly(arylene ether sulfone) as a catalyst. This is the first report to describe the use of metallophthalocyanine-containing polymer as a polymer-supported catalyst to activate carbon dioxide. Catalytic activity (30 g-polymer/g catalyst) was achieved by optimizing the PO/catalyst ratio. NMR measurement revealed that the synthesized copolymer from carbon dioxide and PO had an alternating structure. Thermal properties of the copolymer were determined by thermogravimetric analysis, and the results demonstrated that the copolymer exhibited a high glass transition temperature of 35 °C and decomposition temperature of 247 °C.

Introduction

Carbon dioxide (CO_2) is well-known to be regarded as an environmental pollutant because it is a major cause of the greenhouse effect, which contributes highly to climate change.[1–5] Thus, the reduction of industrial waste CO_2 emissions is now seriously considered by all nations in the world.[2,5–6] CO_2 chemistry is today in the position of CO chemistry at the beginning of last century: it took forty years for CO chemistry to be developed to an industrial level. One can foresee that with the correct approach, new catalysts can be developed to activate CO_2 and enable industrial usage of this carbon source. As a matter of fact, Nature uses carbon dioxide for the synthesis of a myriad of products, through many different ways that are characteristic of microorganisms, plants and algae. A vast scientific and patent literature demonstrate that carbon dioxide is a potential raw material for many fine chemicals and commodities, with low energy input (reactions can occur at room temperature). More recently processes based on the use of catalysts for carbon dioxide conversion have been exploited opening a new potential market for carbon dioxide as a source of carbon.[7]

Among these utilizations of CO_2, the preference is to use carbon dioxide directly as a co-monomer in polymer synthesis. For example, aliphatic polycarbonates can be obtained *via* the copolymerization of CO_2 with epoxides, such as ethylene oxide (EO), propylene oxide (PO), isobutylene oxide (BO) and cycloheptene oxide (CHO). Inoue and co-workers carried out pioneering work on the alternating co-polymerization of carbon dioxide and propylene oxide using diethyl zinc/water as catalyst in 1960.[8–10] Since then, a variety of related catalyst and catalyst precursors containing zinc or other metals have been developed to enhance the catalytic efficiency.[11–13]

For example, aluminium porphyrin complexes have been used for alternating copolymers of carbon dioxide and cyclic ether.[14,15] In particular, (5,10,15,20-tetraphenylporphinato)aluminium chloride (TPPAlCl) complexed with an appropriate quaternary salt such as ethyltriphenylphosponium bromide ($EtPh_3PBr$) or tetraethylammonium bromide (Et_4NBr) was reported to be an effective catalyst for the copolymerization of CO_2 with epoxides.[16,17] In this case, the synthesized polymer using such catalyst exhibited a narrow molecular weight distribution. However, only polymers with rather low molecular weight of 1200–9000 were obtained, and the copolymerization process needed a very long reaction time of 12–40 days. Copolymerization of CO_2 and PO was also carried out using aluminiumphthalocyanine complexes as catalysts.[18–20]

It has also been well-documented in literature that zinc dicarboxylates (for example, zinc glutarate) were the most effective catalysts to yield alternating copolymers from CO_2 and epoxides.[13] We have reported the synthesis of an alternating copolymer from CO_2 and propylene oxide in an extremely high yield by using a supported zinc glutarate.[11,12] The highest catalytic activity was 160 g-polymer g-catalyst^{-1}.[7] It is believed that the enhanced catalytic activity resulted from the increase in the surface area of the catalysts. Considering this connection, it is anticipated that the catalytic activity of designed catalysts could be increased by increasing their solubility in the reaction system. In previous work, we have synthesized a series of polyaromatics containing dicyanine groups on the backbone of these polymers.[21,22] In this work, we aim at preparing soluble poly(arylene ether)s having covalently bound zinc(II) naphthalocyanine units with zinc glutarate as a new catalyst to activate and fix carbon dioxide into a polymer. Compared with insoluble catalysts, soluble and metal-containing catalysts show promise as having high activities for the copolymerization of carbon dioxide and epoxides.

Experimental

Materials

Propylene oxide with a purity of 99.5% was dehydrated by distillation over calcium hydride under dry nitrogen gas flow for 2

DOI: 10.1039/b400624k

h. In some cases, PO was further purified by distillation over sodium hydroxide and calcium hydride simultaneously under dry nitrogen gas for 6 h. The as-treated PO was then stored over 4A molecular sieves prior to use. Carbon dioxide with purity greater than 99.8% was used as received. Phenolphthalein, 4,4′-isopropylidenediphenol (BPA) (Aldrich Chemicals Inc), 1,2-dicyanobenzene (ACROS); fumaronitrile (TOKYO KASEI KOG CO, LTD), bis(4-chlorophenyl)sulfone, dimethylacetamide (DMAc), quinoline, toluene, chloroform, methanol, and acetic acid were obtained from commercial sources and used as received.

Instrumentation

The glass transition temperatures (T_g) were determined using a DSC instrument (model NETZSCH 204) at a heating rate of 20 °C min^{-1} under nitrogen flow of 100 mL min^{-1}. The reported T_g values were recorded from the second scan after first heating and quenching. The ^{1}H-NMR spectra were recorded on a DRX-400 instrument using dimethysulfoxide-d_6(DMSO-d_6) and chloroform ($CDCl_3$) as solvents. Infrared spectra were recorded using the KBr pellet method using an Analect RFX-65A FTIR spectrophotometer. UV-visible spectra were recorded on a SHIMADZU UV-2550 spectrophotometer. Thermogravimetric analysis was carried out employing a Pekin-Elmer thermogravimetric analyzer (TGA/DTA; model TGS-2) under a protective nitrogen atmosphere (100 mL min^{-1}) at a heating rate of 20 °C min^{-1}. In addition, wide-angle X-ray diffraction (WAXD) measurements were performed at room temperature using a Rigaku D/max-1200 to analyze the structure of the catalyst. The 2θ scan data were collected at 0.05° intervals over a range of 4–70°. For a given PPC copolymer, the relative and specific viscosities were measured at concentrations in the range of 0.10–0.50 g dL^{-1}, the [η] value was derived by extrapolating the reduced inherent viscosities to infinite dilution. The number average molecular weight can be calculated from the formula: [η] = $1.11 \times 10^{-4} M_n^{0.8}$ (dL g^{-1}).[23]

Preparation of zinc glutarate

Zinc glutarate was synthesized from zinc oxides and glutaric acid under magnetic stirring as described in previous work.[7]

Preparation of zinc metallophthalocyanine end-capped poly(aryl ether sulfone)s

The syntheses of the metal-containing aromatic copolymers **4** have been described in previous works.[24–26] For the synthesis of copolymer **5**, as depicted in Scheme 1, to a 25 mL three-neck flask equipped with a condenser and nitrogen gas inlet, the metal-containing poly(arylene ether) copolymer **4** (1 g), 1,2-dicyanobenzene (3.8254 g), zinc glutarate (4.958 g), and 50 mL of quinoline were added. Under an atmosphere of nitrogen, the mixture was heated to 220–240 °C for 6–8 hour, and thereafter the reaction mixture became dark blue. The mixture was poured into a mixture of 30 mL methanol and 2 mL of hydrochloric acid (36%), with vigorous stirring. The precipitated deep green to blue particles were washed with acetone, water, dilute hydrochloric acid, and finally with water and ethanol. The precipitates were collected by filtration and extracted by chloroform, using a Soxhlet extractor. The chloroform solution was concentrated and precipitated into methanol. The dark blue fibrous copolymer **5** was produced and dried at 110 °C for 24 hours.

Synthetic procedure for polymers

The copolymerization of CO_2 and PO was carried out in a 500 mL autoclave equipped with a mechanical stirrer. The above synthesized catalyst, *i.e.* zinc metallophthalocyanine end-capped poly(aryl ether sulfone), was further dried at 100 °C for 24 h prior to being used for the polymerization process. Dry catalyst was then introduced into the autoclave as quickly as possible. The autoclave was then capped with its head. The autoclave with catalyst inside was further dried for 24 h under vacuum at 60 °C. Subsequently, the

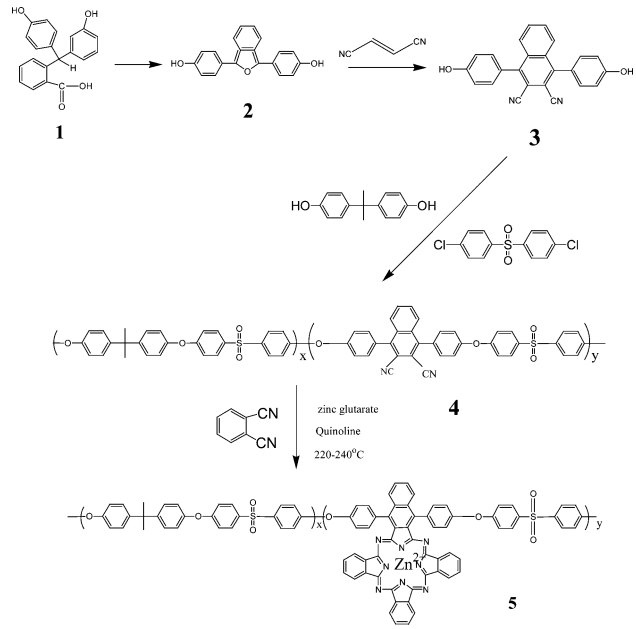

Scheme 1 Synthesis of the metal-containing copolymer **5** (ZM-PAE).

autoclave was purged with carbon dioxide and evacuated alternatively three times, followed by adding purified PO with a syringe. The autoclave was then pressurized to 5.0 MPa using a CO_2 cylinder. The polymerization was performed at 60 °C under stirring for 40 h. The autoclave was cooled to room temperature and the pressure was released. The resulting viscous mixture was removed, diluted with THF and transferred to a separating funnel. The catalyst residual was removed by filtration due to the insolubility of the catalyst in THF. The viscous solution was concentrated to a suitable concentration using a rotary evaporator. Finally, the concentrated copolymer solution was precipitated out in vigorously stirred methanol. The as-made poly(propylene carbonate) (PPC) was collected by filtration and dried for 2 days at 70 °C under vacuum. Meanwhile, the resulting filtrate was distilled to remove methanol and THF to yield a methanol soluble product.

Results and discussion

Synthesis of zinc metallophthalocyanine end-capped poly(aryl ether sulfone)s

Fig. 1 shows the ^{1}H NMR spectrum of the zinc metallophthalocyanine end-capped poly(arylene ether sulfone) **5** (ZM-

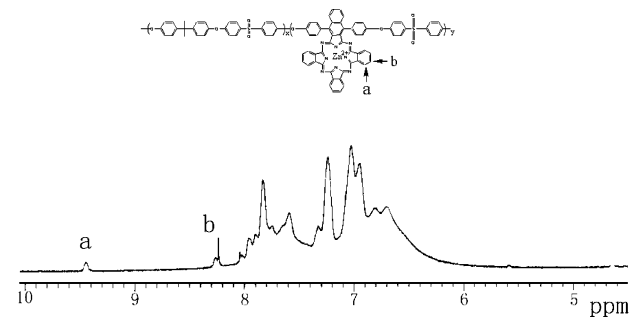

Fig. 1 ^{1}H-NMR spectrum for ZM-PAE obtained at 90 °C, in DMSO-d^6.

PAE); it is evident that the signals of protons **a** and **b** appear at 9.46 and 8.35 ppm (broad peak), respectively. Because protons **a** and **b** are not very close to the core of the large metal-complex ring, the downfield shift effects of the metal-complex ring on the chemical shift of protons **a** and **b** are not significant. The signal intensities of protons **a** and **b** are weak because the metal-complex units constitute about 7.1 mol% as estimated from NMR character-

ization. This value indicates that about 71% of the dicyanobenzene groups were converted and incorporated into the metal-complex rings.

The UV-visible spectrum of the ZM-PAE catalyst is shown in Fig. 2. From this figure, it can be clearly seen that the strong

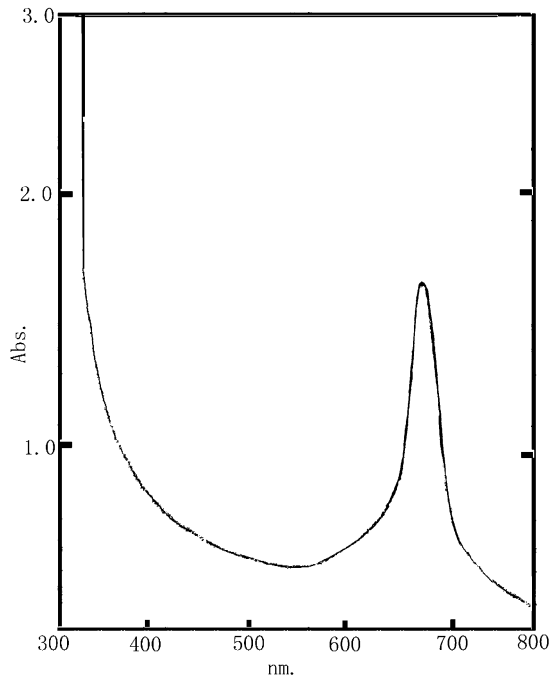

Fig. 2 Optical absorption spectrum of the ZM-PAE copolymer **2** in chloroform.

absorption in the visible range resulted from the metallophthalocyanine rings. The absorption maximum value of the catalyst is 665 nm and was found to be colored gray green as expected. This indicated that the ring closure took place and the copolymer **2** was produced as depicted in Scheme 1.

The X-ray diffraction patterns of the ZM-PAE catalyst and neat zinc glutarate are shown in Fig. 3 and 4, respectively. It can be seen

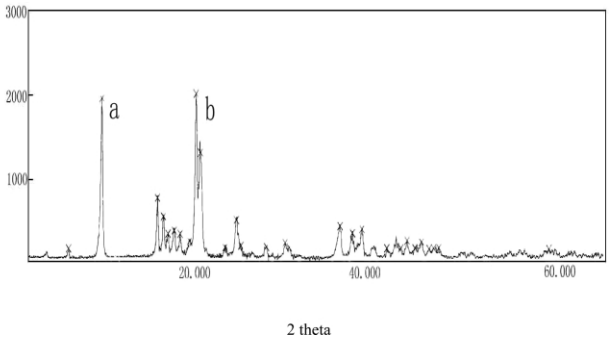

Fig. 3 X-Ray of diffraction pattern of ZM-PAE catalyst.

that two patterns are the same, owing to the existence of zinc glutarate that acts as the salt to produce the covalent metallophthalocyanine rings. To determine its crystalline structure, two peaks (peaks **a** and **b**) located at around 2θ = 12.7, 22.5° were selected to calculate their intensity/FWHM (full width at half-maximum) values. The results are listed in Table 1. The intensity/FWHM or the crystallinity of ZM-PAE catalyst appeared to be good but to be lower when compared with neat zinc glutarate. As exploited in previous work,[7] the catalytic activity of zinc glutarate for the copolymerization between CO_2 and PO is believed to positively proportional to the crystallinity of zinc salts.

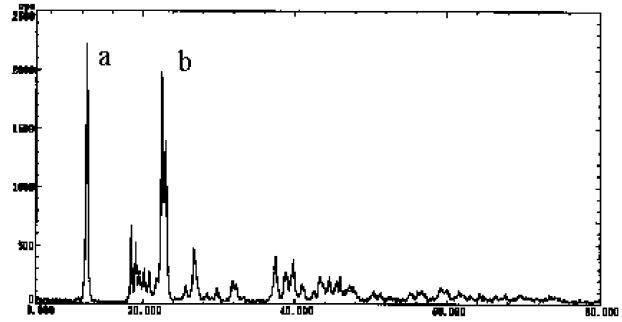

Fig. 4 X-Ray of diffraction pattern of zinc glutarate.

Table 1 X-Ray diffraction data of ZM-PAE catalyst and zinc glutarate

Peak no.	2 theta	FWHM	*d*-value	Intensity/ FWHM
ZM-PAE				
a	12.660	0.235	6.9861	8348.9
b	22.460	0.235	3.9551	8557.4
Zinc glutarate [ref. 7]				
a	12.636	—	—	34,823
b	22.449	—	—	28,815

Copolymerization of CO_2 and PO using ZM-PAE catalyst

As described in Scheme 2, the copolymerization of CO_2 and PO has been extensively studied elsewhere in the literature by using zinc

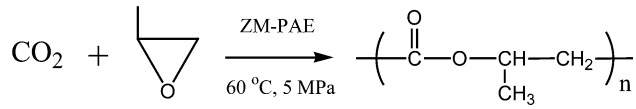

Scheme 2 Copolymerization of CO_2 and PO using ZM-PAE catalyst.

dicarboxylates as catalysts.[7–13] Among these catalysts, zinc glutarate was found to give the highest yield in the synthesis of PPC.[12] The zinc glutarates were generally synthesized as powders from zinc oxide and glutaric acid.[7,13] Due to the inherent insolubility of zinc glutarate in solvents including water, thus the catalyst acts as a heterogeneous rather than homogeneous catalyst in the copolymerization. In order to further increase the catalytic activity of the catalyst, the zinc metallophthalocyanine end-capped poly(aryl ether sulfone) or ZM-PAE was thought to be an new approach. This is due to the solubility of ZM-PAE in PO; in this case, the copolymerization can be carried out homogeneously. Upon the completion of polymerization, ZM-PAE can be separated from the polymerization solution by simply precipitating it out in acetone. The zinc cannot leach into the solution because of the formation of a ZM-PAE complex. All the ZM-PAE catalyst can be isolated from the produced polymer due to their solubility difference. Using the same copolymerization conditions as previous work,[7] the reaction was performed under a pressure of 5.0 MPa with PO either as monomer or solvent. In this process, the autoclave must be dried thoroughly because trace water can reduce the activity and in turn yield low molecular weight PPC. Therefore, the autoclave and the catalyst in the reactor have to be carefully dried at 60 °C under vacuum for 24 h prior to the copolymerization.

Table 2 lists the experimental results for the copolymerization with varying PO/ZM-PAE ratios. By changing the ratio from 83 (mL g-catalyst^{-1}) to 250 (mL g-catalyst^{-1}), an optimum PO/ZM-PAE of 125 (mL g-catalyst^{-1}) can be observed as evidenced in Table 2. Relatively high molecular weight PPCs were yielded ranging from 20 k to 40 k Da. It can also be seen that the catalytic activity increases with increasing cat/PO ratio up to 1/125 and, thereafter, decreases with further increase of the ratio. This behavior is believed to result from the decrease in the solubility of

Table 2 Effect of ZM-PAE/PO ratio on the yield and molecular weight of PPC

PO/ml	Catalyst/g	Zn content/g	PO/catalyst ratio (ml g-catalyst^{-1})	Yield/ g g-catalyst^{-1}	$\bar{M}_n$ (k)
100	0.4	0.06	250	7.6	23.0
100	0.6	0.09	167	13.2	31.0
100	0.8	0.12	125	18.4	35.0
100	1.0	0.15	100	11.6	36.0

Copolymerziation conditions: temperature, 60 °C; reaction time, 40 h; pressure of CO_2, 5.0 MPa, stirred at 125 rpm in a 500 mL autoclave.

ZM-PAE in PO in the presence of the resulting PPC copolymer. For the molecular weight, however, no obvious changes were observed when the cat/PO ratio exceeded 1/167. Even when lower ZM-PAE concentration was used for the copolymerization, no obvious catalytic activity enhancement was afforded, as shown in Table 3.

Table 3 Effect of PO amount on the yield and molecular weight of PPC

PO/ml	Catalyst/g	Zn content/g	PO/catalyst ratio (mL g-catalyst^{-1})	Yield/ g g-catalyst^{-1}	$\bar{M}_n$ (k)
100	0.8	0.12	125	18.4	35.3
200	0.8	0.12	250	17.9	30.2
300	0.8	0.12	375	16.4	57.6
400	0.8	0.12	500	17.2	22.4

Reaction conditions: reaction time, 40 h; pressure, 5.0 MPa, time of dryness 24 h.

The influence of reaction temperature was investigated and the results were tabulated in Table 4. The experimental data showed that the yield increases with increasing temperatures, up to 60 °C, and thereafter decreases dramatically. Therefore, we can conclude that the preferred polymerization temperature ranges from 50 to 60 °C. For the molecular weight of the PPCs, similarly, the relatively high molecular weight PPCs were produced (Table 4).

As listed in Table 5, the investigation of the effect of reaction time on the catalytic activity demonstrated an increase of copolymer yield with the increase of reaction time. We have previously reported the same behavior for neat zinc glutarate.[7] This increment was observed for reaction times less than 40 h, however, this increment extended up to 80 h because of the solubility of the ZM-PAE catalyst. The molecular weight of PPC also increases with increasing reaction time up to 20 h, but no obvious changes were observed with further increments. This implies that the molecular weight of PPC is dependent upon the solubility of the resulting copolymers.

Properties for the synthesized PPC copolymers

^{1}H NMR technique was used to characterize the molecular structure of the synthesized PPC copolymer. The observed peaks were assigned as follows: ^{1}H-NMR ($CDCl_3$), δ (ppm) 1.34 (d, 3H; $-CH_3$), 4.17 (m, 2H; H_2C-), 5.00 (m, 1H; –CH–). By comparing the results with previous work,[12] the synthesized PPC has an alternating molecular structure, because the assignment of random PPC copolymer are of (^{1}H NMR ($CDCl_3$), δ (ppm) 1.16 (d, 3H; $-CH_3$), 3.58 (m, 2H; $-CH_2CH-$), 3.45 (m, 1H; $-CH_2CH-$)). A trace amount of ether unit or poly(propylene oxide) (less than 2 wt%) was observed in the ^{1}H NMR spectrum at 1.16 and 3.58 ppm. These peaks correspond to the protons of CH_3 and CH_2CH in the poly(propylene oxide) units, respectively. Fig. 5 shows the ^{13}C-

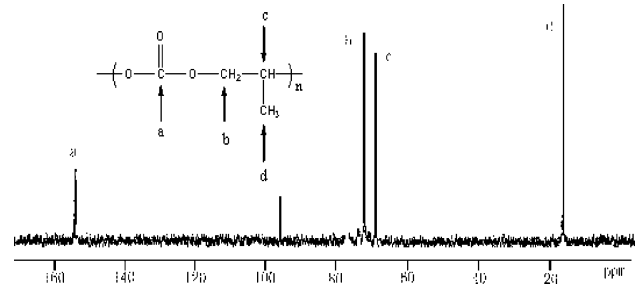

Fig. 5 ^{13}C-NMR spectrum for PPC.

NMR spectrum for the synthesized PPC copolymer. Only four peaks were assigned as follows: ^{13}C-NMR (ClD_3), δ (ppm) 16.1 ($-CH_3$), 69.0 ($-CH_2CH-$), 72.2 ($-CH_2CH-$), 154.2 (OCOO). The results clearly indicated that the synthesized PPC copolymer exhibited a strictly arranged alternating molecular structure. The FT-IR spectrum for the PPC is shown in Fig. 6. The intensive absorptions at 1750 cm^{-1} (s, C=O), 1250 cm^{-1}(s, C–O) and 790 cm^{-1} (s, C–O) show the ester structure of the PPC copolymer.

Thermal properties for the PPC copolymer with varying molecular weights are listed in Table 6. It can be seen that all thermal properties including glass transition temperature (T_g) and 5% weight loss temperatures ($TGA_{-5\%}$) for the alternating PPC increase with increasing molecular weight. For this characteristic, more details have been addressed in previous work.[27] The thermal stability of as-made PPC copolymer is almost the same as that synthesized by using neat zinc glutarate. The alternating PPC copolymer with a molecular weight of > 37000 Da exhibited the highest T_g of > 32.1 °C and $TGA_{-5\%}$ of > 247.2 °C.

Table 4 Influence of temperature on the yield and molecular weight of PPC

PO/ml	Catalyst/g	Zn content/g	PO/catalyst ratio (mL g-catalyst^{-1})	Yield/ g g-catalyst^{-1}	$\bar{M}_n$ (k)	Temperature /°C
100	0.8	0.12	125	0.5	10.0	40
100	0.8	0.12	125	18.2	32.9	50
100	0.8	0.12	125	18.4	35.3	60
100	0.8	0.12	125	0.7	11.7	70

Copolymerization conditions: reaction time, 40 h; pressure of CO_2, 5.0 MPa, stirred at 125 rpm in a 500 mL autoclave.

Table 5 Effect of reaction time on the yield and molecular weight of PPC

PO/ml	Reaction time/h	Zn content/g	PO/catalyst ratio (ml g-catalyst^{-1})	Yield/ g g-catalyst^{-1}	Catalyst/g	$\bar{M}_n$ (k)
100	20	0.12	125	7.5	0.8	10.0
100	40	0.12	125	18.4	0.8	35.3
100	60	0.12	125	19.1	0.8	34.6
100	80	0.12	125	29.4	0.8	35.5

Reaction conditions: pressure, 5.0 MPa, time of dryness 24 h, weight of catalyst 0.8 g.

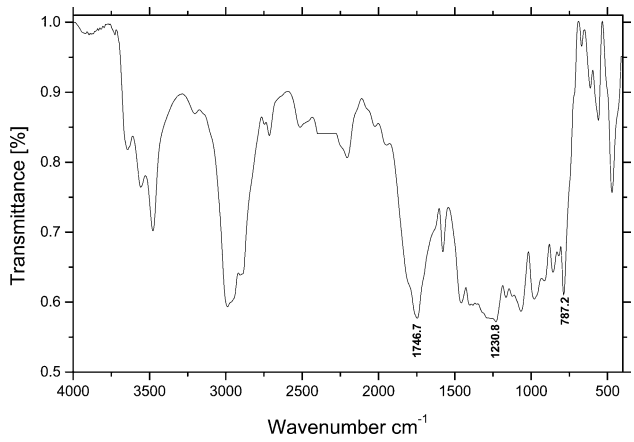

Fig. 6 FT-IR spectrum of PPC.

Table 6 Thermal properties for PPC with varying molecular weights

$\bar{M}_n$ (k)	T_g/°C	TGA_{-5}/°C
31.0	20.2	229.6
35.0	23.9	246.8
36.0	29.3	247.2
37.0	32.1	244.6

$TGA_{-5\%}$: 5% weight loss temperature.

Conclusions

Zinc metallophthalocyanine-containing poly(arylene ether sulfone) (ZM-PAE) can be readily synthesized by reacting zinc glutarate with phthalocyanine group-containing poly(arylene ether sulfone)s. The zinc-containing ZM-PAE was successfully used as catalyst for the copolymerization of carbon dioxide and propylene oxide. The crystalline structure of the ZM-PAE catalyst was confirmed by FTIR and WAXD techniques. Alternating poly(propylene carbonate)s (PPCs) were synthesized using the ZM-PAE catalyst with the highest activity of 30 g of polymer per gram of catalyst. The PPCs exhibited high thermal stabilities with a glass transition temperature of 35 °C and decomposition temperature of 247 °C.

Acknowledgements

We thank the National High Technology Research & Development 863 Program (Grant No: 2003AA302410), the Natural Science Foundation of China (Grant No. 50203016), the Guangdong Natural Science Foundation of China (Excellent Team Project Grant No. 015007), the Guangdong Province Sci. & Tech. Bureau (Key Strategic Project Grant No. A1100402) for financial support of this work.

References

1 K. Kacholia and R. A. Reck, *Clim. Change*, 1997, 35.
2 W. S. Broecker, *Science*, 1997, **278**, 1582.
3 B. D. Santer, K. E. Taylor and T. M. L. Wigley, *Nature*, 1996, **382**, 39.
4 G. A. Meehl and W. M. Washington, *Nature*, 1996, **382**, 56.
5 M. Hanschild and H. Wenzel, *Environmental Assessment of Products*, Chapman & Hall, London, 1997, vol. 2.
6 *Carbon Dioxide Chemistry; Environmental Issues*, eds. J. Paul and C. M. Pradier, Royal Society Chemistry, Cambridge, 1994.
7 Y. Z. Meng, L. C. Du, S. C. Tjong, Q. Zhu and A. S. Hay, *J. Polym. Sci., Part A: Polym. Chem.*, 2002, **40**, 3578–3591.
8 S. Inoue, H. Koinuma and T. Tsuruta, *Polym. Sci., Polym. Lett. Ed.*, 1969, **7**, 287.
9 S. Inoue, H. Koinuma and T. Tsuruta, *Makromol. Chem.*, 1969, **130**, 210.
10 S. Inoue, *Progr. Polym. Sci.*, 1982, **8**, 1.
11 Q. Zhu, Y. Z. Meng, S. C. Tjong, X. S. Zhao and Y. L. Chen, *Polym. Int.*, 2002, **51**, 1079.
12 Q. Zhu, Y. Z. Meng, S. C. Tjong, Y. M. Zhang and W. Wan, *Polym. Int.*, 2003, **52**, 799–804.
13 M. Ree, J. Y. Bae, J. H. Jung and T. J. Shin, *J. Polym. Sci. Part A, Polym. Chem.*, 1999, **37**, 1863.
14 S. Mang, A. I. Cooper, M. E. Colclongh, N. Chauhan and A. B. Holmes, *Macromolecules*, 2000, **33**, 303–308.
15 M. Cheng, E. B. Lobkovsky and G. W. Coates, *J. Am. Chem. Soc.*, 1998, **120**, 11018–11019.
16 A. Rokicki and W. Kuran, *J. Macromol, Sci. – Rev. Macromol. Chem.*, 1981, **C21**(1), 135–186.
17 D. J. Darensbourg and M. W. Holtcamp, *Macromolecules*, 1995, **28**, 7577–7579.
18 K. Kasuga, T. Katoo, N. Kabata and M. Handa, *Bull. Chem. Soc. Jpn.*, 1996, **69**, 2885–2888.
19 K. Kasuga, N. Moriwaki and M. Handa, *Inorg. Chim. Acta*, 1996, **244**, 137–139.
20 K. Kasuga, S. Nagao and M. Handa, *Polyhedron*, 1995, **15**, 69–72.
21 W. Wan, Y. Z. Meng, Q. Zhu, S. C. Tjong and A. S. Hay, *Polymer*, 2003, **44**, 575–582.
22 Y. Z. Meng, I. A. Abu-Yousef, A. R. Hlil and A. S. Hay, *Macromolecules*, 2000, **33**, 9185–9191.
23 M. Kobayashi, Y. L. Tang, T. Tsuruta and S. Inoue, *Makromol. Chem.*, 1973, **169**, 69.
24 H. Mandal, A. S. Hay and J. M. S. Pure, *Appl. Chem.*, 1998, **A35**(11), 1797–1808.
25 Y. Z. Meng, A. R. Hlil and A. S. Hay, *Polym. Adv. Technol.*, 2001, **12**, 206–214.
26 I. Abu-Yousef and A. A. S. Hay, *Synth. Commun.*, 1999, **29**, 2915.
27 X. H. Li, Y. Z. Meng and Q. Zhu, *Polym. Stab. Degrad.*, 2003, **81**, 157–165.

PAPER

www.rsc.org/greenchem

Biobased resin as a toughening agent for biocomposites

G. Mehta,[a] A. K. Mohanty,[b] M. Misra[a] and L. T. Drzal*[a]

[a] *Composite Materials and Structures Center, 2100 Engineering Building, Michigan State University, East Lansing, MI, USA 48824. E-mail: drzal@egr.msu.edu; Fax: 01 517432 1634; Tel: 01 517353 5466*

[b] *The School of Packaging, 130 Packaging Building, Michigan State University, East Lansing, MI, USA 48824*

Received 19th December 2003, Accepted 16th March 2004
First published as an Advance Article on the web 6th April 2004

Biocomposites can be designed and engineered from plant bio-fibres and a blend of unsaturated polyester resin and derivatized vegetable oil to replace existing glass fibre-polyester composites for use in housing applications. Natural fibre composites (biocomposites) would provide environmental gains, reduced energy consumption, lighter weight, insulation and sound absorption properties, thus providing many beneficial additions to the American Advanced Housing program. Biocomposites were made using a non-woven fibre mat (90% Hemp fibre with 10% thermoplastic polyester binder) as reinforcement, and unsaturated polyester (UPE) resin as well as blends of UPE and functionalized vegetable oils as the polymer matrix. All composites were made with 30% volume fraction of fibre, which was optimized earlier. The structure–property relationships of this system as well as the thermo-mechanical properties of these composites were measured. The notched Izod impact strength of biocomposites from biobased resin blends of UPE and functionalized vegetable oil and industrial hemp fibre mat are enhanced by 90% as compared to that of the pure UPE-industrial hemp fibre mat composites. The initial tests also show an improvement in the tensile properties of the composite as a result of the incorporation of the derivatized vegetable oil. The morphological changes of the matrix and composites have been analyzed using electron microscopy.

Introduction

Renewable materials from sustainable sources are becoming increasingly attractive for a variety of applications. Interest in the use of natural fibres has grown during the last decade due to their various advantages. Biocomposites, in general, are materials made by nature or produced synthetically that include some type of natural material in their structure. In our research, biocomposites are also known as natural fibre composites. Biocomposites are formed through the combination of natural cellulose fibres with other resources such as biopolymers or resins or binders based on renewable raw materials. The objective is to combine two or more materials in such a way that a synergism between the components results in a new material that is much better than the individual components. The properties of plant fibres can also be modified through physical and chemical technologies to improve performance of the final biocomposite. Some of the plant fibres with suitable properties for making biocomposites are: industrial hemp, kenaf, henequen, jute, flax, sisal, banana, kapok, *etc*. Biocomposites can be used for a range of applications, for example, building materials, structural and automotive parts, absorbents, adhesives and bonding agents and degradable polymers.[1]

Vegetable oils such as soybean, cotton seed, linseed, castor, are available on a global basis in very large quantities at affordable costs. These naturally hydrophobic plant oils are used as starting materials for a range of resin products currently under study at the Composite Materials and Structures Center (CMSC). Vegetable oils can be transformed to resin precursors that will polymerize when heated in the presence of catalysts. This technology uses the reactivity of the monomers to attack the double bonds present in the oil, forming linkages that can subsequently be reacted into crosslinkable units. Other reactive chemicals can be incorporated into the formulation to facilitate curing.

In this study, biobased resins were made by the addition of a derivatized vegetable oil to the unsaturated polyester resin matrix. This bioresin was then used for the fabrication of a biocomposite using an optimum amount of natural fibre (30% volume). The natural fibre used was a non-woven hemp mat, which contains 10% poly(ethylene terephthalate) (PET) as filler. The resulting composite was approximately 50% biobased.

Experimental

Materials

The polymer matrix used in this project is *ortho* unsaturated polyester resin (UPE), which was obtained from Kemlite Inc. The initiator used was methyl ethyl ketone peroxide (MEKP), and promoter used was cobalt(II) naphthenate (CoNap). Both MEKP and CoNap were obtained from Aldrich. Methyl ester of soybean oil (MESO), SoyGold 1000, was kindly provided by AG Environmental Products. Epoxidized methyl linseedate (EML), Vikoflex 9010, was obtained from Atofina Chemicals. Poly(butadiene-maleic anhydride) (PBMA), Ricon 130MA20 was procured from Sartomer Company Inc. Non-woven hemp fibre mat, (density 274 g m^{-2}) containing 90% randomly oriented hemp fibres and 10% poly(ethylene terephthalate) (PET) as binder was kindly provided by FlaxCraft Inc. All materials were used as such without further purification.

Processing

The required amounts of fibre mats were vacuum dried for 5 hours. The polyester resin (UPE) was mixed well with MEKP and CoNap, in the required amounts and then degassed under vacuum at room temperature for 5 minutes. The fibre mats were individually coated with the degassed resin; they were then placed between two aluminium plates covered with 'Teflon' release sheets. The plates were placed in a compression moulding press (Carver ® Laboratory Press) and the composites were cured at 80 psi for 2 hours at 100 °C followed by 2 hours at 150 °C. For making a control plaque from neat resin, degassed UPE solution was poured over degassed silicone moulds and cured in a conventional oven using the same temperature profile. EML and MESO were mechanically blended with UPE in the ratio of 20% oil, and 80% UPE, by weight. Bioplastics were made by blending the UPE, the functionalized oils

DOI: 10.1039/b316658a

and the curing agents (MEKP and CoNap), followed by curing them in silicone moulds in a conventional oven. Five percent by weight of PBMA was added to one of the blends of MESO and UPE. Biocomposites were also made with hemp fibre mats and blends of UPE and functionalized oils as matrix by compression moulding. Only one kind of derivatized oil (EML) was used in the fabrication of biocomposites. The resulting plastic and composite plaques were cut into required shapes for various tests.

Analysis

The biocomposites, bioplastics and neat polyester samples were evaluated by flexural (United Calibration Corporation, SFM 20) and notched Izod impact (Testing Machines Inc., 43-OA-01) tests using ASTM D790 and ASTM D256 protocols respectively. The impact-fractured surfaces of plastics and composites were examined using Environmental Scanning Electron Microscopy (ESEM, Electroscan Corporation, Model no. 2020). It was equipped with a lanthium hexaboride filament. The imaging pressure (Chamber pressure) was set between 2–3 Torr. Water vapour acted as the imaging gas. The accelerating voltage was set to 20 kV. DMA (TA DMA 2980) was performed to measure storage modulus, loss modulus and tan delta. For this test, rectangular sample bars (50 mm × 12 mm × 3 mm) were placed on the 3 point bending clamp (gauge length 50 mm) in the furnace and heated at the rate of 4 K per minute from 25 to 150 °C at an oscillation frequency of 1.0 Hz. AFM imaging was conducted using a Nanoscope IV atomic force microscope from Digital Instruments (Santa Barbara, CA) equipped with a *J* scanner with a maximum scan area of 125 mm^2. The sample was mounted onto a stainless steel disk using sticky tape (Latham, NY). The microscope was allowed to thermally equilibrate for thirty minutes before imaging. Scanning rates between 1 and 5 Hz were used. Room temperature was maintained at 22 ± 1 °C. Images were recorded in contact mode using standard silicon nitride (Si_3N_4) integral tips (NP type) (Digital Instruments) mounted on cantilevers with a manufacturer-specified spring constant of 0.22 N m^{-1}, length of 120 mm, width of 15 mm, and a nominal tip radius of curvature between 20 and 40 nm. The impact failure surfaces of samples were also observed by scanning electron microscopy. A thin, nanometer thick gold coating was firstly made on the observed failure surfaces. A JEOL 6300 SEM with field emission filament under an accelerating voltage of 10 kV was used to collect SEM images for samples.

Results and discussion

Most unmodified thermosets are brittle materials at ambient temperature. Consequently, most polymers have to be impact modified in order to satisfy end-use requirements for rigid applications. In most cases, the problem can be solved by incorporating rubber domains into the polymer matrix. However, the nature and the size of the elastomeric phase has to be adapted to each polymer matrix.[2] In most cases, it is also desirable to use the minimum amount of rubber modifier, in order not to affect other physical properties such as modulus.

The most important characteristics of an impact modifier are: rubber glass transition temperature, rubber domain particle size in the matrix, quality of dispersion, and adhesion to the polymer matrix. Historically, several technical approaches for toughening have been developed, which can be divided into three categories all based on the incorporation of an elastomeric damping phase: elastomer introduction during polymerization, dispersion of a thermoplastic elastomer phase during compounding (uncrosslinked), and incorporation of elastomeric core-shell particles.

Impact energy is the energy absorbed into the specimen during the impact event divided by its cross-sectional area. For the bioplastics, the impact strength increased after addition of biobased oil into the matrix (Fig. 1). The impact strength of plastic containing MESO was 25% higher than that of neat UPE resin, and impact strength of plastic containing EML is 96% higher than neat UPE

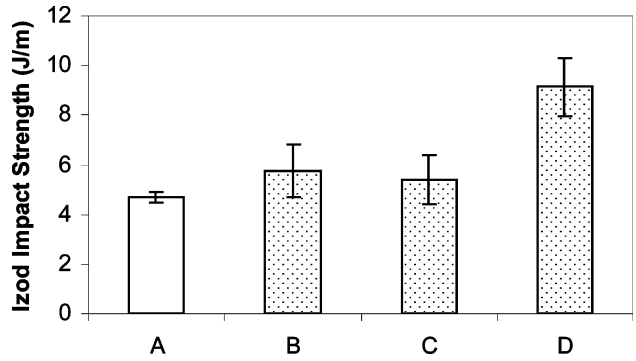

Fig. 1 Impact strength of bioplastics A = UPE control, B = MESO-UPE, C = MESO-PBMA-UPE, D = EML-UPE.

resin. But the trend in flexural properties was opposite to that of impact strength. All bioplastics had lower bending strength and elastic modulus as compared to neat UPE resin (Fig. 2). The

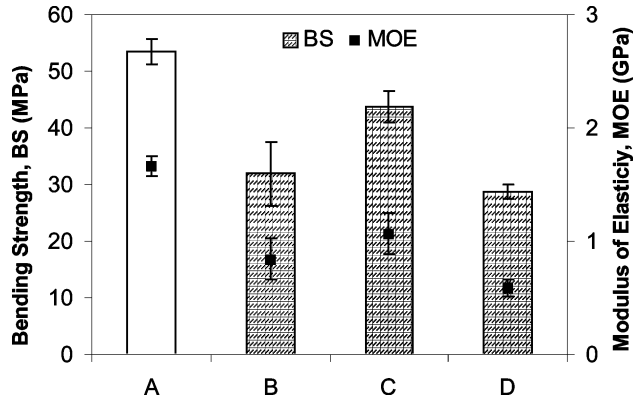

Fig. 2 Flexural properties of bioplastics A = UPE control, B = MESO-UPE, C = MESO-PBMA-UPE, D = EML-UPE.

bending strength of plastic containing modified MESO was 20% lower than strength of neat resin, and its modulus was 30% lower than that of neat resin.

In the case of biocomposites made with blends of oils and resin, the impact strength increased, but the flexural properties decreased. The impact strength of biocomposite containing hemp fibres in a matrix of bioresin, was 96% more than that of biocomposite made with hemp fibres and UPE resin (Fig. 3). However, the bending

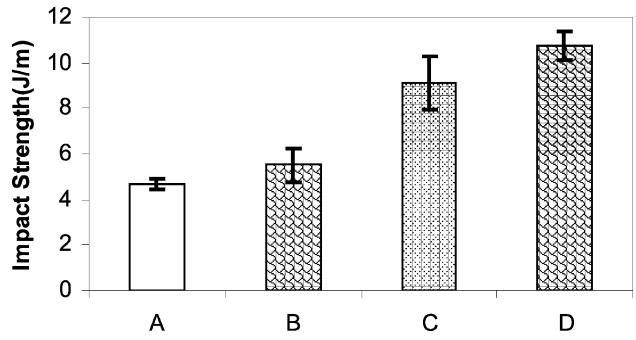

Fig. 3 Impact strength of biocomposites A = UPE plastic, B = untreated hemp-UPE, C = UPE-EML plastic, D = untreated hemp-UPE-EML.

strength of the biocomposite with bioresin was 20% lower than that of biocomposite with neat resin and the modulus of elasticity for this biocomposite was 30% lower than that of biocomposite with neat UPE resin (Fig. 4).

ESEM micrographs of the impact fractured surfaces of the bioplastics show phase separation (Fig. 5 and 6). These pictures showed discrete microstructures of the dispersed phase which are scattered throughout the entire surface.

SEM images (Fig. 7) of the impact fractured surfaces of plastic samples showed contrast between the neat UPE resin and bioresin

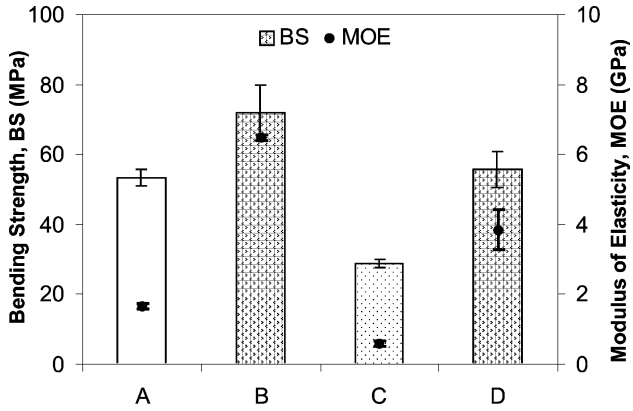

Fig. 4 Flexural properties of biocomposites A = UPE plastic, B = untreated hemp-UPE, C = UPE-EML plastic, D = untreated hemp-UPE-EML.

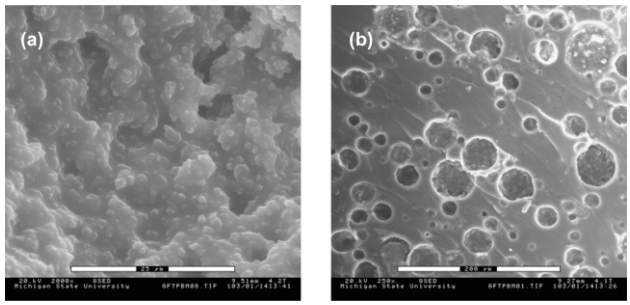

Fig. 5 ESEM micrographs of impact fractured surfaces of bioplastic containing MESO-PBMA-UPE. (a) Magnification 2000X, Scale 25 μm, (b) Magnification 250X, Scale 200 μm.

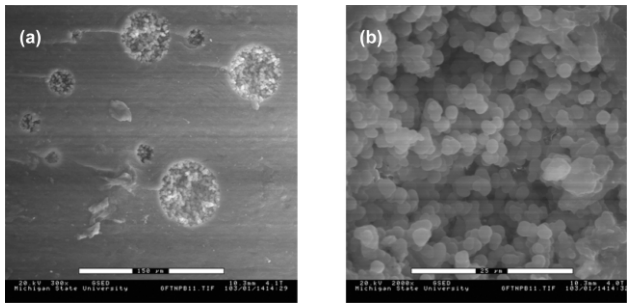

Fig. 6 ESEM micrographs of impact fractured surfaces of bioplastic containing MESO-UPE, (a) Magnification 300 X, Scale 150 μm (b) Magnification 2000X, Scale 25 μm.

(MESO-PBMA-UPE). Phase separation was observed in the bioplastics samples.

From ESEM and SEM images, it was observed that addition of small amount of liquid rubber, PBMA, improved the distribution of the second phase in the bioplastics, by making it more uniformly spread out over the entire surface.

AFM images (Fig. 8–10) also validated the existence of two phases in bioplastic samples, and a single phase in neat polyester resin. As can be seen in Fig. 9, there was uniformity in the distribution of hemispherical shaped craters of the second phase.

According to all ESEM, SEM and AFM images, the second phase seemed to be present in craters or holes, which contain crosslinked molecules of the MESO, UPE and polystyrene. They appeared in different sizes, but had the same content. In Fig. 9, the circular parts contain the second phase, which is the methyl ester of soybean oil. This picture specially looked at the smaller circular particles, and represented different sized domains distributed uniformly across the entire matrix. Fig. 10 shows the inside view of one such crater of the second phase. It was different in structure compared to the neighbouring UPE resin. A lamellar structure was observed inside the circular crater, validating the difference in mechanical properties of the UPE and MESO. The granular looking

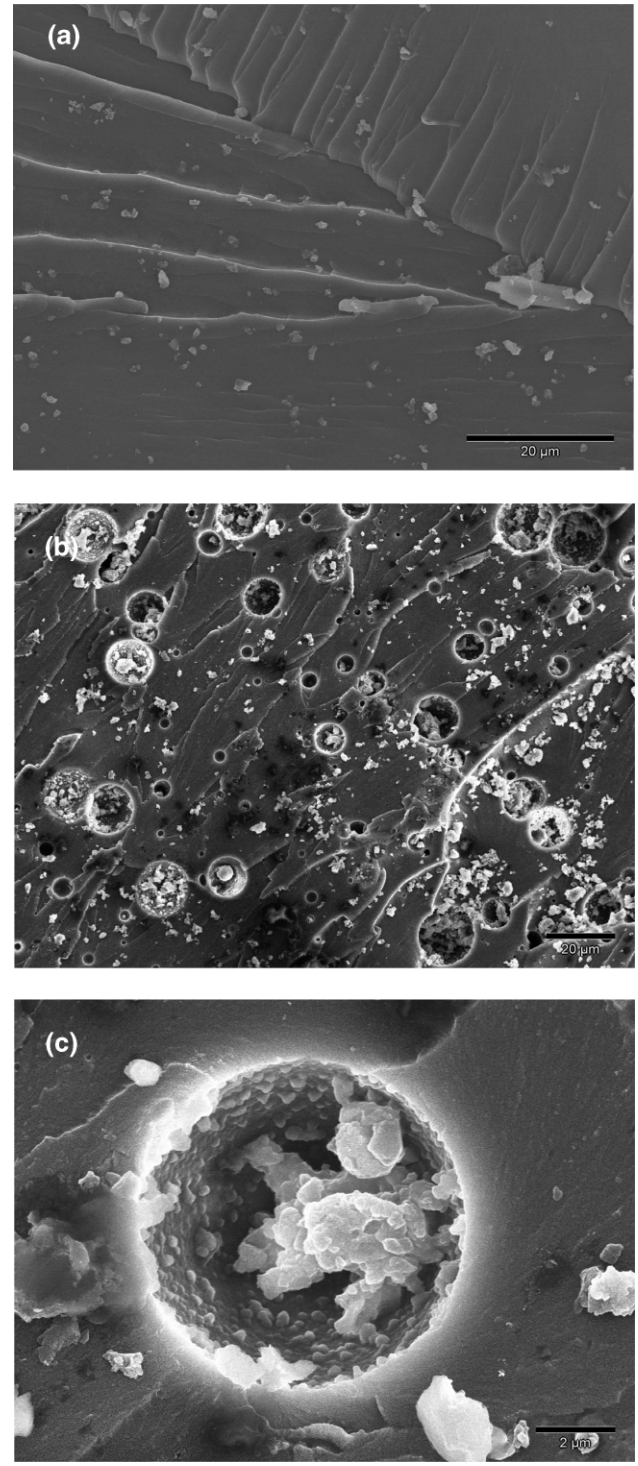

Fig. 7 (a) Impact fractured surface of neat polyester resin seen under SEM, scale 20 μm. (b) Impact fractured surface of bioplastic (MESO-UPE-PBMA) seen under SEM, scale 20 μm. (c) Impact fractured surface of bioplastic (MESO-UPE-PBMA) seen under SEM, scale 2 μm.

objects in Fig. 8 (neat UPE), were probably micro gels formed during curing.

It can be inferred that the lamellar structured second phase particles, absorbed the impact energy, and thus improved the impact strength of brittle neat polyester resin.

Following the trend of flexural properties, the storage modulus for bioplastics decreased in the same manner as the neat resin. As seen with bending strength and modulus of elasticity, there was a 20–30% reduction in the storage modulus of the bioplastic (figure not shown). This result was expected because vegetable oils are intrinsically low modulus materials because of their molecular structure, and when they are added to the polyester matrix, they

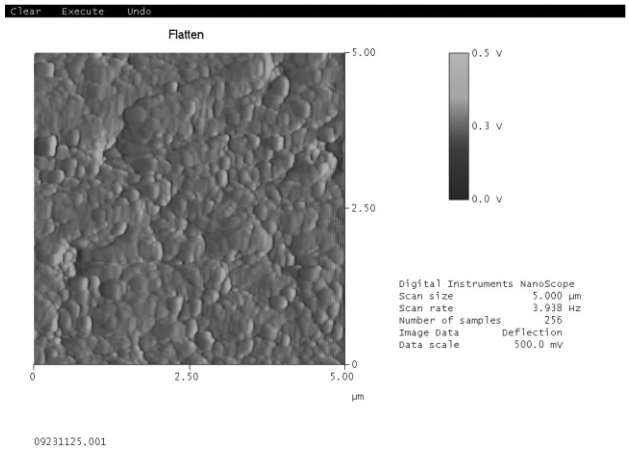

Fig. 8 AFM picture of neat unsaturated polyester resin (deflection image, scan size: 5 μm × 5 μm).

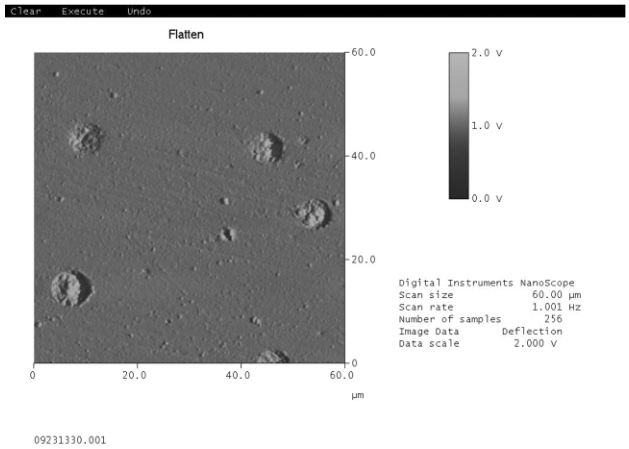

Fig. 9 AFM picture of bioplastic (MESO-UPE-PBMA) (deflection image, scan size: 60 μm × 60 μm).

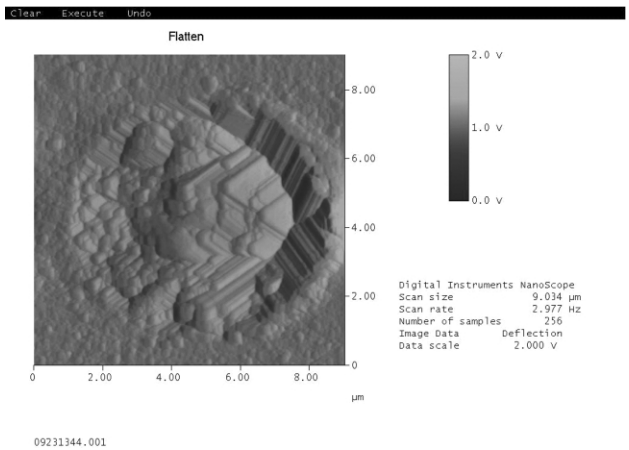

Fig. 10 AFM picture of bioplastic (MESO-UPE-PBMA) (deflection image, 9 μm × 9 μm).

lower the stiffness of the resulting material. The glass transition temperature of neat UPE resin, obtained from a tan delta plot was 95 °C (figure not shown). For all bioplastics, the T_g decreased by 10–12 °C as compared to neat UPE resin. The glass transition temperatures of plastics based on vegetable oils have been reported from −40 to 80 °C in the literature.[3–5]

Traditionally, elastomeric additives have been used for toughening in the free radical cross-linking of unsaturated polyester resin.[6,7] But polyester blends with vegetable based oils can also achieve the same purpose. The blends of oils and polyester resin form semi immiscible systems. Here, the oil phase provided the rubbery structures after curing. The oil phase was acting as an impact modifier, hence, it absorbed impact energy and delayed catastrophic failure.

The main toughening mechanisms which have been identified for thermoplastics as well as thermosets are namely: crazing of the polymer matrix, shear yielding of this matrix, and cavitation of the rubber phase. Depending on the polymer system, either a single mechanism or a combination of different mechanisms will be activated.[8]

The oil phase of the system consisted of small discrete rubbery particles, with an average size of 5–15 μm. They were randomly distributed in the glassy brittle polyester resin matrix. As reported in the literature about rubber toughened thermosets, these oil phase particles relieved the constraints in the matrix through principal mechanisms of cavitation and forming shear bands.[9] This phase separation phenomenon is similar to that in the low profile mechanism of unsaturated polyester resins.

The miscibility and interfacial properties of additive and resin blends play a major role in the toughening process. Improvements in the fracture impact of thermoset polyester resin can be obtained by dispersing elastomer particles with diameters from 0.5 to 5 μm in the blends. The smaller particles produce more microcracks in the matrix and enhance the fracture–impact energy. The additive is immiscible with the resin and gets phase separated from the matrix during curing.

Unsaturated polyester resins systems are very reactive materials, which are initially in a liquid state, and become solid after curing. The morphology of the polyester resin systems is decided by thermodynamics and polymerization kinetics.

Phase separation brings about a change in polydispersity. Usually, the size of additive particles in the matrix is 1–40 microns. A way to reduce this size is to decrease interfacial tension between two phases. Adding a small percentage of coupling agent like maleic anhydride solves this problem. In this system, poly-(butadiene-maleic anhydride) brought about uniformity in the dispersion, as well as uniformity in sizes of the second phase.

Therefore, smaller microcracks were formed in the matrix leading to an increase in impact strength. These microcracks were produced during the large volumetric shrinkage which takes place during polymerization. Microvoids also occurred around the fibres in the composite.

Microvoid formation is an important phenomenon for systems consisting of blends of bioresin and UPE. It compensates for resin shrinkage, but induces intrinsic brittleness. Increased additive content in the UP resin should produce higher impact strength, but if the microvoid content is also enhanced, impact strength is reduced. But in this system, the reverse effect was observed. Even after addition of 20% bioresin into the polyester matrix, the impact strength was improved, with a little sacrifice of modulus of elasticity.

Well-dispersed particles in the resin matrix induced homogeneous distribution of internal stresses due to network formation. Thus, low energy impact fractures in the unsaturated polyester resin composites were eliminated by the use of this additive in the system. The addition of the blends of derivatized oils and UPE in the matrix of the natural fibre biocomposites lead to an increase in the impact strength of the composites.

Conclusions

Using bioresins as polymer matrices provides a two fold benefit over thermoset resins in biocomposites. Their presence can improve the impact strength of the resulting bioplastic, as well as produce a material with higher biobased content. Further experiments are aimed at studying in detail the behavior of the second phase, the actual mechanism of toughening and control of the dispersed phase. Also, the structure–property relationships are to be determined. It is also planned to study the fractured surfaces to find the critical parameters like fibre-matrix adhesion and fracture dynamics.

Acknowledgements

The authors are grateful to NSF-PATH (2001 Award No.0122108) for kindly supporting this project. Collaboration and samples from Kemlite Inc., Joliet, IL and FlaxCraft Inc., Cresskill, NJ are highly appreciated. Authors are also thankful to Atofina Chemicals Inc., Philadelphia, PA, for Vikoflex 9010 sample, and to Sartomer Company Inc., Exton, PA, for poly(butadiene-maleic anhydride) (PBMA), Ricon 130MA20 sample. The help of Dr. H. Miyagawa, CMSC, Michigan State University for SEM imaging, and Dr. X. Liang, CMSC, Michigan State University for AFM imaging is deeply appreciated.

References

1 A. K. Mohanty, M. Misra and G. Hinrichsen, *Macromol. Mater. Eng.*, 2000, **276**/**277**, 1.
2 B. Cherian and E. T. Thachil, *Progr. Rubber Plastics Technol.*, 2001, **17**(4), 205–224.
3 F. Li and R. C. Larock, *J. Polym. Sci., Part B: Polym. Phys.*, 2001, **39**, 60–77.
4 E. Can, S. Kusefoglu and R. P. Wool, *J. Appl. Polym. Sci.*, 2001, **81**, 69.
5 I. Frichinger and S. Dirlikov, in *Toughened Plastics I Science and Engineering*, ed. C. K. Riew and A. J. Kinloch, 1993, (Advances in Chemistry, No. 233), American Chemical Society, Washington, DC, pp. 451–489.
6 L. Suspene, Y. S. Yang and J. P. Pascault, in *Toughened Plastics I Science and Engineering*, ed. C. K. Riew and A. J. Kinloch, 1993, (Advances in Chemistry, No. 233), American Chemical Society, Washington, DC, pp. 163–188.
7 F. J. McGarry and R. Subramanium, in *Toughened Plastics II Novel Approaches in Science and Engineering*, ed. C. K. Riew and A. J. Kinloch, 1996, (Advances in Chemistry Series, No. 252), American Chemical Society, Washington, DC, pp. 133–149.
8 C. B. Bucknall, *Toughened Plastics*, Applied Science Pub. Ltd., London, 1977.
9 A. F. Yee and R. A. Pearson, *J. Mater. Sci.*, 1986, **21**, 2462.

PAPER

www.rsc.org/greenchem

Structure–activity relationships of pyrithiones – IPC-81 toxicity tests with the antifouling biocide zinc pyrithione and structural analogs

Caren A. Doose,*[ab] Johannes Ranke,[a] Frauke Stock,[a] Ulrike Bottin-Weber[a] and Bernd Jastorff[a]

[a] *Center for Environmental Research and Environmental Technology, Department for Bioorganic Chemistry, University of Bremen, Germany*

[b] *School for Engineering and Science, Department for Chemistry, International University Bremen, Campus Ring 8, 28759 Bremen, Germany. E-mail: c.doose@iu-bremen.de*

Received 14th November 2003, Accepted 3rd March 2004
First published as an Advance Article on the web 13th April 2004

Zinc pyrithione (1-hydroxypyridine-2-thione, zinc complex; $ZnPT_2$) is currently viewed as the top prospect for replacing tributyltin antifoulants in ship paints. Thus, the risk assessment of a high scale release of $ZnPT_2$ to the natural environment is of increasing importance. The knowledge of the molecular mechanisms related to biological effects of $ZnPT_2$ and its transformation products is crucial for this assessment and thus for the decision whether pyrithiones are sound or "green" alternatives to organotin antifoulants. A multitude of biological effects of pyrithiones is already known while the underlying molecular mechanisms of action remain obscure. This study presents toxicological data of zinc pyrithione and several structural analogs in rat leukemic cells (IPC-81). The N-hydroxythioamide functional group proved to play a significant role in the molecular mechanisms related to the biological action. Structural analogs, which are deprived of one or more molecular interaction or chemical reaction potentials given by this group (namely pyridine, pyridine 1-oxide and pyridine 2-thione, bis(2-pyridinyl)disulfide, and three methylated metabolites), exhibit far less toxic potential in IPC-81 cells than pyrithiones (*i.e.*, 2-pyridinethione-1-oxides). In particular the trans-metallization products of $ZnPT_2$, iron ($FePT_3$) and copper ($CuPT_2$) pyrithione, and the oxidation product bis(2-pyridinyl)disulfide 1,1′-dioxide (pyrithione disulfide, (PT_2)) have been proven to be as toxic as $ZnPT_2$ and tributyltin chloride in IPC-81 cells. $CuPT_2$, $FePT_3$ and $(PT)_2$ need to be considered as environmental transformations products of $ZnPT_2$.

1 Introduction

1-Hydroxy-2-pyridinethione **1**, known as Pyrithione (PT) or Omadine®, is an aromatic heterocycle related to pyridine. *Via* the sulfur and the oxygen of its N-hydroxythioamide group, it forms complexes with most transition metals.[1–3] For fifty years PT has been noted for its highly bacteriocidal and fungicidal action.[4–6] Often metallization of the bidentate ligand highly augments biocidal action as in the case of zinc pyrithione **2** (Zinc Omadine®, $ZnPT_2$). (Fig. 1).

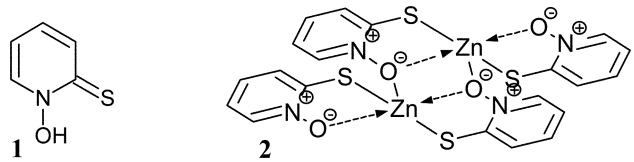

Fig. 1 Pyrithione **1** and zinc pyrithione **2**. In the solid state $ZnPT_2$ exhibits a dimeric structure with pentacoordinated zinc.[10]

$ZnPT_2$, the derivative of PT that is produced prevalently, is a well-known chemical. It is employed as a preservative in various commercial products such as cosmetics or industrial fluids. It is also an effective antidandruff agent, and it has been used in several hair care products for the last 30 years (*e.g.*, Head & Shoulders®, Dove®). Pyrithione also exhibits a broad action against marine fouling organisms and thus finds application as a booster biocide in anti-fouling paints.[7–9]

Due to the ban of organotin antifoulants in ship paints established by the International Maritime Organization (IMO), the use of substitute biocides is of increasing significance. For example, Arch Chemicals, producers of $ZnPT_2$ have announced substantial production growth for 2002 and expect to become leaders in the antifouling biocide market by 2003 or 2004.[11]

Biofouling on ship hulls is caused by a large diversity of aquatic organisms (*e.g.*, different algae, mussels or barnacles). High toxicity against a broad spectrum of different organisms is a feature of antifouling biocides desired by the user. Thus, it is not surprising that pyrithiones have been found to induce a large variety of toxic effects in highly diversified living organisms, which in most cases are non-target organisms.

Pyrithiones have been found to produce teratogenic and general toxic effects in aquatic organisms (fish and sea urchins) at extremely low concentrations†.[12,13] In a comparative investigation using sea urchin eggs, toxicity of pyrithiones is far higher than that induced by tributyltin oxide.[13] Genotoxic effects induced by pyrithiones have been found in mammalian lymphoma cells with and without photoactivation.[14] Pyrithiones are general inhibitors of membrane transport processes in fungi[15] and have been found to distort membrane integrity in bacteria[16–19] and mammalian cultured cell lines.[20] Oxidative damage elicited by pyrithiones has been found in rabbit myocardium tissue.[21] Membrane depolarization induced by pyrithiones has been shown in mammalian cultured cells[22] and fungi.[23] Pyrithione biocides are capable of interaction with common biological molecules (phosphatidyl-ethanolamine, cysteine)[16] and have been shown to cause large decreases in ATP levels in bacteria[18] and fungi.[15] As ionophores, pyrithiones affect homeostasis of different metal cations. This was found in different mammalian cultured cell lines[22,24,25] and rabbits (*in vivo*).[26] Further, pyrithiones affect amino acid metabolism in different mammalian cultured cell lines[25,27,28] as well as nucleoside

† Early life stage tests exhibited significant teratogenic effects (morphologically visible wavy structures of the vertebral column) at very low concentrations of $ZnPT_2$ in larvae of zebra fish and Japanese Medaka.[12] $ZnPT_2$ exhibited EC_{50} values of 9 μg L^{-1} [28 nM] in zebra fish and 5 μg L^{-1} [16 nM] in Japanese Medaka. Kobayashi and Okamura[13] comparatively assessed the effects of tributyltin oxide and seven organotin antifoulant substitutes on sea urchin eggs and embryos. With No Observed Effect Concentrations (NOEC) of 0.03 attoM, $ZnPT_2$ was the most toxic antifoulant tested. $CuPT_2$ exhibited a NOEC value of 3 femtoM.

DOI: 10.1039/b314753c

metabolism in bacteria,[29] different mammalian cultured cell lines[27,28,30] and the isolated salmon sperm DNA/bacterial RNA polymerase model.[29] Pyrithiones affect cellular function regulating molecules (transcription factors NF-κB and AP-1) in different mammalian cultured cells.[24]

Numerous biological effects of pyrithiones are known but the identity of the active species and the molecular causalities of this highly diverse biological activity remain obscure. However, this knowledge is crucial for the assessment of the risk implied by a high scale release of pyrithione biocides to the natural environment, and it is thus important for the decision whether pyrithiones biocides are sustainable alternatives to tributyltin antifoulants.

The present study was aimed at the comparative evaluation of the toxic potentials of $ZnPT_2$ and some structural analogs. Copper pyrithione **3** ($CuPT_2$), iron pyrithione **4** ($FePT_3$) and bis(2-pyridinyl)disulfide ($(PT)_2$) **5** have been selected because they are probable environmental transformation products of $ZnPT_2$, as will be discussed later. Free pyrithione **1** is prone to oxidation and therefore relatively difficult to handle. Thus, sodium pyrithione **6** (NaPT) has been selected to represent the free pyrithione **1** or pyrithionate **1a**. At the low concentractions at which NaPT is active the salt might completely dissociate with the PT moiety entering the acid–base equilibrium according to its pK_a of 4.6 (Fig. 4 and Table 3). Pyridine **7** (Py), pyridine 2-thione **8** (PyS), and pyridine 1-oxide **9** (PyNO) are the closest structural analogs of PT. Bis(2-pyridinyl)disulfide **10** ($(PyS)_2$) is a close analog of $(PT)_2$. Three methylated metabolites of $ZnPT_2$ which have been found in rats[6] have been selected: 2-(methylthio)pyridine 1-oxide **11** (MSPT), 2-(methylthio)pyridine **12** (MSP) and 2-(methyl-sulfonyl)pyridine **13** (MSO_2P). Methylated metabolites are also likely to be part of metabolic pathways of bacteria. For comparison, EC_{50} values of tributyltin chloride **14** (TBT) are given. The substances tested are listed in Table 1.

Toxicities of these "testkit-compounds" were determined with the WST/IPC-81 cell viability assay. This assay has been successfully performed in this laboratory before for hazard assessment and mode of action studies.[31–33] IPC-81 is a cultured promyelocytic leukemia rat cell line,[34] WST-1 reagent is a dye which is electrochemically reduced by living cells. This reduction is seen as changing absorbance (450 nm), which in turn is used as an indicator for cell viability.

The interpretation and discussion of the results has been performed according to the "T-SAR" approach[35] – a bioorganic chemistry approach of "thinking in terms of structure–activity and structure–property relationships". This approach is aimed at the systematic comprehension of the molecular structures of chemicals focusing on features such as chemical reaction and noncovalent interaction potentials, functional groups, stereochemistry and possible transformation or speciation of these chemicals as well as on possible impacts of identified characteristics in biological systems. A systematic characterization of $ZnPT_2$, PT and NaPT according to T-SAR is given in ref. 36 This includes a comprehensive review and classification of observed biological effects of pyrithiones.

2 Experimental

(a) Chemicals

Testkit compounds. All chemicals that were tested for toxicity, except for PyNO and Py, had been packed in 1 and 0.1 μmol portions. This had been done by measuring respective aliquots from a stock solution followed by lyophilization. PyNO and Py were directly applied from stock solutions.

Pyridine **7** of analytical grade was obtained from Bernd Kraft GmbH, pyridine 1-oxide **9** and pyridine 2-thione **8** (97%) from Fluka. Zinc pyrithione **2** 95% and sodium pyrithione **6** 97% were purchased from Sigma. Bis(2-pyridinyl)disulfide 1,1′-dioxide **5** 99% was synthesized as described in ref. 37 and characterized by UV and ESI-MS. Purity of the compounds was assessed using HPLC. Bis(2-pyridinyl)disulfide **10** (97%) was obtained from Janssen. Tributyltin chloride 96% **14** was purchased from Aldrich.

Copper and iron pyrithione **3** and **4** were obtained by drop-wise addition of an excess of aqueous solutions of either cupric nitrate

Table 1 Structural analogs selected for IPC-81 toxicity tests

Molecular structure	Chemical name	Abbr.	No.	Molecular structure	Chemical name	Abbr.	No.
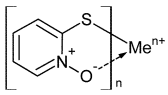 Me = Zn^{2+}, Cu^{2+}, Fe^{3+}	Zinc(II)- Copper(II)- Iron(III)- pyrithione	$ZnPT_2$ $CuPT_2$ $FePT_3$	**2** **3** **4**	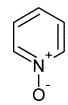	Pyridine 1-oxide	PyNO	**9**
				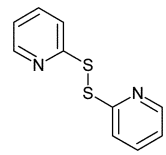	Bis(2-pyridinyl)disulfide	$(PyS)_2$	**10**
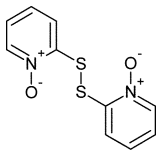	Bis(2-pyridinyl) disulfide 1,1′- dioxide	$(PT)_2$	**5**	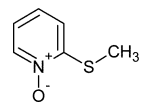	2-(Methylthio) pyridine 1-oxide	MSPT	**11**
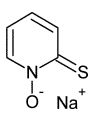	Sodium pyrithione	NaPT	**6**	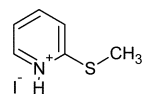	2-(Methylthio) pyridine hydroiodide	MSPHI	**12**
	Pyridine	Py	**7**	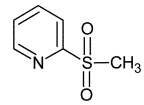	2-(Methylsulfonyl) pyridine	MSO_2P	**13**
	Pyridine 2-thione	PyS	**8**	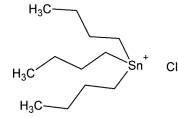	Tributyltin chloride	TBT	**14**

trihydrate or ferric chloride hexahydrate, respectively, (obtained from Fluka puriss. p.a. grade) to a stirred aqueous solution of sodium pyrithione. The metal complex precipitated immediately. To complete the reaction, the stirred mixture was heated to reflux. After cooling to room temperature, the mixture was filtrated. The precipitate was washed with water, and then with small amounts of methanol before lyophilization. The complexes were recrystallized from methanol and characterized by ESI-MS^n, UV/Vis, and in the case of $FePT_3$ by X-ray diffraction.

2-(Methylthio)pyridine 1-oxide **11** was obtained by stepwise addition of methyl iodide (99%, Acros Organics) to an equimolar amount of sodium pyrithione which was dissolved in 250 mL ethanol (room temperature). The mixture was left for 12 hours before the filtrate was separated from a white precipitate. The filtrate was evaporated and the beige precipitate recrystallized from methanol. Faint yellow crystals have been characterized by ^1H NMR and ESI-MS^n. Purity of the compounds was assessed using HPLC.

2-(Methylthio)pyridine **12a** was obtained by stepwise addition of methyl iodide to an equimolar amount of pyridine 2-thione which was dissolved in 300 mL ethanol (room temperature). The mixture was left for 12 hours before precipitated faint yellow crystals were separated from the filtrate. Crystals were washed with small amounts of cold ethanol and then recrystallized from ethanol. Faint yellow crystals of 2-(methylthio)pyridine hydroiodide **12** have been characterized by ^1H NMR and ESI-MS^n. Purity has been controlled by HPLC. Attempts failed to completely dry and exactly portion the free base, which was obtained by addition of an aqueous solution of sodium hydroxide to an aqueous solution of **12**. Therefore, **12** was used for toxicity tests accompanied by control experiments with sodium iodide, which exhibited no toxic effect.

2-(Methylsulfonyl)pyridine **13** has been obtained by stepwise addition of an excess of 30% H_2O_2 (Acros Organics) to a solution of 2-(methylthio)pyridine hydroiodide **12** which was dissolved in diluted acetic acid (Fluka) and heated to reflux. During addition the solution was permanently stirred. After the mixture was cooled to room temperature it was treated with concentrated sodium hydroxide (Fluka) and then extracted with *tert*-butylmethyl ether (Acros Organics). The clear colorless oil has been characterized by ESI-MS^n. Purity of the compounds was assessed using HPLC.

Chemicals for the WST/IPC-81 assay. Cell culture medium, serum and phosphate buffer were purchased from GIBCO BRL Life technologies, antibiotics and glutamine were obtained from PAA Laboratories and WST-1 Reagent (2-(4-Iodophenyl)-3-(4-nitrophenyl)-5-(2,4-disulfophenyl)-2H-tetrazolium monosodium salt) was purchased from Roche Diagnostics.

(b) The WST/IPC-81 cell viability assay

Cultures of IPC-81 were grown in RPMI 16/40 medium (Roswell Park Memorial Institute 160 Medium[38,39]) (supplemented with 0.2% $NaHCO_3$, 1% Penicillin/Streptomycin and 1% Glutamine) with 10% horse serum at 37 °C and a pH of 6.8 (5% CO_2).

In advance of the preparation of testkit stock solutions, compounds were suspended in DMSO to improve their solubilities. Final DMSO concentration in test media did not exceed 0.5%. Control experiments exhibited no toxic effects of DMSO in IPC-81 cells at this concentration. The stock solutions of the testkit compounds were prepared in culture medium and added to 96 well plates. Each plate contained three replicates of two substance dilution series, control and blank wells. Cells were added at a concentration of 15×10^5 cells mL^{-1} (in RPMI with 8% heat inactivated foetal calf serum) and cultivated for 48 hours. After 44 hours 10 μL of WST-1 reagent (diluted 1 : 4 with phosphate buffer) were added and cells were incubated for four hours. After incubation absorbance in each well (450 nm) was measured with a microplate-reader (MRX Dynatech). Cell viability was expressed as a percentage of absorbance compared to absorbance of controls.

1 : 1 dilution series generally started from 1 mM concentrations. If necessary, additional tests were performed with higher or lower dilution, respectively. Each dose–response curve was recorded for 3–6 repetitions (9–18 replicates).

(c) Effect data evaluation

The obtained data were normalised using blanks with no cells (mean response $\rightarrow 0$) and unexposed cells (mean response $\rightarrow 1$) on each microtiter plate. Dose–response curves were fitted to normalised data using the cumulative density function of a lognormal distribution. Wherever suitable, *i.e.* when the mean response at the highest concentration was lower than 0.5, EC_{50} values were calculated from the location parameter of the fitted density functions. EC_{50} values are only reported here if they did not exceed the highest concentration tested. Calculations were performed with the R language and environment for statistical computing, version 1.7, using the R package nls (nonlinear least squares).

3 Results

The viabilities with means and standard deviations as well as fitted dose–response curves are given in Fig. 2. For comparison all dose–response curves of the testkit compounds are shown together in Fig. 3. $\log_{10}EC_{50}$ values with standard deviations, respective EC_{50} values as well as the slopes *b* are given in Table 2.

Py **7**, PyNO **9**, MSPHI **12** and MSO_2P **13** exhibited no toxic effect in IPC-81 cells at concentrations below 1000 μM. EC_{50} values for PyS **8**, MSPT **11**, and $(PyS)_2$ **10** ranged from 60 to 480 μM. $ZnPT_2$ **2**, $CuPT_2$ **3**, $FePT_3$ **4**, NaPT **6** and $(PT)_2$ **5** exhibited very similar EC_{50} values ranging from 0.36–0.48 μM. TBT **14** exhibited an EC_{50} of 0.69 μM. $(PT)_2$ exhibited the lowest EC_{50} value of all pyrithione analogs tested.

For most substances the deviations in the dynamic range of the dose–response curves were relatively large. This might be due to the natural variability of the cells used combined with an "all-or-nothing" effect of the substances. This allows small concentration inaccuracies to cause relatively large deviations in viability. Orders of magnitudes and differences in the toxic potentials of the compounds tested are nevertheless evident. Differences in curve shapes will not be discussed in detail because of the high deviation in the dynamic range of the dose–response curves.

4 Discussion

The present results indicate two main structure–activity relationships of pyrithiones: (i) substances exhibiting the 2-thiopyridine-1-oxide structure ($ZnPT_2$, $CuPT_2$, $FePT_3$, NaPT and $(PT)_2$) exhibit far higher toxic potentials than those without this structure (Py, PyNO, PyS and $(PyS)_2$ as well as MSO_2P and MSPHI); (ii) the pyrithione complexes tested and sodium pyrithione exhibit similar and very low (nanomolar) effect concentrations. Both features can be explained with characteristics of the molecular structure of pyrithione considering physico-chemical data of pyrithione and its metal complexes.

Due to tautomerism and acid–base equilibria, pyrithione is subject to speciation in aqueous solution at physiological pH (Fig. 4). According to[40,41] the thione form is preferred by the factor 52 in water. The pK_a data obtained in the literature differ as shown in Table 3 and for calculations performed in this paper an average value of 4.6 has been used. According to Hendersson–Hasselbalch,

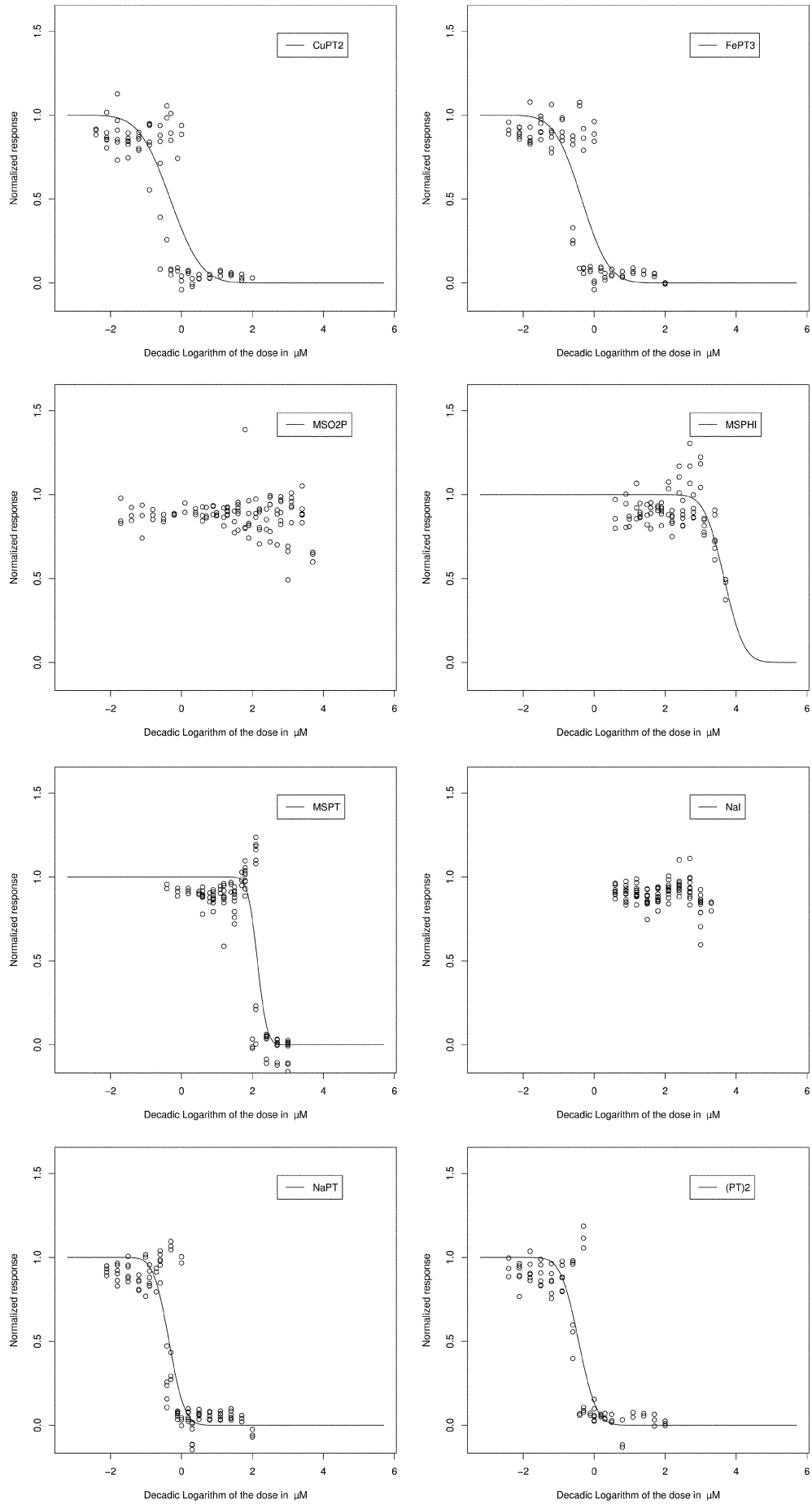

Fig. 2 Viabilities with means and standard deviations as well as fitted dose–response curves for compounds tested.

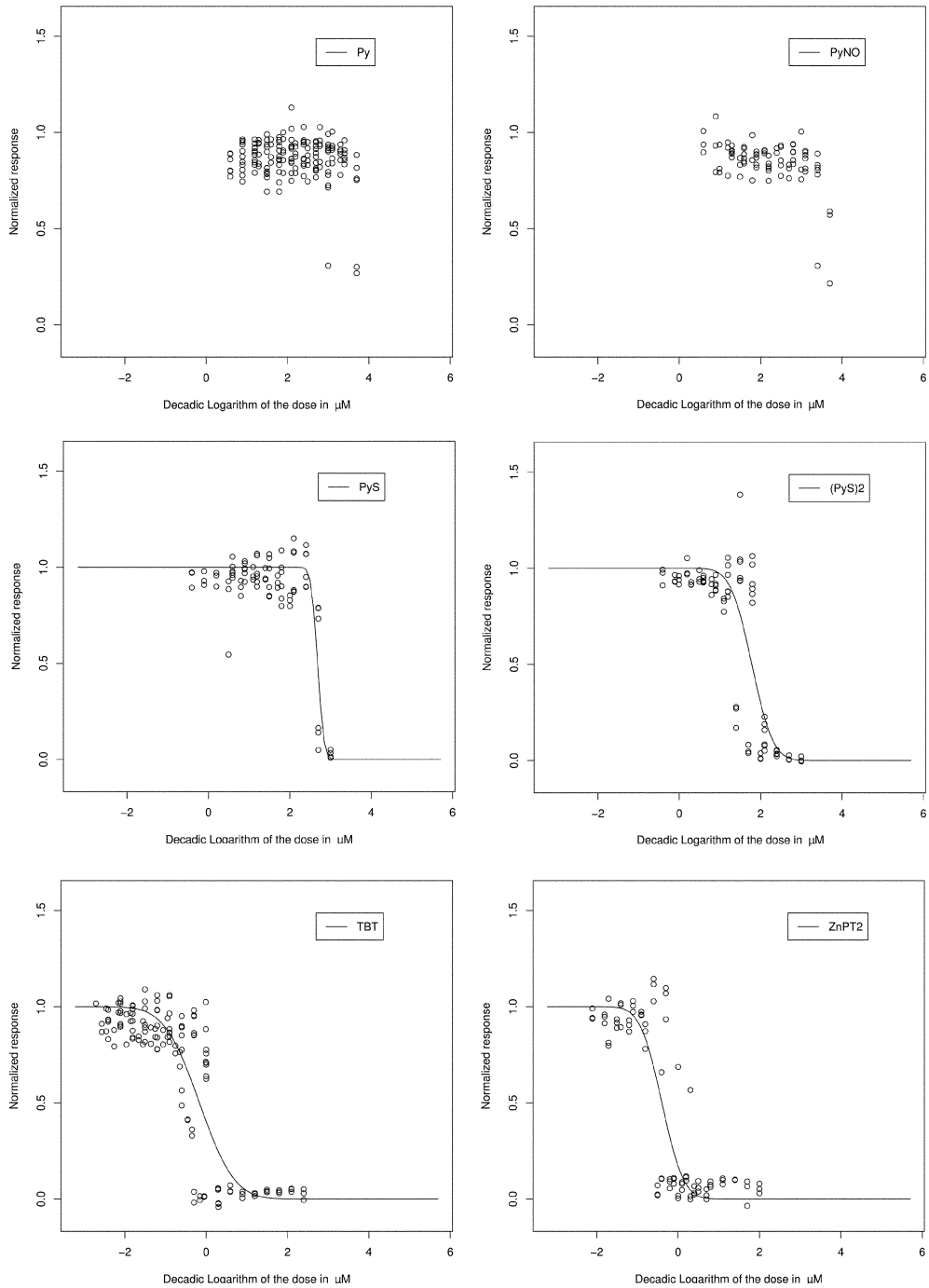

Fig. 2 cont.

at pH 7 deprotonated pyrithione exists in about 250-fold excess over the neutral form (pK_{a1} neglected).

The pyridine ring is capable of hydrophobic and π–π-interactions, whereas the N-hydroxythioamide group introduces highly polar properties to the molecule. The neutral molecule exhibits strong H-bond donation potential due to the exocyclic proton. The ability to enter a strong intramolecular H-bond may, however, hamper intermolecular H-bonds. Pyrithione exhibits H-bond acceptor potential due to several free electron pairs. The N-oxide group possesses a highly bi-polar structure. In the deprotonized forms of pyrithione, one negative ionic interaction potential is present. Pyrithione exhibits two potential nucleophilic sites, sulfur being a stronger nucleophile than the nitrogen-bound oxygen. Electrophilic potential, which is predominantly located at the nitrogen, may be hampered due to a missing leaving group.

According to eqn. 1 pyrithione is a reducing agent:

$$\text{R–SS–R} + 2e^- + 2H_3O^+ \rightleftarrows 2\text{R–SH} + 2H_2O \qquad E'_0 = -0.34‡ \tag{1}$$

Thus, free pyrithionate may generate $(PT)_2$ in the presence of mild oxidants as *e.g.* atmospheric oxygen or ferric ions. Oxidation of PT when exposed to air yielding $(PT)_2$ has been observed in our laboratory (Fig. 7).[36]

The chemical structure of the N-hydroxythioamide group in the pyrithionate anion species gives rise to a bidentate character due to the negative charge and the adjacent strong electron donor potential. This allows coordination to metal cations such as zinc(II), copper(II) or iron(III).

‡ Data obtained from[44] for PT *vs.* Ag/AgCl/KCl_{sat} and from[43] for NaPT *vs.* SCE have been converted to E'_0 (SHE at pH 7) for the partial reaction $(PT)_2 + 2e^{\ominus} \rightarrow 2PT^{\ominus}$.

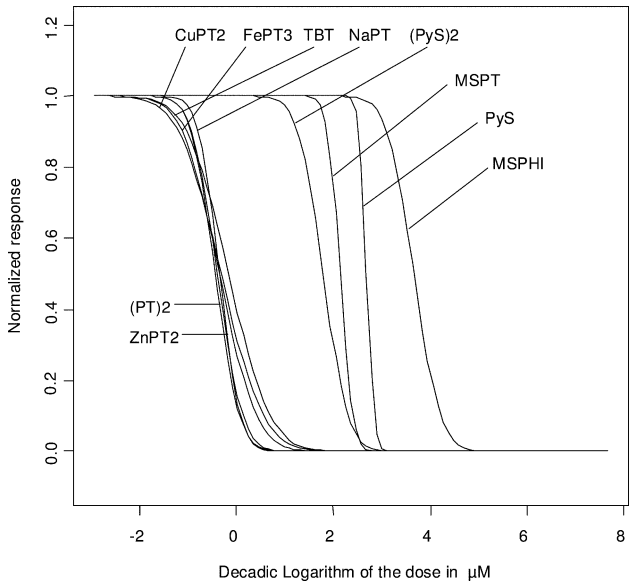

Fig. 3 Compiled dose–response curves for compounds tested.

Table 2 $\log_{10}EC_{50}$ values with standard deviations and respective EC_{50} values calculated from the dose–response curves of the testkit compounds in IPC-81 cells. Slopes *b* and number *n* of dilution series. All concentrations are given in [µM]

	$\log_{10}EC_{50}$	EC_{50}	*n*	*b*
$(PT)_2$	−0.44 ± 0.1	0.36	9	0.40
$ZnPT_2$	−0.40 ± 0.1	0.40	9	0.42
$FePT_3$	−0.35 ± 0.1	0.44	9	0.60
NaPT	−0.35 ± 0.07	0.45	12	0.34
CuPT2	−0.32 ± 0.2	0.48	9	0.69
TBT	−0.16 ± 0.1	0.69	15	0.68
(PyS)2	1.8 ± 0.1	60	9	0.41
MSPT	2.2 ± 0.07	140	12	0.21
PyS	2.7 ± 0.04	480	9	0.13
MSO_2P	≥ 3[a]	≥ 1000	12	
MSP(HI)	> 3	> 1000	9	
Py	> 3[a]	> 1000	18	
PyNO	> 3[a]	> 1000	9	

[a] No dose–response curve was fitted to the obtained data because the response was too low in the dose range measured.

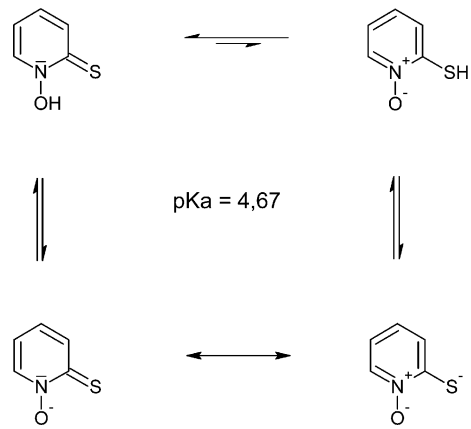

Fig. 4 Tautomerism and dissociation of PT.

In the presence of metal cations pyrithione is therefore subject to additional speciation as shown in Fig. 5 for $ZnPT_2$.

As shown in Fig. 6 and Table 4, at three calculated concentrations of applied $ZnPT_2$ ($ZnPT_{2(total)}$) pyrithionate is predominant.

Table 3 pK_a values of PT

	Method	
	UV spectral	polarographic
pK_{a2}	4.67 [40]	4.6 [43]
	4.40 [42]	
pK_{a1}	−1.95 [40]	

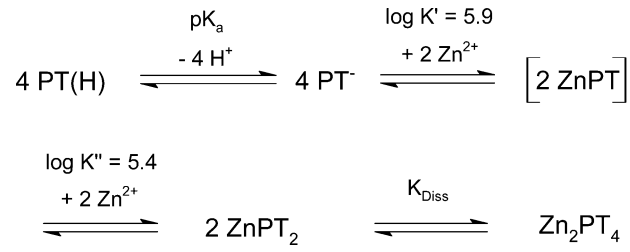

Fig. 5 Chemical equilibria of $ZnPT_2$.

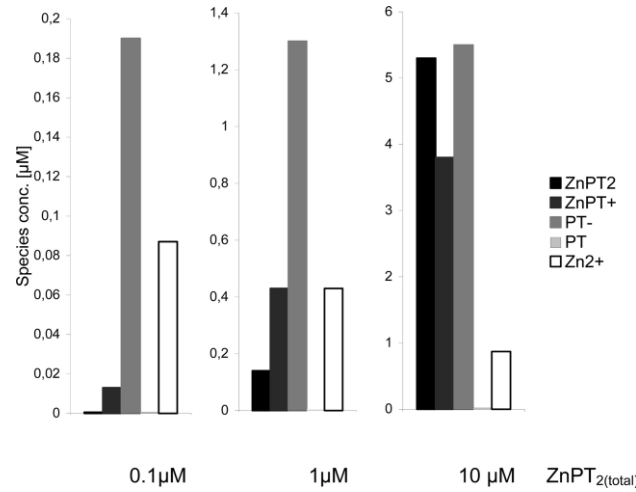

Fig. 6 Speciation of $ZnPT_2$ at different $ZnPT_2$(total) concentrations in aqueous solution at pH 7 resulting in various pyrithione species and free zinc(II). $ZnPT_2$ = zinc pyrithione 1 : 2, $ZnPT^+$ = zinc pyrithione 1 : 1, PT^- = pyrithionate, PT = free pyrithione, Zn^{2+} = free zinc(II) cations.

Table 4 Speciation of $ZnPT_2$. Different pyrithione species and free zinc(II) in aqueous solution of $ZnPT_2$(total) at pH 7. Concentrations are given in [µM]

$ZnPT_{2(total)}$	0.1	1	10
$ZnPT_2$	0.00059	0.14	5.3
$ZnPT^+$	0.013	0.43	3.8
$PT^{\ominus}$	0.19	1.3	5.5
PT	0.00074	0.0051	0.022
Zn^{2+}	0.087	0.43	0.87

Proportions of different pyrithione species and free zinc vary significantly at different $ZnPT_{2(total)}$ concentrations.§

Additional metal cations as *e.g.* Fe(III) or Cu(II) would split up the speciation even more according to the respective complex stability constants (Table 5). This speciation has been observed for PT, $ZnPT_2$ and $FePT_3$ in our laboratory (Fig. 7).[36] It also complicates the development of HPLC analysis methods for pyrithiones.

Each metal complex species of pyrithione exhibits characteristic molecular interaction potentials as *e.g.* positive ionic charge in the

§ Data have been calculated according to the Mass Law and the Henderson–Hasselbalch equation with the pK_a value of PT (Table 3) and stability constants of $ZnPT^+$ and $ZnPT_2$ (Table 5).

Table 5 Stability constants of pyrithione with zinc(II), iron(III) and copper(II)

	Zn^{2+}	Fe^{3+}	Cu^{2+}
log*K′*	5.3 [1]	4.7 [2]	> 8.5 [2]
	5.9 [2]		
log*K″*	5.4 [2]		

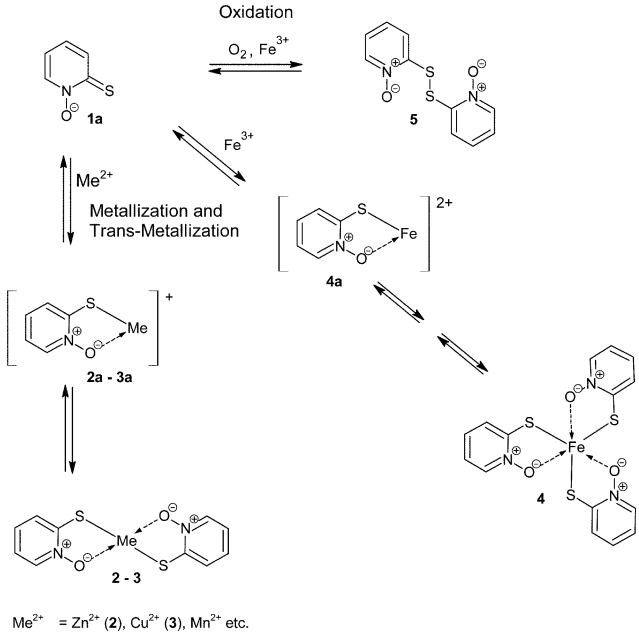

Fig. 7 Abiotic transformation pathways of pyrithiones.

case of the 1 : 1 complex species $ZnPT^+$. $ZnPT_2$, $CuPT_2$ and $FePT_3$ exhibit an increased lipophilic character as compared to the ionic species.

Due to this speciation, different bioavailable pyrithione species might be formed according to the chemical properties of the respective medium (*e.g.*, the metal cation content and pH). In the biological system these species may exert their particular molecular interaction potentials. The neutral species, *i.e.* the free PT, the Cu(II) 1 : 2 or the Fe(III) 1 : 3 complex, could *e.g.* diffuse across the hydrophobic bilayers of cell membranes, immediately dissociating when entering the cytosol. Pyrithione species could coordinate to the active-site metal in metalloenzymes, intercalate in nucleic acids or interfere with electrochemical membrane gradients. It could enter ionic interactions with phospholipid head groups of membrane lipids or disulfide exchange reactions.

Many of these conceivable interactions of pyrithiones with biomolecules have their origin in the N-hydroxythioamide structure of pyrithione. This structure exhibits an inherent neighboring group effect that enables the molecule to chelate Lewis acids of appropriate size and LUMO, and to carry a negative charge. PT possesses a larger number of interaction potentials than would be the sum of interaction potentials of Py, PyNO and PyS.

This explains the toxicity differences of compounds that possess the 2-thiopyridine-1-oxide structure to those without this structure. These results corroborate with findings of Shaw *et al.*,[45] Leonard *et al.*,[46] Albert *et al.*,[2,47] Chandler and Segel[15] and Möller *et al.*,[14] which showed that pyridine derivatives with oxygen bound to the pyridine nitrogen and sulfur (=S/–SH) located adjacent to the nitrogen exhibit far higher biocidal action than structural analogs.

The speciation of the pyrithione metal complexes explains the similarity in toxicity of the metal complexes of pyrithione and NaPT. According to the metal content of the physiological medium different metal complexes of pyrithione could, at low concentrations, afford similar identities and proportions of bioavailable species. However, in the case of $FePT_3$ one would expect a lower effect concentration according to stoichiometry.

Notably, the $(PT)_2$ is as toxic as the pyrithiones although it exhibits the 2-thiopyridine-1-oxide structure in derivatized form thus lacking the negative charge which supports the chelating character. This can be explained by its neutral and hence more lipophilic character compared to the charged pyrithione species. Higher lipophilicity could enhance transport of this species across the hydrophobic membrane bilayers. $(PT)_2$ then could generate PT in the biological medium according to the redox equilibrium $(PT)_2 + 2e^{\ominus} \leftrightarrows 2\ PT$ (see eqn. 1). This would explain the difference from MSPT, which also possesses the 2-thiopyridine-1-oxide structure in derivatized form but is not in equilibrium with free pyrithione. However, IPC-81 cells may also exhibit molecular structures and regulating processes amenable to interaction or reaction with $(PT)_2$ itself.

5 Conclusion

According to the Green Chemistry principles, chemical products should be designed to effect their desired function while minimizing their toxicity.[48] This of course is challenging in the case of antifouling biocides since their purpose is to prevent fouling by toxic action.

Since the N-hydroxythioamide group appears to be the origin of pyrithione toxicity, care has to be taken that this group breaks down irreversibly in biotic or abiotic pathways. Thus, different environmental conditions need to be considered, in particular with respect to the possible formation of $CuPT_2$, $FePT_3$ and $(PT)_2$ (Fig. 7). These highly toxic compounds might form in environmental media, since oxidants and metal cations like Cu(II) and Fe(III) are ubiquitous. Cupric and ferric ions are present in high concentrations in shipping environments (shipping lines, harbors). Cupric oxide is used as an additive in antifouling paints. The environmental occurrence and fate of $CuPT_2$, $FePT_3$ and $(PT)_2$ need to be investigated and monitored in order to validate sustainability of pyrithione antifoulants that has been recommended by manufacturers.

Manufacturers currently refer to reports of rapid degradation and detoxification of $ZnPT_2$ in synthetic seawater under anaerobic and aerobic conditions.[7,49] Unfortunately, test protocols and the chemical structure of some of the identified transformation products were not provided on request. Other studies showed that microbiological activity of aqueous solutions of NaPT was not affected after storage at 40 °C for three months.[50] Mixtures of cupric carbonate and NaPT, which in long term decay tests were tested for their efficacy as a synergetic wood preservative, exhibited no decay in biological activity for six years.[51]

Investigation of the molecular causalities of the molecular mechanisms of pyrithione action is an attractive research field, and resulting knowledge would aid the decision whether pyrithione antifoulants are sustainable alternatives to tributyltin antifoulants. This requires further investigation on a more mechanistic level beyond the scope of the present study.

Acknowledgements

The authors would like to thank NATO who provided financial support for the establishment and development of the Test Battery Ecotoxicity/Toxicity with the NATO collaboration linkage grant.

References

1 J. Sun, Q. Fernando and H. Freiser, *Anal. Chem.*, 1964, **36**(13), 2485–2488.
2 A. Albert, C. W. Rees and A. J. H. Tomlinson, *Br. J. Exptl. Pathol.*, 1956, **37**, 500–511.
3 B. L. Song, Z. S. Lu, D. Z. Niu and Y. Cao, *Chin. Chem. Lett.*, 1990, **1**(2), 117–118.
4 G. A. Hyde and J. D. Nelson Jr., *Cosmet. Drug Preserv.*, 1984, 115–128.

5 J. G. Black and D. Howes, *Clin. Toxicol.*, 1978, **13**(1), 1–26.
6 W. B. Gibson, A. R. Jeffcoat, T. S. Turan, R. H. Wendt, P. F. Hughes and M. E. Twine, *Toxicol. Appl. Pharmacol.*, 1982, **62**(2), 237–250.
7 Olin Corporation, *Harmful effects of the use of anti-fouling paints for ships: Environmental risk assessment of zinc pyrithione anti-fouling biocides*, MEPC 42/5/10, International Maritime Organization, Marine Environment Protection Committee, 4th September 1998, http://www.imo.org/index.htm.
8 N. Voulvoulis, M. D. Scrimshaw and J. N. Lester, *Appl. Organomet. Chem.*, 1999, **13**(3), 135–143.
9 D. E. Audette, R. J. Fenn, J. C. Ritter, G. Polson and P. A. Turley, The Euro-Mediterranean Centre on Insular Coastal Dynamics, *Costs and benefits. From antidandruff to antifoulant: a non-persistent alternative to TBT and alternative antifoulants – an international conference*, Foundation for International Studies, Malta, 4–6 December 1995.
10 B. L. Barnett, H. C. Kretschmar and F. A. Hartman, *Inorg. Chem.*, 1977, **16**(8), 1834–1838.
11 PCI interview, Robert Martin, Arch Chemicals, http://www.archbiocides.com/marine/news.asp, 20-9-2002.
12 K. Goka, *Environ. Res.*, 1999, **81**(1), 81–83.
13 N. Kobayashi and H. Okamura, *Mar. Pollut. Bull.*, 2002, **44**, 748–751.
14 M. Möller, W. Adam, C. R. Saha-Möller and H. Stopper, *Toxicol. Lett.*, 2002, **136**, 77–84.
15 C. J. Chandler and I. H. Segel, *Antimicrob. Agents Chemother.*, 1978, **14**(1), 60–68.
16 A. J. Dinning, I. S. I. Al-Adham, P. Austin, M. Charlton and P. J. Collier, *Lett. Appl. Microbiol.*, 1998, **85**(1), 132–140.
17 I. S. I. Al-Adham, A. J. Dinning and I. A. Eastwood, *J. Ind. Microbiol. Biotechnol.*, 1998, **21**, 6–10.
18 A. J. Dinning, I. S. I. Al-Adham, I. M. Eastwood and P. J. Collier, *Abstr. Gen. Meet. Am. Soc. Microbiol.*, 1995, **95**, 151), ISSN: 1060-2011.
19 S. M. A. Abdel Malek, I. S. I. Al-Adham, C. L. Winder, T. E. J. Buultjens, K. M. A. Gartland and P. J. Collier, *J. Appl. Microbiol.*, 2002, **92**, 729–736.
20 W. T. Gibson, M. Chamberlain, J. F. Parsons, J. E. Brunskill, D. Leftwich, S. Lock and R. J. Safford, *Food Chem. Toxicol.*, 1985, **23**(1), 93–102.
21 E. J. Lesnefsky and J. Ye, *Am. J. Physiol.*, 1994, **266**, H384–392.
22 K. E. Dineley, J. M. Scanlon, G. J. Kress, A. K. Stout and I. J. Reynolds, *Neurobiol. Dis.*, 2000, **7**, 310–320.
23 E. Ermolayeva and D. Sanders, *Appl. Environ. Microbiol.*, 1995, **61**(9), 3385–3390.
24 C. H. Kim, J. H. Kim, S. J. Moon, K. C. Chung, C. Y. Hsu, J. T. Seo and Y. S. Ahn, *Biochem. Biophys. Res. Commun.*, 1999, **259**(3), 505–509.
25 M. Alirezaei, A. Nairn, J. Glowinski, J. Prémont and P. Marin, *J. Biol. Chem.*, 1999, **274**(45), 32433–32438.
26 R. C. Spiker Jr. and H. P. Ciuchta, *Am. Ind. Hyg. Assoc. J.*, 1980, **41**(4), 248–253.
27 G. J. Kontoghiorghes, A. Piga and A. V. Hoffbrand, *FEBS Lett.*, 1986, **204**(2), 208–212.
28 G. Imokawa and K. Okamoto, *J. Soc. Cosmet. Chem.*, 1983, **34**(1), 1–11.
29 M. M. Khattar and W. G. Salt, *J. Chemother.*, 1993, **5**, 175–177.
30 D. M. van Reyk, S. Sarel and N. H. Hunt, *Int. J. Immunopharmacol.*, 1992, **14**(5), 925–932.
31 C. Hoffman, H. Genieser, M. Veron and B. Jastorff, *Bioorg. Med. Chem. Lett.*, 1996, **21**, 2571.
32 J. Ranke, K. Mölter, F. Stock, U. Bottin-Weber, J. Poczobutt, J. Hoffmann, B. Ondruschka, J. Filser and B. Jastorff, *Ecotoxicol. Environ. Saf.*, 2003, in press10.1016/S0147-6513(03)00105-2, available at the EES website.
33 S. Ruchaud, M. Zorn, E. Davilar-Villar, H. Genieser, C. Hoffmann, B. Gjersten, S. Doeskeland, B. Jastorff and M. Lanotte, *Cell. Pharmacol.*, 1995, **2**, 127.
34 N. Lacaze, G. Gombaud-Saintonge and M. Lanotte, *Leuk. Res.*, 1983, **7**(2), 145–154.
35 B. Jastorff, R. Stoermann and U. Woelcke, *Struktur-Wirkungs-Denken in der Chemie*, Universitätsverlag Aschenbeck und Isensee, Bremen, Oldenburg, 2003.
36 C. Doose, *Pyrithiones: From Molecular Structure to Biological Action – Implementation of the T-SAR-approach for the understanding of delicate analytes and versatile biocides*, Dr. rer. nat. Dissertation, University of Bremen, Germany, 2003.
37 D. H. R. Barton, C. Chen and G. M. Wall, *Tetrahedron*, 1991, **47**(32), 6127–6138.
38 R. Freshney, *Culture of animal cells a manual of basic technique*, 4 edn., Wiley-Liss. Inc., New York, 2000.
39 A. Moore, R. Gerner and H. Franklin, *J. Am. Med. Assoc.*, 1967, **199**, 519–524.
40 R. A. Jones and A. R. Katritzky, *J. Chem. Soc.*, 1960, 2937–2942.
41 J. N. Gardner and A. R. Katritzky, *J. Chem. Soc.*, 1957, 4375–4387.
42 B. Lynch and M. R. Smyth, *Voltammetric determination of some heterocyclic mercaptans*, ed. M. R. Smyth and J. G. Vos, Elsevier Science Publishers B.V., Amsterdam, The Netherlands, 1986, pp. 97–103.
43 A. F. Krivis, E. S. Gazda, G. R. Supp and M. A. Robinson, *Anal. Chem.*, 1963, **35**(8), 966–968.
44 I. Pardo, M. Angulo, R. M. Galvin and J. M. R. Mellado, *Electrochim. Acta*, 1996, **41**(1), 133–139.
45 E. Shaw, J. Bernstein, K. Losee and W. A. Lott, *J. Am. Chem. Soc.*, 1950, **72**, 4362–4364.
46 F. Leonard, F. A. Barkley, E. V. Brown, F. E. Anderson and D. M. Green, *Antibiot. Chemother.*, 1956, **6**(4), 261–266.
47 A. Albert, C. W. Rees and A. J. H. Tomlinson, *Recl. Trav. Chim.*, 1956, **75**, 819–824.
48 P. Anastas and J. Warner, *Green Chemistry – Theory and Practice*, Oxford University Press, Oxford, UK, 2000.
49 T. Madsen, L. Samsoe-Petersen, K. Gustavson and D. Rasmussen, *Environmental project: Ecological assessment of antifouling biocides and nonbiocidal antifouling paints*; The Danish Environmental Protection Agency, DHI Water & Environment, Miliøstyrelsen, Environmental project: No. 531, 2000.
50 J. D. Nelson and G. A. Hyde, *Cosmet. Toiletries*, 1981, **96**(3), 87–90.
51 T. P. Schultz, T. Nilsson and D. D. Nicholas, *Wood Fiber Sci.*, 2000, **32**(3), 346–353.